1-1-2014

Preliminary Investigation of Cellular Lipid Extraction Using Electroporation as an Enhancement Technique

Robert McComas

Preliminary investigation of cellular lipid extraction using electroporation as an enhancement technique

By

Robert G. W. McComas

A Thesis
Submitted to the Faculty of
Mississippi State University
in Partial Fulfillment of the Requirements
for the Degree of Master of Science
in Chemical Engineering
in the Dave C. Swalm School of Chemical Engineering

Mississippi State, Mississippi

May 2014

Preliminary investigation of cellular lipid extraction using electroporation as an enhancement technique

By

Robert G. W. McComas

Approved:

_____

R. Mark Bricka
(Co-Major Professor)

_____

W. Todd French
(Co-Major Professor and Graduate Coordinator)

_____

Jason Keith
(Committee Member)

_____

Keisha B. Walters
(Committee Member)

_____

Achille Messac
Dean
Bagley College of Engineering

Name: Robert G. W. McComas

Date of Degree: May 16, 2014

Institution: Mississippi State University

Major Field: Chemical Engineering

Major Professor: Dr. R. Mark Bricka and Dr. W. Todd French

Title of Study: Preliminary investigation of cellular lipid extraction using electroporation as an enhancement technique

Pages in Study: 153

Candidate for Degree of Master of Science

This study investigated the use of electroporation as an extraction method of lipids in oleaginous microorganisms. Electroporation is the process of placing a voltage gradient across a lipid membrane to create pores that vary in size and longevity with voltage magnitude and pulse duration. Once the voltage gradient is removed, the lipid membrane will seal the pore. The use of electroporation on oleaginous microorganisms to extract stored lipids could be a useful tool if the microorganism is allowed to regenerate and produce more lipids. Three high-lipid media were investigated: soybeans, *Rhodococcus opacus* (bacteria), and *Rhodotorula glutinis* (yeast). This study investigates varied voltage magnitude, pulse duration, quantity of pulses, and distance between electrodes. Electroporation proved to be moderately successful for lipid removal when using low voltages and long pulse durations. However, electroporation removed only a small percentage of the intracellular lipids.

DEDICATION

This paper is dedicated to my family. My wife, Catherine, and my daughter, Vivian, have been the inspiration that I needed to complete this report. My wife has endured many hardships throughout this process and I will always be in her debt for continually encouraging me to complete my thesis. Also, my mother, father, brother, mother- and father-in-law, and grandparents have given me the support and positive energy that were required to complete this thesis.

ACKNOWLEDGEMENTS

I would like to acknowledge Dr. Mark Bricka and Dr. Todd French for their insight, guidance, and belief in my ability to complete this work. I would also like to thank Dr. Jason Keith, Dr. Keisha Walters, Dr. Hossein Toghiani, and Dr. Gouchang Zhang for their comments and input for this report. I am also thankful for my fellow graduate students, Richard Lusk, Jacqueline Hall, Amy Parker, Preshanth Buchireddy, and Jericus Witlock, for their continued support and insight throughout my research. Also, I would like to acknowledge all of the undergraduate students who worked diligently in support of my lab efforts: Rosemary Weathersby, Catherine Brimhall, Jordan Elmore, Brittany Clune, and Melissa Spark. Without their assistance, I could not have completed all of the experiments necessary to complete my research. Publication of this thesis would not have been possible without all the support I received.

TABLE OF CONTENTS

DEDICATION ii

ACKNOWLEDGEMENTS iii

LIST OF TABLES vi

LIST OF FIGURES viii

CHAPTER

I. INTRODUCTION 1

II. LITERATURE REVIEW 4

2.1 Oleaginous Microorganisms 4
2.2 Electroporation Background 8
2.3 The Five Stages of Electroporation 17
2.3.1 Induction Step 18
2.3.2 Expansion Step 19
2.3.3 Stabilization Step 20
2.3.4 Resealing Effect 20
2.3.5 Memory Effect 21
2.4 Pore-based Electroporation Model 22
2.5 Current State of the Science (2008-2013) 24

III. OBJECTIVES 27

IV. METHODS AND MATERIALS 29

4.1 Overview 29
4.2 Method Required to Electroporate Oleaginous Microorganisms and Soybeans 31
4.2.1 Inoculation 32
4.2.2 Incubation 37
4.2.3 Electroporation 39
4.2.4 Analysis 43
4.2.5 Supernatant Analysis 47
4.2.6 Soybean Electroporation 48
4.3 Experimental Matrix 49

V. DATA ANALYSIS 54

5.1 *Rhodococcus opacus* (Bacteria) 56
5.2 Soybeans 58
5.3 *Rhodotorula glutinis* (Yeast) 60
5.3.1 Matrix 1 – Low Voltage and Single Pulse 61
5.3.2 Matrix 2- High Voltage and Single Pulse 68
5.3.3 Matrix 3- Low voltage, pulse duration, and number of pulses 76
5.3.4 Matrix 4: High voltage, pulse duration, and number of pulses 83
5.4 Scanning Electron Microscopy 90
5.4.2 Irreversible Electroporation Experiments 94

VI. CONCLUSIONS AND RECOMMENDATIONS 97

6.1 Conclusion 97
6.2 Recommendations 98

REFERENCE 99

APPENDIX

A. DATA WITH PARAMETERS 110

A.1 Soybean Data 111
A.2 Data Collected for *R. glutinis* 113

APPENDIX

B. SAS OUTPUT 119

B.1 Soybean SAS Output 120
B.2 Matrix 1 SAS output 127
B.3 Matrix 2 SAS output 132
B.4 Matrix 3 SAS output 139
B.5 Matrix 4 SAS output 147

LIST OF TABLES

2.1 List of oleaginous microorganisms proven to accumulate 25% lipids on a dry mass basis 7

4.1 Experimental design for a Box-Behnken three-variable matrix 50

4.2 Experimental design for a Box-Behnken three-variable matrix with parameters for Matrix 1 52

4.3 Experimental design for a Box-Behnken three-variable matrix with parameters for Matrix 2 52

4.4 Experimental design for a Box-Behnken three-variable matrix with parameters for Matrix 3 53

4.5 Experimental design for a Box-Behnken three-variable matrix with parameters for Matrix 4 53

5.1 Output from regression model run on soybean electroporation data 60

5.2 Matrix 1 parameters 61

5.3 Minimum ridge analysis of Matrix 1 Box-Behnken experimental design (from Appendix B.2, SAS Output) 63

5.4 Output from regression model run on Matrix 1 electroporation data 64

5.5 Eigenvalues and eigenvectors from ridge analysis of Matrix 1 67

5.6 Matrix 2 parameters 69

5.7 Minimum ridge analysis of Matrix 2 Box-Behnken experimental design 70

5.8 Minimum ridge analysis of Matrix 2 Box-Behnken experimental design 71

5.9 Minimum ridge analysis of Matrix 2 Box-Behnken experimental design 74

5.10 Matrix 3 parameters 76

5.11 Minimum ridge analysis of Matrix 3 Box-Behnken experimental design 78

5.12 Output from regression model run on Matrix 3 electroporation data 79

5.13 Output from regression model run on Matrix 3 electroporation data 82

5.14 Matrix 4 parameters 84

5.15 Minimum ridge analysis of Matrix 4 Box-Behnken experimental design 86

5.16 Output from regression model run on Matrix 4 electroporation data 87

5.17 Output from regression model run on Matrix 3 electroporation data 90

5.18 Data collected during irreversible EP experiments....95

A.1 Soybean data with experimental parameters....111

A.2 Matrix 1 data with experimental parameters 113

A.3 Matrix 2 data with experimental parameters 114

A.4 Matrix 3 data with experimental parameters 115

A.5 Matrix 4 data with experimental parameters 117

LIST OF FIGURES

2.1 A) Microphotograph of red blood cell before electroporation, B) Microphotograph of electroporated red blood cell (Source: Chang and Reese, 1990) 9

4.1 Flow chart of electroporation experimental process 30

4.2 A) Keeping the media in a sterile environment during cell transfer, B) Inoculation loop 32

4.3 Agar and growth media in a New Brunswick Scientific constant motion incubator 34

4.4 Cell colonies on surface of YM agar after 2 days of incubation 35

4.5 Lipid accumulation media (left), YM media after 20 hours (right) 36

4.6 Inoculated bottles in constant motion incubator 37

4.7 Comparison chart of OD reading versus cell mass for 5-day growth cycle of *R. glutinis* 38

4.8 Teflon™ cuvette for EP experiment 39

4.9 Experimental setup for electroporation using Teflon™ cuvette 41

4.10 Transferring oil-rich media to Teflon™ cuvette for electroporation experiment 42

4.11 Removing electroporated cells from Teflon™ cuvette 43

4.12 Concentrated cell puck after centrifugation 44

4.13 A) Freeze drier with samples attached, B) Cell masses will change from a dark pink to light pink when freeze drying is complete 45

4.14 The top layer is cell mass and methanol: the bottom layer is chloroform and lipids 46

4.15 TurboVap loaded with amber vials to evaporate chloroform 47

5.1 Lipid extraction data collected during *R. opacus* Bligh and Dyer 57

5.2 Graph of lipid percentage in crushed soybeans with boundaries (noted with bold lines) of literature-reported lipid percentages at 19 and 23% 59

5.3 Graph of lipid percentage data collected during Matrix 1 tests with control experiments on left and EP experiments on right 62

5.4 Model prediction for Matrix 1 variables (voltage, pulse duration, and electrode spacing): A) Surface graph comparing voltage and electrode spacing on lipid extraction, B) surface graph comparing pulse duration and electrode spacing on lipid extraction, and C) surface graph comparing voltage and pulse duration on lipid extraction. (see Appendix B.2: SAS Output) 65

5.5 Data collected during Matrix 2 tests with control experiments on left and EP experiments on right 69

5.6 Model prediction for Matrix 2 variables (voltage, pulse duration, and electrode spacing): A) Surface graph comparing voltage and electrode spacing on lipid extraction, B) surface graph comparing pulse duration and electrode spacing on lipid extraction, and C) surface graph comparing voltage and pulse duration on lipid extraction 72

5.7 Data from Matrix 2 grouped by electrode spacing (control=0 and electroporated cells= 10, 15, and 20) 75

5.8 Graph of data collected during Matrix 3 tests with control experiments on left and EP experiments on right 77

5.9 Model prediction for Matrix 3 variables (voltage, pulse duration, and number of pulses): A) Surface graph comparing voltage and number of pulses on lipid extraction, B) surface graph comparing pulse duration and number of pulses on lipid extraction, and C) surface graph comparing voltage and pulse duration on lipid extraction. 80

5.10 Data from Matrix 3 grouped by pulse duration (control=0 and electroporated cells= 10, 505, and 1000) 83

5.11 Graph of data collected during Matrix 4 tests (control experiments on left and EP experiments on right) 85

5.12 Model prediction for Matrix 4 variables (voltage, pulse duration, and number of pulses): A) Surface graph comparing voltage and number of pulses on lipid extraction, B) surface graph comparing pulse duration and number of pulses on lipid extraction, and C) surface graph comparing voltage and pulse duration on lipid extraction. 88

5.13 SEM photo of *Rhodotorula glutinis*, not subjected to EP.....91

5.14 SEM microphotographs of *R. glutinis* after EP treatment (3000 volts, 100 microseconds, and 59 pulses) 92

5.15 SEM of irreversible EP experiments illustrating cell membrane failure (490 volts, 10 seconds, and 3 pulses).....93

5.16 Enhanced SEM of irreversible EP experiments with cell membrane failure (490 volts, 10 seconds, and 3 pulses) 93

5.17 Average percent intracellular lipid extracted during the irreversible electroporation experiments.....96

CHAPTER I

INTRODUCTION

Oleaginous microorganisms, bacteria, yeast, or algae that accumulate more than 20% of their biomass as lipids, have proven to efficiently produce lipids in the form of phospholipids and triglycerides (Kaneko, H 1976; Wynn, J 2005; Yoon 1983; Alvarez 1996). Microorganisms are able to accumulate lipids when cultivated under conditions of limited nitrogen and an excess of carbon, usually using glucose, media. Research completed by Alvarez et al. (1996) has shown lipid production of bacteria as high as 78% lipid/ dry cell mass (DCM). Several strains of bacteria and yeast proven to accumulate lipids have been a focus of intensive research since the 1970's. Kaneko et al. (1976) validated the production of lipids for 30 different strains of yeast. Once a microorganism accumulates lipids, they are extracted using techniques that destroy the oleaginous microorganism. One method for extracting lipids from microorganisms involves separating the cells from their growth media using a centrifuge or filtration, drying the cell mass, and then using solvent extraction to remove the lipids entrained in the cell mass (Wynn 2005). This method is costly for large-scale production.

Soybeans are oleaginous plant media and are grown primarily for their protein and oil content (Smith and Huyser 1987). Soybean seeds contain 19%-23% oil depending on the time of year they were harvested and the amount of precipitation occurring during growth phases (Sharma et al. 2002 and Dornbos and Mullen 1992). The

two primary methods for extracting oil from soybeans are solvent extraction and mechanical pressing. The mechanical method utilizes a screw press and removes the oil contained in the soybean seed (Bargale et al. 1999). This method is cost-intensive and inefficient; therefore, methods were developed that utilize solvent extraction, typically hexane, to remove oil from soybeans that have been machined to flakes (Ramsey and Harris 1982). Solvent extraction can remove up to 86% of the oil contained in the soybean. After the oil is extracted, the soybean flakes are rinsed to remove the solvent so the flakes can be recovered and used for animal feed, soy products, and protein supplements. After processing, the soybean oil recovered in the extraction process is suitable for human consumption and/or biodiesel production (Farsaie et al. 1985).

The potential of using a living microorganism to produce an alternative fuel has been the focus of research for the last several years (Qiang et al. 2008). In 2008, the world consumed over 85,462 barrels of crude oil per day (www.eia.gov). The amount of crude oil in the world is limited and scientists and engineers have been searching for alternative sources of oil for decades, with renewable fuel resources currently under development. Wynn et al. (2005) state that some strains of bacteria and yeast have been proven to produce and accumulate lipids under certain living conditions. Researchers are formulating methods to cultivate oleaginous microorganisms using large-scale processes while maximizing lipid yield (Li 2008). One challenge in this process is developing an economical process to extract lipids from the microorganism while maintaining cell viability, allowing the cell to recover and maintain all functions.

One such process, referred to as electroporation (EP), creates disruptions in a cell's lipid membrane layer through voltage potential. EP creates pathways, or pores, in

the lipid bi-layer which surrounds cells. Experiments completed by Weaver et al. (1996) proved this technology can be utilized to inject deoxyribonucleic acid (DNA) into a living cell while allowing the cell to remain intact. When an experiment is completed under the proper conditions, the cell closes its pores and is still viable after electroporation. After an experiment, if the cell sample is placed in optimal living conditions – optimal temperature, excess nutrients, and proper mixing – the cells are able to completely recover and reseal any deformations formed during EP. The pores formed during EP are dependent on the pulse duration and pulse amplitude (Smith and Weaver 2008). Therefore, under the optimal parameters, a pore could be created with the appropriate dimensions to allow lipids to be released and recovered from oleaginous media while maintaining cell viability so the cells could recover and store additional lipids.

CHAPTER II

LITERATURE REVIEW

2.1 Oleaginous Microorganisms

The demand for alternative energy sources is increasing since traditional fuel sources are depleting and petroleum prices are increasing (Zhang 2014). One possible source for alternative fuels is oleaginous microorganisms, yeast, fungi, algae, and bacteria, since they are renewable, environmental friendly, generate energy from multiple carbon sources, do not remove food sources from the global market, and provide comparable energy densities as traditional sources (Wynn and Ratledge, 2005; Canakci and Sanli, 2008). The most promising aspect of oleaginous microorganisms is their ability to generate large lipid contents on a mass basis, some instances lipid content as high as 87% w/w dry biomass basis (Koutb and Morsy, 2011; Gao et al., 2013; Hetzler et al., 2013).

Oleaginous microorganisms are able to accumulate lipids in nitrogen or phosphorus depleted environments when the carbon source is in excess (Wynn and Ratledge, 2005). Adenosine triphosphate (ATP) is referred to as the "molecular unit of currency" and transfers energy in cells which promotes cell division (Knowles 1980). Microorganisms in nitrogen depleted environments are unable to produce ATP which is necessary to generate new cells therefore, they begin to store energy if an excess of consumable carbon is available (Hall, 2012). As a result of nitrogen depletion, the

enzymes in the citric acid cycle become inactive which leads to isocitrate not being metabolized. This produces an excess of isocitrate and citric acid. Once the citrate is in excess it comes in contact with an enzyme, ATP:citrate lyase which cleaves the citrate to and forms acetyl-coenzyme A, oxaloacetate, ADP and inorganic phosphate. Acetyl-coenzyme A is vital fatty acid biosynthesis. Oxaloacetate is immediately converted to malate by malate dehydrogenase and then the malate is then converted to pyruvate by the malic enzyme. A product of the malate cleavage is reduced nicotinamide adenine dinucleotide phosphate (NADPH) which is necessary for long acyl chain that are derived from acetyl-coenzyme A. For a cell to accumulate lipis these two components are necessary, NADPH and acetyl-coenzyme A (Wynn and Ratlegde, 2005).

Every microorganism is not able to accumulate lipids since the ability to accumulate lipids is dependent on the activity of the malic enzyme. Non-lipid accumulating microorganisms switch off the gene controlling the activity of the malic enzyme after nitrogen has been depleted. The microorganisms that accumulate large amounts of lipids, up to 87% dry mass basis, do not deactivate the gene controlling the malic enzyme (Hetzler et al., 2013; Wynn and Ratledge, 2005).

Numerous studies have been completed to determine the microorganisms that accumulate lipids and the amount of lipids they are able to generate. Table 2.1 lists several microorganisms that are known to accumulate more than 25% lipids on a dry mass basis. The microorganisms listed in Table 2.1 have been published in the literature to accumulate excess lipids using various carbon sources. There have been additional experiments to determine the optimal amount and type of carbon source to maximize the amount of lipids cells accumulates (Alvarez, 1996; Daniel et al., 1999; D'Annibale et al.,

2005; Davis, 1964; Makula et al, 1975; Raza et al., 2007; Holdsworth and Ratledge, 1988; Kavadia et al. 2001)

Table 2.1 List of oleaginous microorganisms proven to accumulate 25% lipids on a dry mass basis

Organism	Lipid Content (%w/w)	Reference
Yeast		
Candida sp. 107	42	Wynn and Ratledge, 2005
Cryptococcus albidus	65	
C. curvatus D	58	
Waltomyces lipofer	64	
Lipomyces starkeyi	63	
Rhodosporidium toruloides	66	
Rhodotorula glutinis	72	
Trichosporon beigelii	45	
Yarrowia lipolytica	36	
Fungi		
Zygomycetes		Wynn and Ratledge, 2005
Conidiobolus nanodes	26	
Entomophthora coronata	43	
Cunninghamella japonica	60	
Mortierella isabellina	86	
Rhizopus arrhizus	57	
Mucor alpine-peyron	38	
Ascomycetes		
Aspergillus terreus	57	
Fusarium oxysporum	34	
Pellicularia practicolo	39	
Microalga and Thraustochytrids		
Prokaryota		Wynn and Ratledge, 2005
Spirulina platensis	25	
Eukaryota		
Chlorella vulgaris	52	
Crypthecodium cohnii	50	
Nannochloropsis oculata	45	
Thraustochytrids		
Schizochytrium sp	40	
Thraustochytrium aureum	25	
Bacterium		
Rhodococcus opacus	87	Alvarez et al. 1996
Rhodococcus ruber	26	Alvarez et al. 1997a
Acinetobacter sp. Strain 211	25	Alvarez et al. 1997b
Pseudomonas aeruginosa strain 44T1	38	De Andres et al. 1991

2.2 Electroporation Background

External electric fields have been utilized in physical chemistry and biophysics to investigate the ionic-electric properties and reactivity of molecules and molecular organisms (Neumann et al. 1989). When an electric field is introduced to a microorganism the cell membrane becomes porous. This phenomenon, known as EP, is defined as an increase in electrical conductivity of a cell membrane introduced by an external source, and has been researched for several decades. Sale and Hamilton (1967a) stated that in 1958, researchers noticed that an unexplained form of "electrical breakdown" occurred in an electrically stimulated membrane. Ten years later it was observed that a microorganism was still viable after a strong electric pulse (Sale and Hamilton 1967). These observations piqued the scientific community's interest, and numerous experiments have been conducted to advance the understanding of the mechanism of this phenomenon. In the late seventies and early eighties, it was observed that an increase of the membrane specific conductance was measured within microseconds of the application of a high-intensity electric field (Abidor et al., 1979; Benz et al., 1979; Benz and Zimmermann, 1980a; Benz and Zimmermann, 1980; Benz and Zimmermann, 1981; Benz and Conti, 1981; Chernomordik et al., 1982; Teissie et al., 2005). Further experimental analyses showed that the electric field interaction was initiated at the lipid portion of the cell membrane. This observation led to further experiments to model the behavior of lipid systems under the influence of electric fields and to study the mechanism controlling EP (Weaver and Chizmadzhev, 1996).

The aspects of EP that are currently understood are to the result of experiments that measured the electric current through planar bilayer lipid membranes (BLM).

During these studies, a structural rearrangement of the lipid membrane was observed. Experiments were completed on red blood cells; Figure 2.1 is an example of the indentations observed after EP of red blood cells.

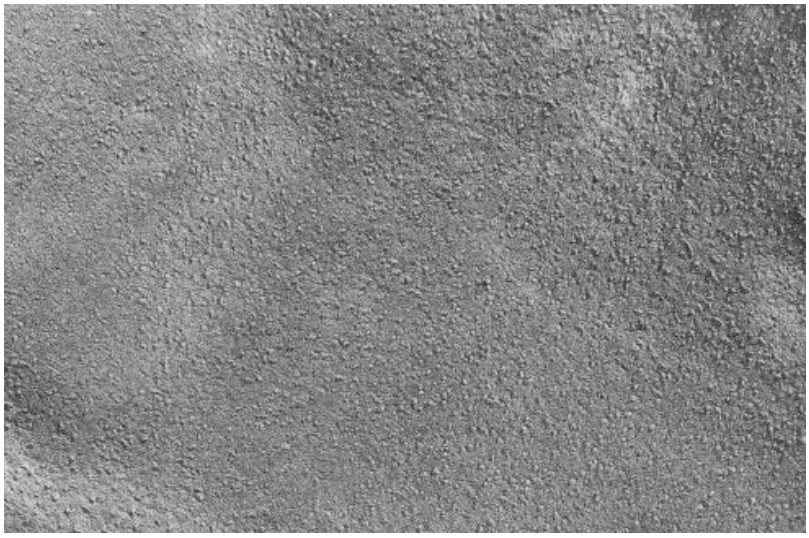

(A)

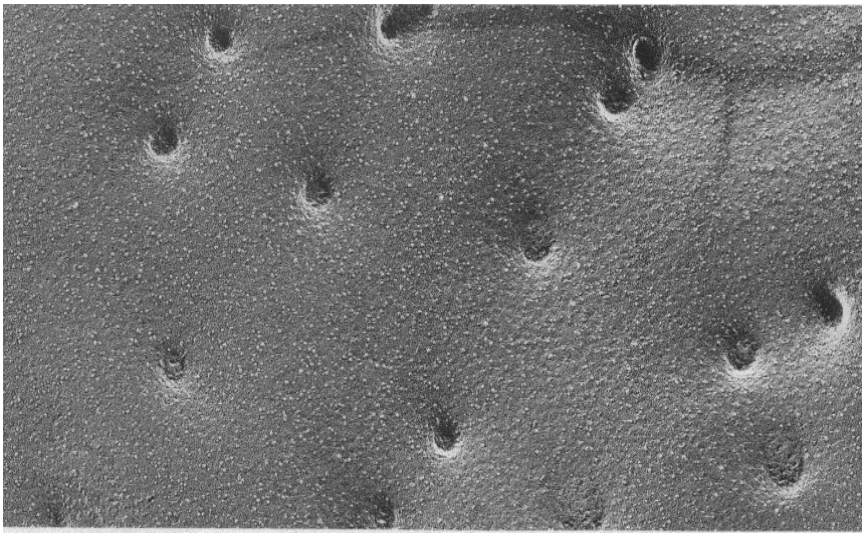

(B)

Figure 2.1 A) Microphotograph of red blood cell before electroporation, B) Microphotograph of electroporated red blood cell (Source: Chang and Reese, 1990)

These rearrangements were observed using an electron microscope. The observation of the indentions of the red blood cell led to the explanation that pores are formed as a result of applying an external electric pulse (Weaver and Chizmadzhev 1996, Gross, 1986). Researchers have been conducting experiments to better understand the mechanism driving EP, since currently the understanding of the mechanism for EP is very limited. Experiments have been performed to better understand electroporation, using three systems: (1) cell suspensions, (2) individual cells, and (3) a pure BLM. The three systems share a common characteristic, a lipid membrane. Therefore, the outcome of an experiment using a BLM could assist in predicting the outcome of a similar test on one of the alternate systems – cell suspensions or individual cells (Weaver and Chizmadzhev 1996). A BLM was utilized for a majority of the experiments because of the ease of variable measurement and manipulation of bulk properties. Also, several experiments can be completed on a single lipid membrane to measure the effect of multiple pulses and to test the stress and strain exerted on a lipid membrane.

Over the last 20 years, electric field pulse techniques have received a great deal of attention, especially in cellular and molecular biology. EP has become popular for cell manipulation and to study electrically induced structural rearrangements in cell membranes. This process has many proven applications, including: (1) transfection, transfer of a foreign media, DNA or virus, from one cell to another cell, or cells; (2) introduction of fluorescent probes; (3) loading cells with molecules for drug delivery purposes; and (4) transporting DNA into and across tissue for therapeutic purposes (Weaver and Chizmadzhev 1996). EP can occur in a time frame of nanoseconds for extreme voltages, 300 kilovolts (kV)/centimeter (cm), and even microseconds for lower

voltages, 0.7 kV/cm (Beebe et al. 2003). Although this phenomenon has been researched for decades, there is still little information about the mechanism that forms the pores produced during electroporation.

EP is the process of placing a voltage across a cell membrane that exceeds the dielectric point. This polarizes the charge of a cell, such that the membrane reorients and forms pores of the cell membrane. The most appealing aspect of EP is that, under the right conditions (pulse length, pulse strength, and number of pulses), the cell is still viable after the procedure. If the cell is given the proper amount of time to recover from an EP experiment (some cells may take minutes and others may take hours), the cell will resume growing and reproducing (Wang 2007). While understanding of the EP mechanism is increasing daily, knowledge is still limited (Weaver 2006).

Historically the study of EP has focused on the deformation of a BLM. The effect of electric pulses and voltage differences on a BLM has been researched extensively. Initially, it was thought that the mechanism of electric forces on a lipid membrane caused an irreversible breakdown by electrocompression (Crowley, 1973; Dimitrov, 1984). Experiments have studied the number of DNA molecules with different characteristics, shapes, sizes, and charges, which are taken up by electroporated cells at varying pulse strengths and durations. These experiments were conducted by placing cell cultures in DNA-rich environments, inducing a voltage potential, and measuring the amount of DNA available in the media after the voltage source was removed. These experiments have been completed on populations of cells (Mir et al., 1988; Chakrabarti et al., 1989; Lambert et al., 1990); as well as analyzed on an individual cell level (Bartoletti et al., 1989; Prausnitz et al., 1993, 1994; Gift and Weaver, 1995). During an EP experiment

involving the introduction of exogenous DNA to a microorganism, the typical results include 0.01% of the electroporated cells accepting the exogenous DNA. For example, if the experiment included 10,000,000 cells affected by EP the accepted the targeted DNA would be 1,000 cells (Chang et al., 1992).

An important effect of EP is the modulation of the membrane potential difference due to the dielectric characteristics of the lipid membrane. A cell membrane can be visualized as an insulating shell containing a conductive medium, in suspension of a conductive medium. This dielectric discontinuity affects the electric field line distribution (Teissie et al., 2005). Analyzing this discontinuity has led to the steady state expression of the voltage, U:

$$U=1.5R_{cell}\, E \cos\theta \qquad \text{(Eq 2.1)}$$

In Eq 2.1, the vesicle is assumed to be a sphere, R_{cell} is the radius of the spherical cell, E is the field strength, and θ is the normal angle between the membrane and the direction of the applied field. The field effect is position-dependent on the cell membrane surface. This causes one side of the vesicle to be hyperpolarized while the adjacent side is simultaneously depolarized (Teissie et al., 2005). The predictions made above were validated experimentally using videomicroscopy on lipid vesicles with potential fluorescent probes (Kotnik, et al., 1997; Teissie and Rols, 1993).

The membrane potential difference is reached after an extremely short charging time, microseconds (Neumann et al., 1989; Chang et al., 1992; Kotnik et al., 1997). Charging time ($\tau_{membrane}$) is dependent on the dielectric properties of the cell membrane and the resistance of the medium surrounding the cell. The cell membrane is more

complex than the manufactured BLM since a cell membrane does not have a uniform thickness and curvature. The $\tau_{membrane}$ is dependent on the resistance of the cytoplasm (r_{int}), external buffer resistance (r_{ext}), and resistance of the cell membrane (C_{memb}) as shown in Eq. 2.2 (Wang 2007).

$$\tau_{membrane}=R_{cell}C_{memb}:(r_{int}+r_{ext}/2) \quad \text{(Eq. 2.2)}$$

This charging time was documented by Lojewska et al. (1989) to be several microseconds and then verified experimentally using videofluorescence on a spherical lipid bilayer (Lojewska et al., 1989).

An external electric field will induce a position-dependent modulation of the membrane potential difference, which is linearly related to the intensity of the applied field (Teissie et al., 2005). The theoretical models produced assume that the following two criteria are met:

1. The cell is spherical, and
2. The membrane is a dielectric.

It should be noted that microbial cells are not perfect spheres; this must be taken into consideration when predicting deformation of the cell membrane.

There are two types of electroporative experiments that can be completed: irreversible electrical breakdown and reversible electrical breakdown. With irreversible electrical breakdown, the cell is not viable after a voltage is applied. There are two forms of irreversible electrical breakdown. The first is an immediate cell rupture where the applied voltage exceeds the transmembrane voltage or the pulse duration, or it exceeds both parameters simultaneously. The second form of irreversible electrical breakdown is

a condition known as cell lyses, or destruction of the cell membrane. Cell lyses is usually attributed to an imbalance in the cell caused by unequal transport of media through the ionic pathways formed as a result of electroporation. Initial studies that discuss the non-thermal killing of biological systems were published in 1967 and discussed how large electric pulses irreversibly affected the system, killing cells (Sale, 1967b). Conversely, during reversible electrical breakdown, the cell is able to repair itself and remain intact.

Most BLM experimental configurations show that the electrode voltage and the transmembrane voltage are equal after membrane charging (Weaver and Chizmadzhev 1996). Experiments conducted to measure the transmembrane current have shown that after a step change in the applied voltage at the electrodes has occurred, a steady-state transmembrane current is achieved (Abidor et al., 1979). As the electrode voltage increases, the measured transmembrane current migrates towards the saturation current, the point when increasing voltage produces no increase in current. Once the saturation current has been reached, the cell membrane is ruptured. This was proven experimentally by lowering the voltage after the saturation current was reached, and the measured current was the same as if there were no membrane present in the solution (Weaver and Chizmadzhev, 1996).

It was also found that the membrane lifetime decreases with increasing voltage. Electrical breakdown of cell membranes has two stages: (1) a steady-state current stage, and (2) a fluctuating current stage. A membrane can survive larger voltages if the pulse length is shortened. For reversible EP, the pulse length must not exceed 1 millisecond (Freeman 1994). If the pulse duration is less than 1 millisecond, a cell membrane will

have a transition into a long excited state with a large conductance and fluctuating current. This state is termed the "stress state."

Determining the mechanism of membrane rupture needs to include investigation of the time dependence on each parameter. It is best to focus on the transmembrane voltage. An increase in transmembrane voltage of 100mV will cause a tenfold decrease in $\tau_{membrane}$. Subsequently, it was observed that as the transmembrane voltage increases from 200mV to 1.4V, $\tau_{membrane}$ will decrease by six orders of magnitude, reducing the amount of time necessary to form a pore. This theory is consistent with pore theory (Weaver and Chizmadzhev, 1996).

The charge relaxation method was used in experiments that focused on oxidized membranes compiled of cholesterol, which were charged to a transmembrane voltage of 1V for 400 ns. After the voltage pulse, the membrane was mechanically stable and was recharged with the same result (Benz et al., 1979). This was the first observed and documented reversible electrical breakdown.

In 1982, the reversible electrical breakdown of a cell membrane was studied using the voltage clamp technique (Chernomordik, et al., 1982; Sukharev, et al., 1982; Abidor, et al., 1982). The voltage clamp technique applies a constant voltage to a membrane while monitoring the current across an ion channel. This method is best known for characterizing the ion flux across a specific membrane. Several reproducible characteristics of membrane current were observed in these experiments. After reversible EP was confirmed, EP became the main interest of future BLM experiments, since the cell membrane could be manipulated and remain intact, thus leaving the cell viable. This method proved experimentally that successive 20-μs square voltage pulses with varying

magnitudes on an oxidized cholesterol membrane had reproducible membrane current characteristics (Weaver and Chizmadzhev, 1996).

When a cell is electroporated, the first consequence is the deformation of the cell due to the induced electric field. The cell shape will change from a spheroid to an elliptical shape. This deformation was explained theoretically and experimentally in the mid-70s (Harbich and Helfrich, 1979; Helfrich, 1974). Recently, membrane conductance has been included as a factor in explaining electroporation. Hyuga et al. (1991) proposed that the ratio of cell interior conductance to the conductance of the exterior solution has an effect on the efficiency of EP (Hyuga, Kinosita, and Wakabayashi, 1991). However, these assumptions aided in predicting the deformation time constants. The time constants had been under the control of arbitrary parameters which were adjusted during experiments completed by Teissie et al. (2005). In some instances, membrane conductance occurred instantaneously with the induced field, as long as the membrane conductance was on the time scale of nanoseconds (Winterhalter and Helfrich, 1988; Hyuga, et al., 1991). However, this theory does not hold true to experimental observations. The membrane conductance does not remain constant during the period a cell is subjected to an induced field. The direction of elongation is dependent on the ratio of the conductivities inside the cell and the conductivity of the buffer solution. When rext/ rint <1, a prolate spheroid (i.e., a sphere where the polar diameter is greater than the equatorial diameter) is produced with its polar axis parallel to the induced field. This increase in length along the induced field will cause a rise in sensitivity of the cell to the field (Teissie et al., 2005). Referring to Eq 2.1, it can be visualized that the portion of the cell facing the electrodes will have a higher transmembrane voltage since the electric

field is parallel to the elongated cell and the value of θ from Eq 2.1 is equal to pi or 0. Therefore, at these values of theta, U will be at a maximum.

Popov et al. (1991) proved this cell deformation experimentally using multiple pulses (Riske and Dimova, 2005; Tekle, et al., 2001; Popov, et al. 1991). More recent studies have utilized nanosecond pulses to analyze the electromechanical stresses from an induced field. The results of these studies showed that the transitory stretching force was at a maximum if the buffer solution had a low conductivity (Sukhorukov, et al., 1998; Muller, et al., 2001). These forces, when present, commonly occur in the nanosecond range, which is before the modulation of the transmembrane potential, which occurs in the μs range (Puc, et al., 2004).

After reversible EP, there is an imbalance in the osmotic forces acting on a cell due the transport of ions that occurs while the pores are present. This will cause swelling of a cell, which causes a tension in the cell membrane. This tension is another variable to consider in the electrodeformation caused by EP (Kinosita and Tsong, 1977; Golzio, et al., 1998).

2.3 The Five Stages of Electroporation

Teissie et al. (2005) proposed that five steps exist during the electrically induced formation of a pore in cell membrane. This theory was published in a review of the current knowledge of EP in 2005. The steps are listed below (Teissie, 2005):

1. Induction Step: An external electric field is induced on the transmembrane potential up to the critical permeabilizing voltage, voltage that produces pores;

2. Expansion Step: Time-dependent membrane transition occurs once the electric field is maintained at an overcritical value;
3. Stabilization Step: Recovery of the cell membrane takes place as soon as the electric field is lower than the sub-critical value;
4. Resealing Step: First order resealing occurs that can be on the order of several seconds to many minutes; and
5. Memory Effect: Under the right parameters, the cell is still viable; however, the structural and physiological characteristics of the cell membrane take much longer to repair, often hours. After this period, the cell will return to its "normal" state.

2.3.1 Induction Step

Since studies have been utilizing electric fields to alter the behavior of microorganisms, it has been shown that a critical voltage exists where a pore will be induced in a cell's membrane when the critical voltage is applied. A cell membrane rupture, which is dependent on the lipid membrane and the pulse duration, occurred at a transmembrane voltage of approximately 200mV (Abidor, et al., 1979). This observation was first considered to be a "leakiness" occurring in the cell membrane after an electric pulse over the critical voltage was introduced. This phenomenon was first observed by Teissie and Tsong (1981) when using radiolabelled sucrose (Teissie and Tsong, 1981). Electrical conductance studies and light scattering experiments have been conducted to detect how quickly the induction step actually occurs. It was observed that membrane leakiness occurs less than a microsecond after an electric pulse is first induced. It was shown that cell diameter plays a significant role in the deformation time constant (Neumann and Kakorin, 1996; Asgharian and Schelly, 1999; Kakorin and Neumann,

1998). It was observed that cells with more curvature had better permeabilization. This led to the hypothesis that the curvature affected the packing between the membrane layers in small cells (Neumann and Kakorin, 1998). This theory was experimentally investigated and confirmed by controlling the packing between the membranes, which showed that permeabilization was reduced (Tonsing, et al., 1997).

EP will induce a critical transmembrane voltage that will result in a leaky cell, which is why this is referred to as the induction step. Additionally, the amount of permeabilization is directly related to the pulse strength and duration. It was observed that with a strong nanosecond pulse, a leaky state was reached, which proved that this step is swift with some contribution from electromechanical stress (Sukhoruko, et al., 1998; Muller, et al., 2001; Hibino, et al., 1991). However, it was discovered that an electrical pulse only affects certain sections of a cell membrane. This enables the cell membrane to stay mechanically sound, because a majority of the cell membrane is still intact. The field intensity is highest at the poles facing the electrodes, and a majority of the pores form around these poles.

When discussing the induction step, it is vital to understand that the electric field controls two major aspects. The first one is the onset of pore formation, caused by the critical voltage being surpassed and resulting in an imbalance in the membrane conductivity. Secondly, the intensity of the field will drastically affect the geometry of the cell and the size of the pore that is to be formed.

2.3.2 Expansion Step

Once a pore is formed, the next step is to understand what is happening to the cell membrane. Experiments using direct video imaging were conducted to better understand

the events occurring in the cell membrane after pore formation; specifically, what is happening to the membrane as pores form. Video imaging revealed that pores were formed in less than a microsecond, and the reorganization of the membrane was on a much larger time scale. It was also seen that increasing the pulse duration had no affect on the geometry of the pores being formed. Pore geometry is directly related to pulse intensity. The pulse duration directly manipulates the density of the membrane at the affected poles (Gabriel and Teissie, 1999).

2.3.3 Stabilization Step

This step predominates once the induced field's voltage drops below the transmembrane's critical voltage. When this occurs, the membrane conductance drops rapidly (Hibino, et al., 1993). Also, there is a decrease in the flow of molecules across the lipid bi-layer after the voltage is dropped below the critical voltage since as much as 75% of transport occurs during the induced pulse (Gabriel, 1995). Despite the voltage decrease, there is still flow. When the voltage drops below the critical level, the pores are still present. The pores do not increase in size; in fact, they are slowly decreasing in size, leading to the next step of electroporation.

2.3.4 Resealing Effect

Assuming that no permanent damage to the cell membrane has occurred, the cell membrane can reseal. Experiments found that the resealing process was highly dependent on the surrounding temperature (Rols and Teissie, 1990; Neumann, et al., 1998).

The resealing process that occurs in an experimental apparatus utilizing a BLM can differ greatly from the resealing process that occurs in a living cell. Experiments have shown that it may take a couple of seconds for pores to reseal in a BLM, whereas it may take several minutes to hours for a living cell to fully recover from an electric pulse. Two aspects that can affect the kinetics of pore resealing are the amount of drug delivery transported to the cell (e.g., DNA injection or induction of a drug for synthesis), and the physical treatment of cells (e.g., extreme temperature, pH, or external pressure changes) (Rols and Teissie, 1992). If a cell is kept at low nutrient conditions and low temperatures, it will take much longer to reseal any pore that has been formed. The cell requires energy to reseal the created pore; for the cell to efficiently complete this task, an abundance of nutrients is necessary. Experiments have been completed on the pore resealing time at 4^{o}C; at this temperature, the cell took several hours to fully recover due to the reduced kinetics at lower temperatures (Lopez, et al., 1988).

Many experiments have been completed to better explain the resealing process of electroporation. In the last decade, it has been postulated that pore resealing is a cellular process, rather than an alteration in the lipid matrix of the cell membrane (Teissie et al., 2005). Extensive studies have been completed to accurately estimate the time scale required to reseal a lipid membrane. Studies have shown that when dealing with a BLM, the resealing time is on the magnitude of microseconds, but when dealing with a cell membrane, the time varies from seconds to hours (Neumann et al., 1989).

2.3.5 Memory Effect

When a pore is formed due to EP, the characteristics of the lipid membrane surrounding the pore have likely been altered. This can cause the membrane to have a

"memory." Cell membrane memory refers to the cell membrane maintaining a pore, much smaller than the original pore, after the pulse has been discontinued. This is referred to as cell membrane memory, since subsequent EP events will result in pore formation at the same site as previous pore sites. Complete cell resealing prevents cell lyses (complete cell membrane failure resulting in death of the cell). However, the cell's membrane has been altered. Instances have been studied where the cell was not terminated during the induced field phase, but, due to lipid membrane reconfiguration, the cell perished minutes after the pulse was stopped. The cell membrane failure that occurred during these experiments was attributed to the cell membrane not resealing the pore created during EP (Gabriel and Teissie, 1995). However, this is not typical, and only affects a fraction of electroporated cells. Therefore, a majority of the electroporated cells remain viable after electroporation.

It has been shown that a BLM is still in a state of reorganization minutes after an electric pulse (Koronkiewicz, et al., 2002). This leads to the theory that a cell will have major lipid movement during an electric pulse and EP may have long-term effects on the structure of the cell membrane.

2.4 Pore-based Electroporation Model

As discussed previously, the foundation for a pore-based model is to associate a critical voltage with any pore that forms on a cell's membrane. Once an electric field is induced, select areas of the cell's membrane become charged. The flow created by the induced field will charge the extra- and intracellular electrolytes. As discussed earlier, the poles of a spherical cell will become charged first (small θ Eq (1)), causing pores to form early at the pole. Once the transmembrane voltage has reached 1V, the amount of

pores created increases drastically. This is the point where the transmembrane voltage begins to decrease. If the induced field is terminated, this will result in reversible EP, with the cell membrane remaining viable after the pore reseals (Weaver and Chizmadzhev, 2006). Once the electric field is terminated, the transmembrane voltage quickly drops to zero because the poles are extremely conductive at this point. A portion of metastable pores will remain during this phase, while smaller pores disappear. During an electric pulse, cell membrane pores are at a maximum. A majority of the molecular transport occurs at this point. This was predicted in transient aqueous pore models for artificial planar BLMs (Freeman, et al., 1994; Vasilkoski, et al., 2006; Barnett and Weaver, 1991, Puc 2003).

Initially, pores were modeled as defects in the cell membrane and only recently has it become possible to simulate this phenomenon using computer programs. These molecular dynamic simulations support the basic transient aqueous pore concepts (Tieleman, et al., 2003; Hu, et al., 2005).

The basis for the transient aqueous pore model is the entry of water and other aqueous electrolytes into a fluid BLM, which is favored as the electric field in the lipid region of the bilayer increases (Weaver and Chizmadzhev, 2006). The transient aqueous pore theory was discussed in a seven-paper series published in 1979 which began with, "Electric Breakdown of Bilayer Lipid Membranes: I. The main experimental facts and their Qualitative discussion" (Abidor et al., 1979; Pastushenko, 1979a; 1979b; 1979c; 1979d; Chizmadzhev, 1979; Arakelyan, 1979;).

The theoretical models illustrate the three common aspects that contribute to reversible electroporation:

1. Chemical composition of the membrane
2. Pulse protocol
3. Feedback at the pore level associated with the spreading resistance due to pore expansion

Weaver and Chizmadzhev (2006) state that experiments have been conducted to analyze the individual steps of EP, but there is still much that needs to be studied in more depth to fully understand the mechanism of electroporation.

2.5 Current State of the Science (2008-2013)

The current research effort started in 2006 and the state of the science has progressed since the first experiment was conducted. The ability to perform more complex computations has allowed the models used to predict EP to become more comprehensive (Kotnik, et al., 2013; Noguchi, 2008). In addition to the creation of more complex predictive models for electroporation, research has been completed to determine EP efficacy for extraction of intracellular substances from microorganisms and plants (Zhan, et al., 2010; Suga and Hatakeyama, 2009; Ohshima, et al., 2000).

Cell contents are currently extracted via alkaline lyses and mechanical disintegration coupled with chemical extraction. These methods destroy the entire cell and lead to costly purifications of the desired intracellular material. Through electroporation, for as long as 10 seconds, the cell membrane is lysed and the organelles are left intact, thus reducing the amount of purification necessary to obtain the preferred protein (Haberl, et al., 2013). Using EP to enhance the extraction of sugar from beets has been investigated with promising results (Loginova, et al., 2011). The effects of EP have

also been investigated on several energy crops: wood chips, switchgrass, and corn. To effectively electroporate cells on large scales, new apparatus had to be created and optimized to increase the efficiency of electroporation. Therefore, EP protocols have been adapted to allow larger scale experiments to be completed (Sack, et al., 2010). The necessity to increase the scale for sugar extraction from beets has allowed researchers to focus on this task. However, extraction of intracellular components requires cell lyses in most cases. Specifically, for intracellular extraction from plant material, the viability of the cell is not a concern because the plant has been harvested prior to electroporation.

EP advances in the medical field include the treatment of cancerous cells and tumors using a combination of electroporation and chemotherapy (Haberl, et al., 2013). Chemotherapeutics act on dividing cells and affect normal tissue as well as cancerous tissues. Chemotherapeutic drugs have poor membrane permeability, which requires the dosage to be high for tumor eradication. Pretreating tumors with EP increases the permeability of the cancerous cells, which allows the chemotherapy to be more efficient. This method for cancer treatment is referred to as electrochemotherapy (Jarm et al., 2010; Sersa, 2012). The future of electrochemotherapy is promising for melanoma nodules and chest wall breast cancer (Sersa, et al., 2012).

Many studies over the last 40 years have aimed at postulating a prediction mechanism when varying electric fields are applied to a BLM or cellular membrane. Much progress has been made, and understanding has increased to coincide with an improvement in the techniques used to monitor the cell membrane on a molecular level. Also, the computational aspect of modeling has improved to allow more complex mathematical analysis to be completed on the cell membrane. However, the results from

computational simulations remain inadequate if they are not verified with experimental data. While our knowledge of EP has greatly increased over the last 40 years, many data gaps still exist, including the following:

1. Molecular transport
2. Mechanism of membrane recovery
3. Cellular stress
4. Multiple pulse stress increases

Advances are being made every day to alleviate the unknowns in these fields, but more work is needed to fully understand the EP phenomenon. While modeling the effect of EP on oleaginous microorganisms is beyond the scope of this study, the possibility of lipid extraction utilizing EP is under investigation.

CHAPTER III

OBJECTIVES

The purpose of this study was to investigate the effect of electroporation on oleaginous microorganisms and soybeans. Oleaginous microorganisms are increasing in popularity as a source to generate alternative fuel due to their ability to accumulate excess lipids under specific conditions (Li 2008). Alternative fuel production using oleaginous microorganisms has increased in popularity recently for the following reasons:

1) Crude oil costs are increasing
2) Amount of crude oil extractable from the current sources is finite
3) Microorganisms are able to convert sugars into triglycerides for energy storage (Yoon 1983 and Wynn 2005)
4) Global food market is affected by producing alternative energy using vegetable oil (Smith and Huyser, 1987)
5) Oil production of plants is directly correlated to the growing conditions of the oleaginous plant (Dornbos and Mullen, 1992) and the growth environment of oleaginous microorganisms is easily manipulated (i.e. temperature, available nutrients, and proportions of nutrients).

Once the oleaginous microorganisms have accumulated oil, the current method of extracting the triglycerides uses chemical solvents to destroy the microbes (Wynn and Ratledge, 2005). This study investigated electroporation (EP), a nonlethal method to

extract accumulated oil from the microorganism's interior. EP involves placing a voltage across a cell membrane to induce pores, which allows a cell to remain intact if the appropriate parameters are applied. EP is typically utilized to inject DNA into cells (Weaver and Chizmadzhev, 1996). EP creates pores in a cell's lipid bilayer and these pathways have the possibility of allowing intracellular material to be released. The experiments used in this investigation attempted to extract lipids and triglycerides from oleaginous microorganisms. To date, the utilization of EP to extract triglycerides has not been documented in published literature.

Little research has been completed on the use of EP as an extraction method. The purpose of this study is to test EP as a lipid extraction method on oleaginous media, soybeans, *Rhodotorula glutinis,* and *Rhodococcus opacus*. Four parameters were varied during each experimental matrix to investigate and optimize, if possible, the effect of EP on lipid extraction. Four parameters (voltage, electrode spacing, pulse duration, and number of pulses) were investigated using the Box-Behnken experimental design.

The goal of this research is to determine the potential of EP for intracellular lipid extraction of soybeans, *R. opacus*, and *R. glutinis*. If EP is a viable method for lipid extraction, then the process will be optimized for the investigated soybeans and oleaginous microorganisms.

CHAPTER IV

METHODS AND MATERIALS

4.1 Overview

This study investigates EP as a viable method of lipid removal and then explores the parameters necessary for lipid extraction of bacteria, soybeans, and yeast. The tests were performed on a small scale and then implemented on a larger scale, examining larger electroporated volumes. Oleaginous, oil-producing microorganisms were grown and research was completed to determine the most applicable growth media. After the correct growth medium was identified, attempts were made to extract the lipids contained within the bacteria, soybeans, and yeast. Determining the feasibility of EP as an extraction technique is the first phase of this study. Phase two is to determine the optimal parameters, if electroporation successfully extracts intracellular lipids. Phase two may also involve establishing parameters for future studies. If phase one is successful and EP is a feasible extraction method for oleaginous media, then phase two is to determine the parameters that affect lipid removal and optimize settings for lipid extraction. The steps involved in this experiment are: inoculation, incubation, centrifugation, EP, and analyzation. The sections that follow will discuss the steps required for yeast, *Rhodotorula glutinis* (*R. glutinis*) EP, and bacteria, *Rhodococcus opacus (R. opacus)*, EP. While this chapter emphasizes yeast EP, bacteria EP followed the same protocol. The soybean EP method is also discussed in this chapter.

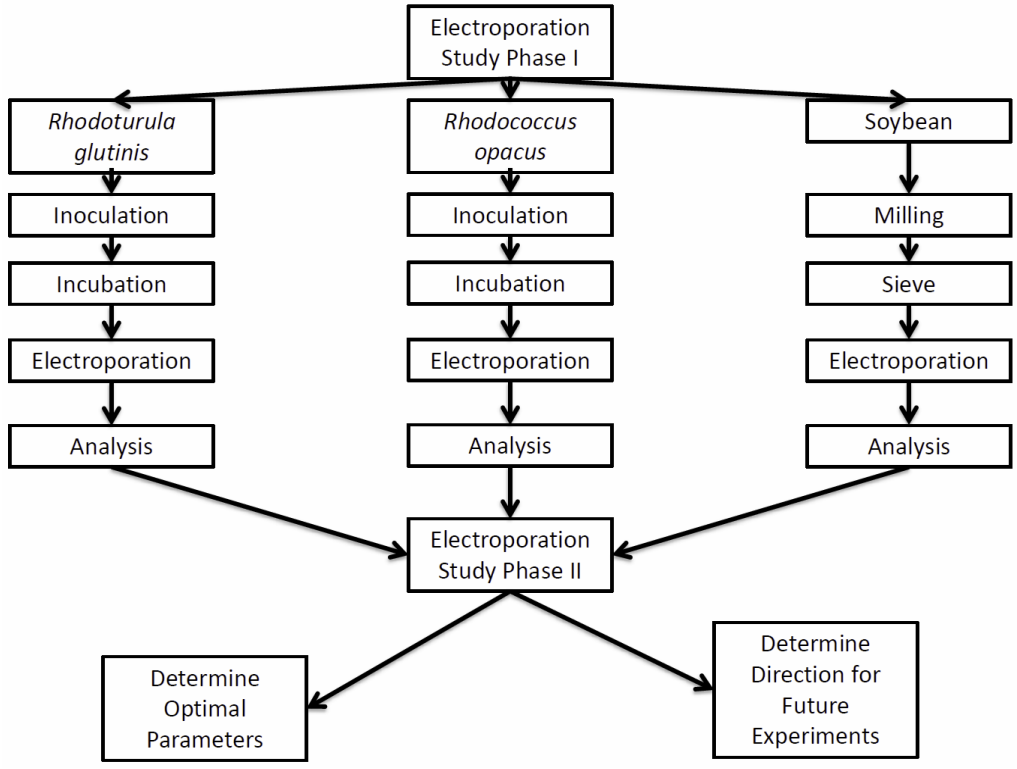

Figure 4.1 Flow chart of electroporation experimental process

This study utilized a Harvard Apparatus BTX 830 electroporator. Each experiment contained control samples and treated samples. The treated samples were exposed to EP and the untreated samples were not exposed to EP. The untreated cells' lipid content is assumed to be the baseline for initial lipid content of the entire colony of cells. It was crucial that each test include a control because the lipid concentrations of the microorganisms were not equal between batches.

The lipid content of each sample is tested using a process known as the modified Bligh and Dyer, a derivative of the Bligh and Dyer method (Bligh and Dyer 1959). During this process, the solvents chloroform and methanol were used to extract the lipids contained by each organism. Each set of experiments had a negative control comprised

of samples that had not been electroporated. The control samples were used as a baseline to compare the treated samples. A control is utilized for every experiment since each growth culture is unique and microbe lipid content varies between growth cultures. Once a sample was processed, the average lipid content of the control was compared to the average lipid percentage of the treated cells. This comparison was then analyzed statistically to test for any significant differences. The Statistical Analysis Software (SAS) v9.2, SASv9.2 was used to test the effect of the independent variables on the dependent variable. If a test showed a significant variance for a particular parameter, this information was used in further experiments. The statistical analysis was used to determine the optimal parameters for successful electroporation. Another benefit of statistical analysis is determining which parameters of EP have the most effect on lipid extraction and which parameters would be of interest in future studies.

4.2 Method Required to Electroporate Oleaginous Microorganisms and Soybeans

Experiments conducted by S.H. Yoon and J.S. Rhee in 1983 on *R. glutinis* produced high lipid mass/cell dry mass (CDM). Also, *R. glutinis* has been proven to generate large cell mass per liter values while maintaining high lipid yields (Yoon and Rhee, 1983). Several growth media were tested and they successfully generated lipid yields as high as 56% lipid mass/CDM while maintaining cell mass values of 10 grams/liter (g/L) of growth media. The Microbiology Laboratory at Mississippi State University had a proven method to produce yeast with high cell mass and lipid content.

4.2.1 Inoculation

Inoculation is the three-step process used to transfer a pure strain of *R. glutinis* or *R. opacus* from a frozen pure culture to growth media. The three steps are: (1) pure culture transfer, (2) cell cultivation in Yeast Mold (YM) media, supplied by Fischer Scientific, and (3) transfer of yeast to a lipid accumulation media. Before explaining the three steps, it is vital to understand the process of maintaining a sterile environment while transferring cells to new media. Each step that requires a sterile environment is completed within 1-2 inches of a flame provided by a Bunsen burner. As seen in Figure 4.2A, when a tube, flask, or vial is to be sterilized with a flame, the tube is held at a 45º angle to the bench top with the lid of the container loosened.

(A)

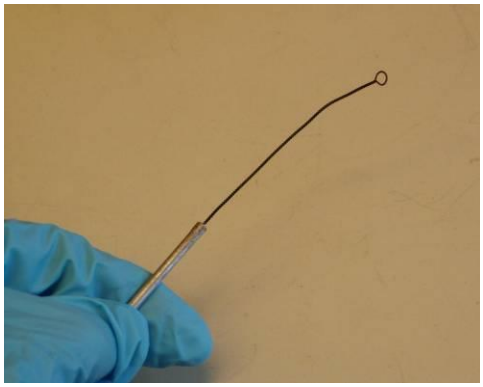

(B)

Figure 4.2 A) Keeping the media in a sterile environment during cell transfer, B) Inoculation loop

The container is kept close to the flame, within the area adjacent to the flame that is referred to as the "dead zone" (i.e., an area located approximately 2 inches around the flame of the Bunsen burner). Since few microorganisms present in the lab are able to

survive in the temperatures near the Bunsen burner's flame, the lid is removed and the top of the container is passed through the flame three times. The inoculating loop, seen in Figure 4.2B, or pipette tip that is used for the transfer of cells must also be sterilized by passing it through the flame. Therefore, an inoculating loop must be heated, by flame, to the point at which the metal is glowing hot. However, both the loop and pipette must be cooled afterwards to ensure the bacteria or yeast is not killed during transfer. During the cooling stage, it is vital that the loop or pipette remain in the dead zone. Following these procedures will decrease the possibility of contaminants propagating in the nutrient-rich growth media.

The three steps necessary to transfer and grow oleaginous microorganisms are discussed below.

1. To maintain a pure yeast strain, the yeast is stored in a Revco -80^{o}C freezer (Thermo Scientific, Asheville, North Carolina). Maintaining the cells at this temperature allows the organisms to remain dormant. Freezing the cells in a medium allows the strain to remain pure by slowing the growth of mutations. A sterilized inoculating loop is used to scrape the surface of the frozen sample of bacteria or yeast. The loop with the thawed cells in the center is kept sterile, and then placed in a tube containing yeast mold (YM) agar (Fischer Scientific, Pittsburgh, Pennsylvania). The YM agar is prepared with deionized water. Allowing the loop to contact the YM agar successfully transfers the microorganisms. A cap is placed loosely on the test tube containing the agar and yeast, to reduce contaminants while allowing minimal air flow. The test tube is then placed in a 30^{o}C incubator (New Brunswick Scientific;

Edison, New Jersey) at 130 rpm for 2 days. As seen on the left side of Figure 4.3, the inoculated agar tubes are allowed to cultivate in a constant-temperature environment.

Figure 4.3 Agar and growth media in a New Brunswick Scientific constant motion incubator

The yeast colonies formed on the agar, Figure 4.4, will be used to inoculate a liquid YM broth. Figure 4.4 illustrates the individual yeast colonies on the surface of the YM agar.

Figure 4.4 Cell colonies on surface of YM agar after 2 days of incubation

2. Cell cultivation in YM broth is performed by transferring the cells from the surface of the YM agar to a sterile bottle of autoclaved YM broth (Fisher Scientific, Pittsburgh, Pennsylvania) for 2 days. Media were sterilized via Amsco Steris steam sterilizer (Westbury, New York) at 121°C and 15 atmosphere for 15 minutes. While working in a sterile environment, the inoculating loop is raked across the surface of the agar to collect colonies of cells. The loop is placed in the YM broth and the cells are released by shaking the loop. Once the culture is released from the loop to the broth, the loop is removed and the cap is replaced. Next, the YM broth is swirled to homogenize the solution. The YM broth is incubated for 20 hours in a 30°C 130 RPM constant motion incubator, similar to that pictured in Figure 4.3.

3. After the cells have incubated in the YM broth for 20 hours, the sterilized lipid accumulation media is inoculated with 5% volume/volume, v/v, of yeast-rich YM broth. The lipid accumulation media has low nitrogen content, which promotes lipid accumulation (Yoon and Rhee, 1983). The media has an excess of sugar equal to or greater than 60 grams/liter. This sugar amount is triple the usual amount required to sustain microorganism colonies. The microorganisms will continue to consume the excess sugar and store lipids after the nitrogen source is depleted. This allows the cells to accumulate lipids (Yoon and Rhee, 1983 and Alvarez et al., 1996).

Figure 4.5 Lipid accumulation media (left), YM media after 20 hours (right)

4.2.2 Incubation

Inoculated bottles, containing cells and media, are placed in a constant motion (30 RPM), constant temperature (25ºC), New Brunswick Scientific Model I26 incubator (Edison, New Jersey), Figure 4.6. Once a bottle has been placed in the incubator, the cells are allowed to incubate for 5-7 days, depending on the desired lipid content.

Figure 4.6 Inoculated bottles in constant motion incubator

After 1 day, an increase was observed in the opacity of the growth media. This observation is verified by a Genesys 20 Spectrophotomter (Thermo Scientific, Brookfield, Wisconsin) optical density (OD) reader. Optical density is measured every 24 hours during the incubation step. To take an OD reading the device is calibrated with 18-Mohm water in a plastic cuvette that has been cleaned with a lint-free cloth. Next 1.5 mL of the cell rich growth media is removed under sterile conditions, placed in a separate

cuvette, wiped with a lint-free cloth, and positioned in the OD reader, where the measurement is recorded. The OD reading allows for the stationary phase to be determined. This is the stage when cell reproduction has decreased and lipid accumulation is maximized. This information is vital, since cells accumulate lipids in the stationary phase. Cells begin storing energy and lipids in this phase, and experience a drastic reduction in cell reproduction (Alvarez et al., 1996). Figure 4.7 illustrates the amount of time required for the microorganisms to reach the stationary phase.

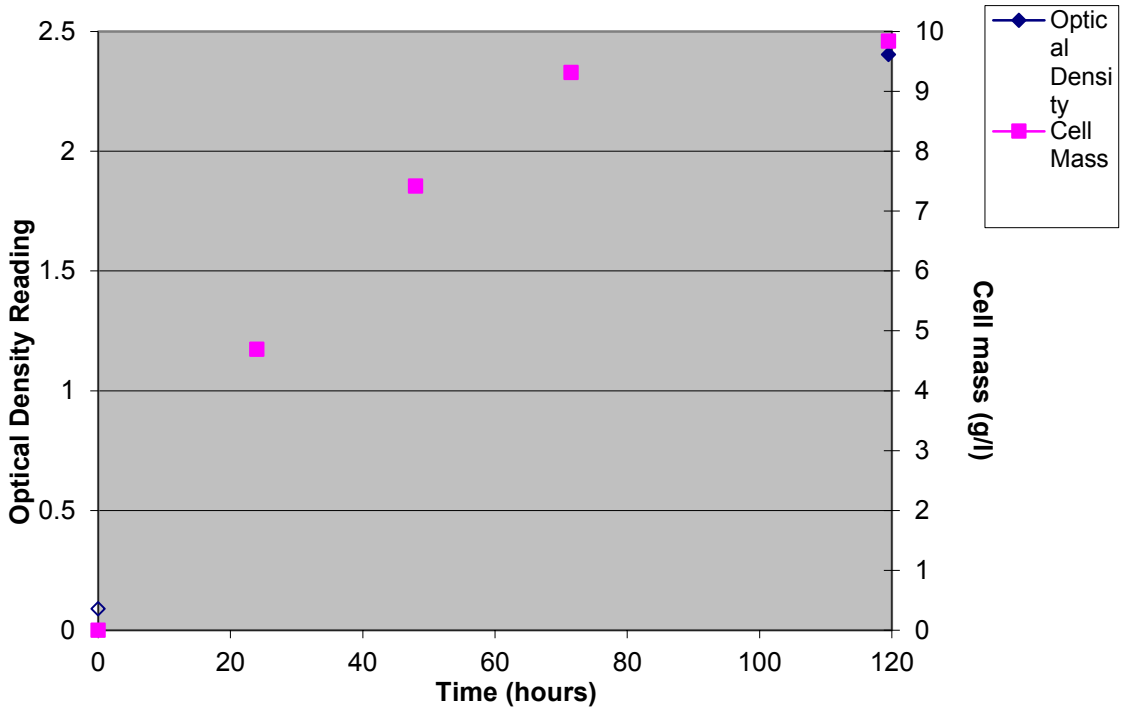

Figure 4.7 Comparison chart of OD reading versus cell mass for 5-day growth cycle of *R. glutinis*

4.2.3 Electroporation

EP is performed using an ECM 830 manufactured by Harvard Apparatus. The ECM 830 has a voltage range of 5-3000 volts and a pulse duration range of 10 μs–10 s. Features of this instrument include multiple pulses and memory storage for multiple experimental parameters. The cuvette used during the EP step consists of a Teflon™ block that is 6 inches long and 1.5 inches wide. Teflon™ is used because it is resistant to hexane, chloroform, and acetone which are used between EP experiments to clean the cuvette. This machined block is designed to hold two stainless steel electrodes with a valley between the electrodes and a depth half the width of the electrodes, as seen in Figure 4.8.

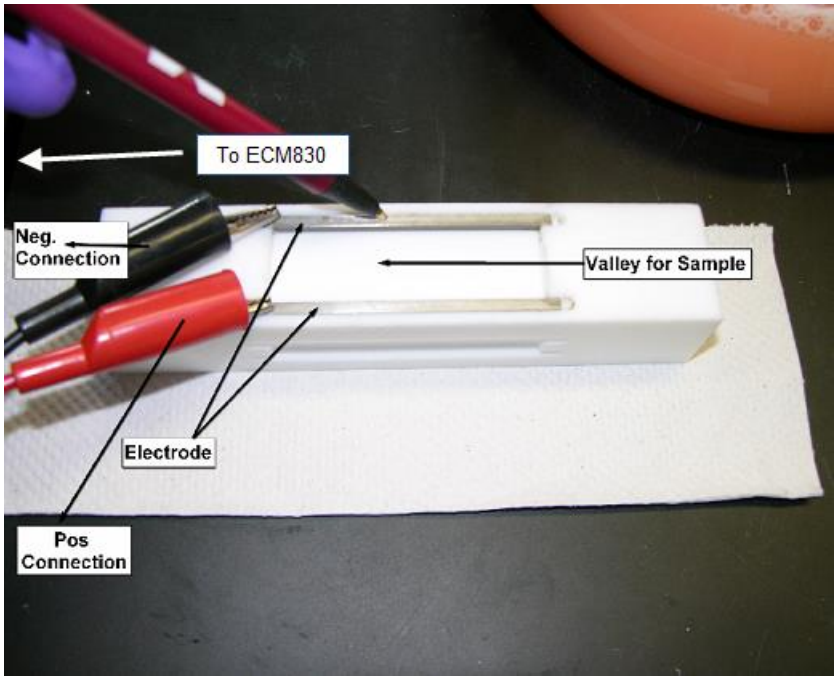

Figure 4.8 Teflon™ cuvette for EP experiment

The machined Teflon™ cuvette allows electrode spacing to be varied at distances of 5 mm, 10 mm, 15 mm, and 20 mm with volumes of 1 ml, 2 ml, 3 ml, and 4 ml, respectively. Each side of the cuvette is machined to accommodate one electrode spacing, as seen in Figure 4.8. This enables the system to be analyzed using a variety of electrode spacings and sample volumes. Between each experiment, the cuvette is cleaned with acetone, chloroform, and hexane, and then dried. After cleaning, the cuvette is ready for the volume of cells and media mixture to be placed in the valley between the electrodes. At this point an experimental run can begin. Preliminary investigations concluded that a minimum dry cell mass (DCM) of 0.15 gram is needed for the modified Bligh and Dyer protocol. This requires the cuvette to be filled and emptied multiple times until a media volume of 16-20 ml has been electroporated for a single experiment. This volume is necessary since the growth media has a concentration of approximately 10 grams/liter. Each experiment requires the cuvette to be filled multiple times; therefore, each cell placement is subjected to identical parameters. After the valley is filled with the sample, a plastic safety cover is placed over the experiment (see Figure 4.9).

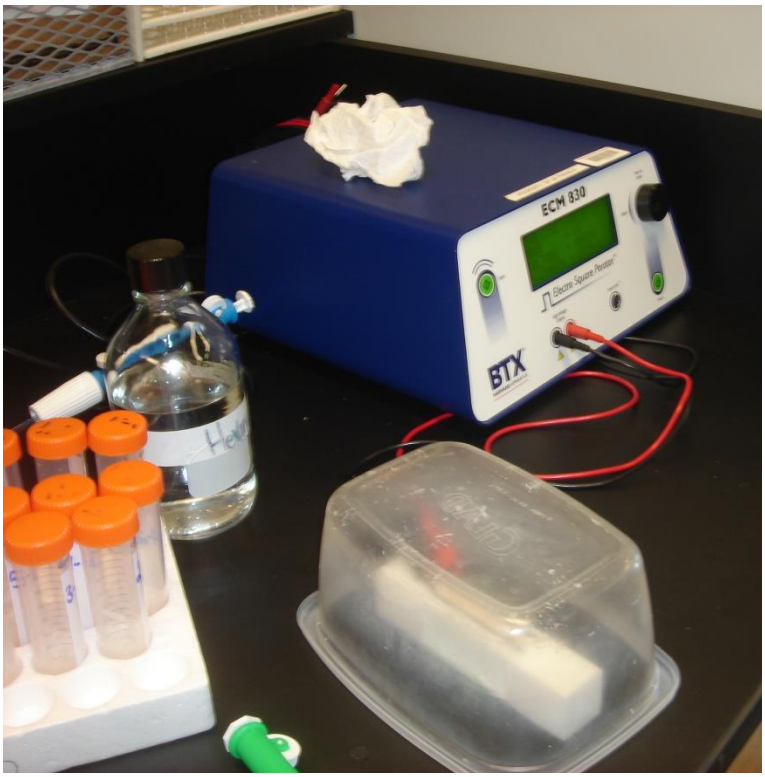

Figure 4.9 Experimental setup for electroporation using Teflon™ cuvette

The leads from the cuvette to the ECM 830 are connected. Then the appropriate parameters are programmed to the ECM 830 and the run is initiated using the Start button. This will initiate the EP process with the ECM 830 inducing the programmed parameters.

Figure 4.10 Transferring oil-rich media to Teflon™ cuvette for electroporation experiment

Once the treatment has been completed, the induced pulse duration and voltage are recorded. The cell media is then removed from the valley using a pipette and placed in a clean plastic centrifuge tube. Figure 4.11 illustrates the process of pipetting the electroporated cells from the cuvette.

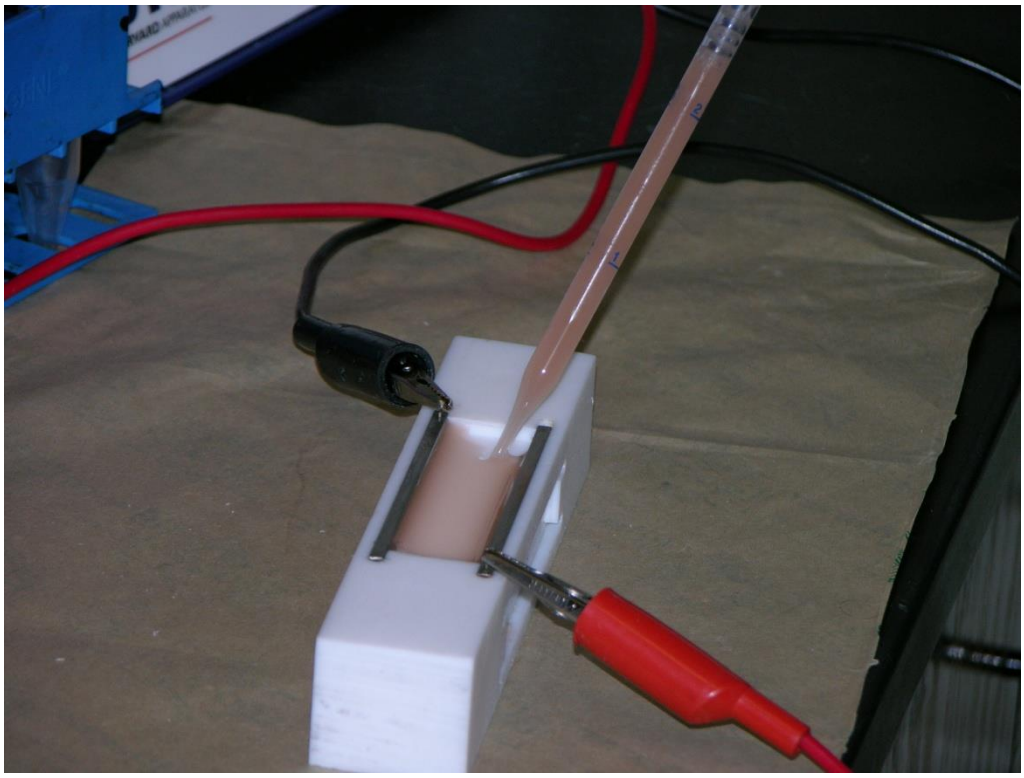

Figure 4.11 Removing electroporated cells from Teflon™ cuvette

This process is continued until approximately 16 ml of culture has been electroporated. After the treated cells are removed, the cuvette valley is filled with hexane to extract any residual material that may have adhered to the walls of the cuvette. The hexane is removed to a glass storage tube using a pipette; the hexane wash is set aside for analysis. The cuvette is then rinsed with acetone, allowed to dry, and prepared for the next experiment.

4.2.4 Analysis

After treatment, three sets of tubes are produced, (a) the first set contains the electroporated cell mixture, (b) the second set contains non-electroporated (control) cells, and (c) the third set contains the hexane wash from the cuvette. The tubes containing the electroporated cells are centrifuged using a Sorvall ST40 (Thermo Scientific, Asheville, North Carolina) for 15 minutes at 1500 rpm and the cell-free media is pipetted from the top and added to the hexane wash. The remaining cell pellet is pictured in Figure 4.12.

Figure 4.12 Concentrated cell puck after centrifugation

The tube containing the hexane wash and the supernatant (liquid above the concentrated cell mass) is then hand shaken for 30 seconds to homogenize the solution. After mixing, the hexane and supernatant are again centrifuged using a Sorvall ST40 (Thermo Scientific, Asheville, North Carolina) for five minutes at 3000 rpm to separate the layers. The hexane layer is removed using a Pasteur pipette and placed in a 20-ml glass storage tube with a Teflon-coated cap and stored at 5°C for further analysis. The plastic tubes containing the electroporated cells (cell puck in Figure 4.12) are placed in a freezer for 2 hours and then freeze-dried for 24 hours. The freeze drier (Labconco Freezone 2.5; Labconco, Kansas City, Missouri) operates at –50°C and 0.133 millibar and removes all liquid from the sample, thus allowing an accurate DCM to be determined.

The freeze dryer has large glass sample holders, which are attached to the apparatus by ports on the exterior of the freeze dryer, as seen in Figure 4.13.

(A) (B)

Figure 4.13 A) Freeze drier with samples attached, B) Cell masses will change from a dark pink to light pink when freeze drying is complete

The DCM is measured on a Mettler Toledo AB265-S/FACT (Columbus, Ohio) scale that is accurate to five decimal places. The recorded DCM is used later to determine the percentage of the cell mass that is lipids using Equation 3.1.

$$Lipid\ Percentage = \frac{Mass\ of\ Amber\ Vial_{Final} - Mass\ of\ Amber\ Vial_{Intial}}{DCM} * 100 \qquad \text{Eq. 3.1}$$

The dried cells are then subjected to a chemical extraction via a modified Bligh and Dyer technique, explained in the next section. This process uses a mixture of an organic solvent, chloroform, and an organic alcohol, methanol. The lipids are extracted to the

chloroform and the remainder of the cell mass remains in the methanol phase. The chloroform layer is transferred to a tared amber vial.

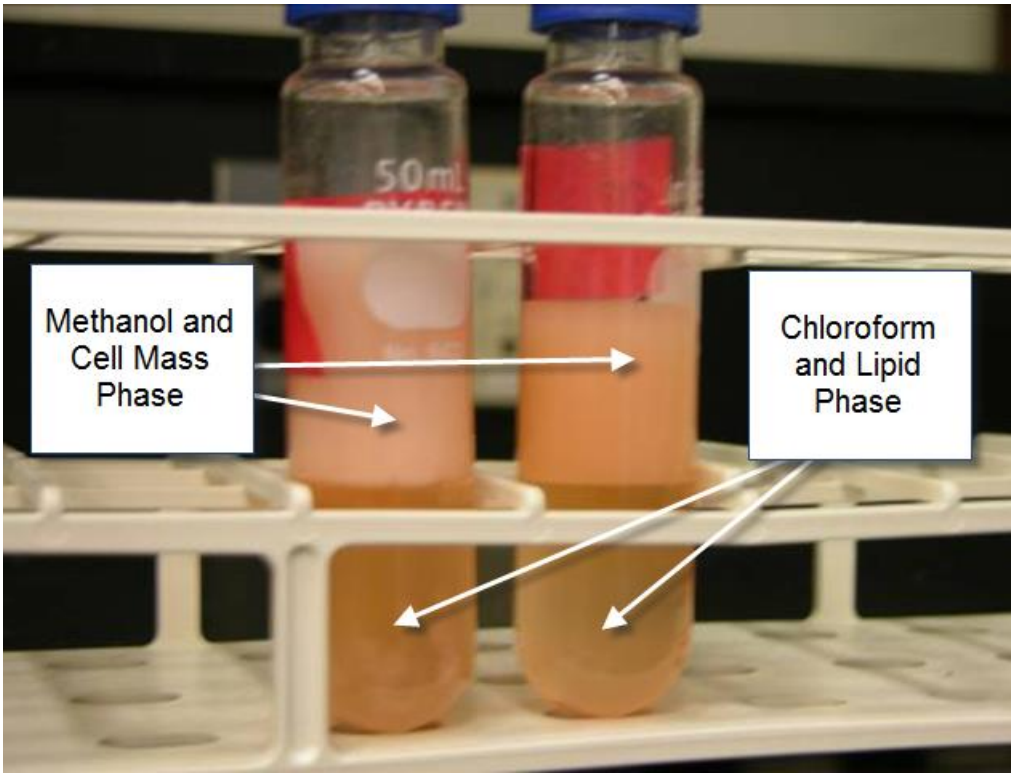

Figure 4.14 The top layer is cell mass and methanol: the bottom layer is chloroform and lipids

The following steps occurred during the modified Bligh and Dyer procedure:

1. Suspend freeze-dried pellet in 5 mL of deionized water by vortex (Innova 2000; New Brunswick Scientific; Edison, New Jersey).
2. Add 12.5 mL of methanol and 6.25 mL of chloroform and shake for 10 minutes.
3. Add additional 6.25 mL of chloroform and 12.5 mL of deionized water with 0.5% NaCl (the NaCl enhances separation), and shake for 15 minutes.
4. Centrifuge (Sorvall ST 40; Thermo Scientific, Asheville, North Carolina) for 20 minutes at 1800 rpm.
5. Extract bottom layer, lipid dissolved in chloroform, using a Pasteur pipette and filter through fiberglass wool into a previously weighed amber vial.

After completing the chemical extraction, lipid content is determined gravimetrically (after chloroform is evaporated). Chloroform separation is accomplished by evaporating the chloroform with a turbovap (Caliper TurboVap LV; Caliper Life Sciences, Hopkinton, Massachusetts). The TurboVap LV uses a heated water bath, 30°C, and a steady flow of nitrogen thus minimizing the time needed to evaporate the chloroform. Figure 4.15 illustrates the turbovap with amber vials.

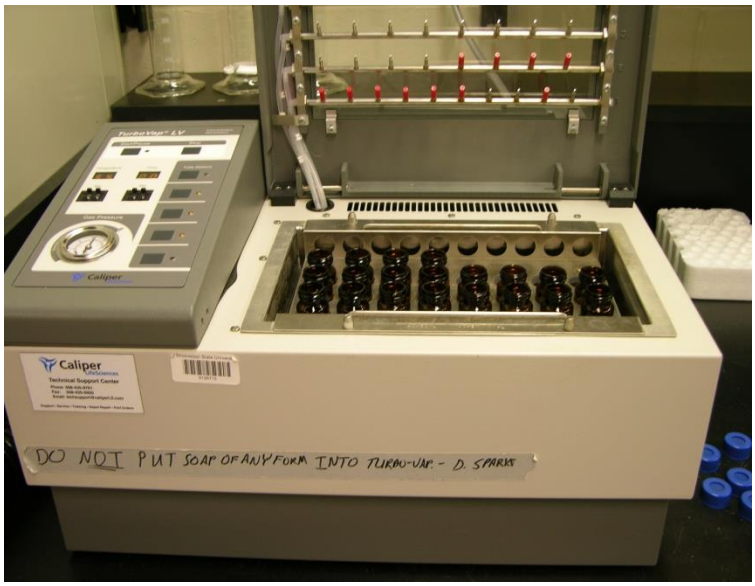

Figure 4.15 TurboVap loaded with amber vials to evaporate chloroform

The difference between the initial mass and the final mass is assumed to be the total lipids extracted through the modified Bligh and Dyer process.

4.2.5 Supernatant Analysis

Analysis of the post-EP cuvette hexane wash and cell supernatant is the next step. 10 ml of hexane and 0.5 grams of sodium chloride are added to the hexane wash. The sodium chloride aids in the removal of water from the hexane phase and the added hexane will reduce the likelihood that water is pipetted while removing the hexane phase.

After the sodium chloride and additional hexane have been added, the solution is placed on a vortex to mix all of the solution uniformly and get all possible lipids in the hexane phase. The hexane is removed using a Pasteur pipette, transferred to a tared 15-ml centrifuge tube, and evaporated off using the turbovap. The final weight of the centrifuge tube is recorded. Extreme caution must be taken when pipetting the hexane wash, so as not to pipette any supernatant. The supernatant is a water phase, which will not evaporate in the turbovap. This will give a false lipid mass during the gravimetric analysis. The difference in mass recorded for this phase is assumed to be lipids released from the electroporated cells. A significant amount of error is associated with this method because of the reliance on the gravimetric scale.

A modified version of ASTM 6584, Standard Test Method for Determination of Total Monoglyceride, Total Diglyceride, Total Triglyceride, and Free and Total Glycerin in B-100 Biodiesel Methyl Esters by Gas Chromatography, was implemented to prepare the samples for a more precise quantitative analysis of the mono's, di's, and triglycerides in the supernatant. A fellow Mississippi State University graduate student, Jericus Whitlock, prepared and conducted these tests on an Agilent 6890N gas chromatogram with a flame-ionization detector (GC-FID; Agilent Technologies Inc., Wilmington, Delaware). This analysis did not detect a measurable amount of lipids in the supernatant of the electroporated cells in any experiment.

4.2.6 Soybean Electroporation

Three steps are utilized to electroporate soybean hulls. The steps are bean machining, EP, and analysis. The soybeans were machined with the use of a crusher. Mechanical crushing involved the use of a hammer to remove the seed exterior followed

by mortar and pestle to grind the seeds' soft interior. The crusher removed the soybeans from their hard exterior seed coat and allowed the cotyledon to be exposed, thus allowing the oil contained in the cell to be extracted more readily. After crushing, the soybeans were sieved through an 841-micron (mesh No. 20) sieve to ensure uniformity for testing purposes. Once crushing and sieving were completed, the soybeans were electroporated using a buffer solution of 1X phosphate-buffered saline (PBS).To prepare 1 liter of 1X PBS, 8 grams (g) NaCl, 0.2 g KCl, 1.44 g Na_2HPO_4, and 0.24 g KH_2PO_4 were dissolved in 800 mL of water. The pH was adjusted to 7.4 with HCl and water was added until 1 liter of solution was obtained. Prior to electroporation, a negative control was tested by placing the crushed soybeans in the 1X PBS solution, placing this mixture in the cuvette, and removing this mixture. The negative control's purpose was to simulate EP without an induced voltage. The purpose of the negative control was to test the effect of the buffer solution on the soybean lipid content. Lipids that remained in the soybeans were then tested using the modified Bligh and Dyer procedure. The amount of lipids remaining in the soybeans after EP was then compared to the amount of lipids contained in untreated soybeans.

4.3 Experimental Matrix

The Box-Behnken three-variable experimental design was implemented in this study instead of a three-level full factorial experimental matrix. The Box-Behnken experimental design was chosen since this study's original objective was to optimize the parameters necessary to extract lipids from oleaginous microorganisms. Box-Behnken experimental matrices manipulate the independent variables by assigning a maximum, +1, median, 0, and a minimum, -1, to each independent variable. This allows a

determination of which independent variable has a significant effect on the dependent variable. A three-level Box-Behnken design employs three center point replication experiments. Center point replications allow an experimenter to determine if the mean of the extremes for the independent variables in the experimental matrix are statistically significant from the mean of the median parameters. Box-Behnken experimental matrices are used to optimize parameters to produce desired yields (Box, 1960). Table 4.1 illustrates the format for a typical three-variable matrix design. Each three-variable experimental matrix includes 15 experiments with coded values: -1, 0, and 1.

Table 4.1 Experimental design for a Box-Behnken three-variable matrix

Test #	X1	X2	X3
1	-1	-1	0
2	+1	-1	0
3	-1	+1	0
4	+1	+1	0
5	-1	0	-1
6	+1	0	-1
7	-1	0	+1
8	+1	0	+1
9	0	-1	-1
10	0	+1	-1
11	0	-1	+1
12	0	+1	+1
13	0	0	0
14	0	0	0
15	0	0	0

The order of the coded experiments is listed in Table 4.1. In Table 4.1, the negative signs represent the minimum value, the positive signs represent the maximum value, and the 0 represents the median value for each independent variable. The experimental matrix design developed by Box-Behnken has the ability to optimize

multiple independent variables. Three independent variables were used during each experiment (voltage, pulse duration, electrode spacing or voltage, pulse duration, number of pulse) and the dependent variable (percent lipids extracted) was the same for each experimental design. Table 4.2 is an example of the Box-Behnken three-variable matrix used for Matrix 1 experiments. For the example in Table 4.2, the voltage (V) values are 10 V, 250 V, and 490 V, which correspond to the coded values -1, 0, and 1, respectively. Each independent variable is assigned a minimum, median, and maximum value, which are equally spaced. For the voltage example, there are 240 volts between the values to be tested. The parameters for each experimental matrix are listed in Tables 4.2-4.5. Matrices 1 and 2 tested voltage, pulse duration, and electrode spacing and matrices 3 and 4 tested voltage, pulse duration, and multiple pulses. The parameters for each matrix were chosen based on the limitations of the electroporator, ECM830. Voltage and pulse duration have the greatest impact on pore formation (Weaver and Chizmadzhev, 1996); therefore, electrode spacing was replaced with multiple pulses to maintain voltage and pulse duration.

Table 4.2 Experimental design for a Box-Behnken three-variable matrix with parameters for Matrix 1

Test #	Voltage (V)	Pulse Duration (μs)	Electrode Spacing (mm)
1	10	10	10
2	490	10	10
3	10	990	10
4	490	990	10
5	10	500	5
6	490	500	5
7	10	500	15
8	490	500	15
9	490	10	5
10	250	990	5
11	250	10	15
12	250	990	15
13	250	500	10
14	250	500	10
15	250	500	10

Table 4.3 Experimental design for a Box-Behnken three-variable matrix with parameters for Matrix 2

Test #	Voltage (V)	Pulse Duration (μs)	Electrode Spacing (mm)
1	1000	10	15
2	3000	10	15
3	1000	90	15
4	3000	90	15
5	1000	50	10
6	3000	50	10
7	1000	50	20
8	3000	50	20
9	3000	10	10
10	2000	90	10
11	2000	10	20
12	2000	90	20
13	2000	50	15
14	2000	50	15
15	2000	50	15

Table 4.4 Experimental design for a Box-Behnken three-variable matrix with parameters for Matrix 3

Test #	Voltage (V)	Pulse Duration (μs)	Number of Pulses
1	10	10	59
2	500	10	59
3	10	1000	59
4	500	1000	59
5	10	505	19
6	500	505	19
7	10	505	99
8	500	505	99
9	500	10	19
10	260	1000	19
11	260	10	99
12	260	1000	99
13	260	505	59
14	260	505	59
15	260	505	59

Table 4.5 Experimental design for a Box-Behnken three-variable matrix with parameters for Matrix 4

Test #	Voltage (V)	Pulse Duration (μs)	Number of Pulses
1	10	20	59
2	490	20	59
3	10	100	59
4	490	100	59
5	10	60	19
6	490	60	19
7	10	60	99
8	490	60	99
9	490	20	19
10	250	100	19
11	250	20	99
12	250	100	99
13	250	60	59
14	250	60	59
15	250	60	59

CHAPTER V

DATA ANALYSIS

The analysis documented herein focuses on investigating the effect of EP on three different oil-rich media: bacteria (*Rhodococcus opacus)*, soybeans, and yeast (*Rhodotorula glutinis*). The Box-Behnken three-variable, three-level design was followed in developing an experimental design for this study. This design consists of 15 individual experiments in which the three independent variables are set at three different levels (Box and Behnken, 1960). For matrices 1 and 2, the three independent variables were voltage, pulse duration, and electrode spacing. The variables manipulated for matrices 3 and 4 were voltage, pulse duration, and number of pulses. Each experiment was repeated three times to ensure that every data point was characteristic to the parameter settings under investigation, and statistical analysis was performed to determine significant differences between the lipid content means. The results were compared based on percentage of lipids extracted from each cell. The following equation was used for all lipid comparisons:

$$\left(\frac{Lipid\ Mass_{Remaining\ intracellular}}{\text{DCM}}\right) * 100 = \%\ LipidExtracted_{Chemically} \qquad \text{(Eq. 5.1)}$$

The amount of lipids removed from the control cells (non-electroporated) for each matrix varied. Therefore, individual matrix data was compared to the control cells from that particular matrix (i.e. each experimental matrix had a unique set of control data points). To compare electroporated (treated) cells and non-electroporated (control) cells, it was assumed that the average amount of lipids removed from the control cells is equal to the initial amount of lipid present in each cell. With this assumption, a decrease in total lipids extracted chemically should be seen in the electroporated cells. The hypothesis of this experiment was that electroporation would remove intracellular lipids which would be evident by lower percentages of intracellular lipids in the treated cells.

The lipids extracted chemically are the amount of lipids remaining intracellular. The hypothesis of these experiments is the amount of intracellular lipids of electroporated cells will be lower than the intracellular lipids in the controls. All lipid percentages reported are the amount of lipids extracted chemically on a dry mass basis. Therefore, if the hypothesis is correct then the percentage of intracellular lipids of electroporated cells should be less than the percentages of the control cells.

The Box-Behnken experimental design was utilized to optimize this response. Also, to ensure that all trends were correctly identified, the experimental matrix was randomized, each experiment was assigned a number, and a random number generator (Microsoft Excel) was used to determine the order in which experiments were performed. The order of the variables in a Box-Behnken design are set to give a characteristic image of the effect of the independent variables on the dependent variable. When the output is analyzed, a saddle point, a maximum point, or a minimum point is used to infer the theoretical optimal parameters.

The results of the completed experiments have been divided into three sections: bacteria, soybeans, and yeast. Once this research was in progress, yeast became the main focus; consequently, the yeast section is the major focus of this data analysis discussion.

The results were analyzed as the difference between the control and the treated sample. Statistical Analysis Software, SAS, v9.2 was utilized for its Canonical Analysis, Ridge Analysis, and its capacity to create three-dimensional and contour graphs. SAS v9.2 was used for data analysis of every matrix and made accessible to Mississippi State University students through the University's Information Technology Services (ITS) Department.

5.1 *Rhodococcus opacus* (Bacteria)

Alvarez et al. (1996) achieved 78% lipid mass/CDM using *R. opacus* incubated in a mineral salt medium (MSM). In an attempt to replicate the Alvarez results, direct correspondence with Alvarez was initiated to gain more knowledge of the procedures used to obtain 78% lipid mass/CDM. The MSM recipe used by Alvarez was then replicated in the lab. However, even when using the procedures used by Alvarez, the author could not reproduce the 78% lipid percentage.

In the first stages of this lipid research, there were problems with reproducibility, variance between repeated experiments, and low lipid production. The data collected during this stage of the study are presented in Figure 5.1.

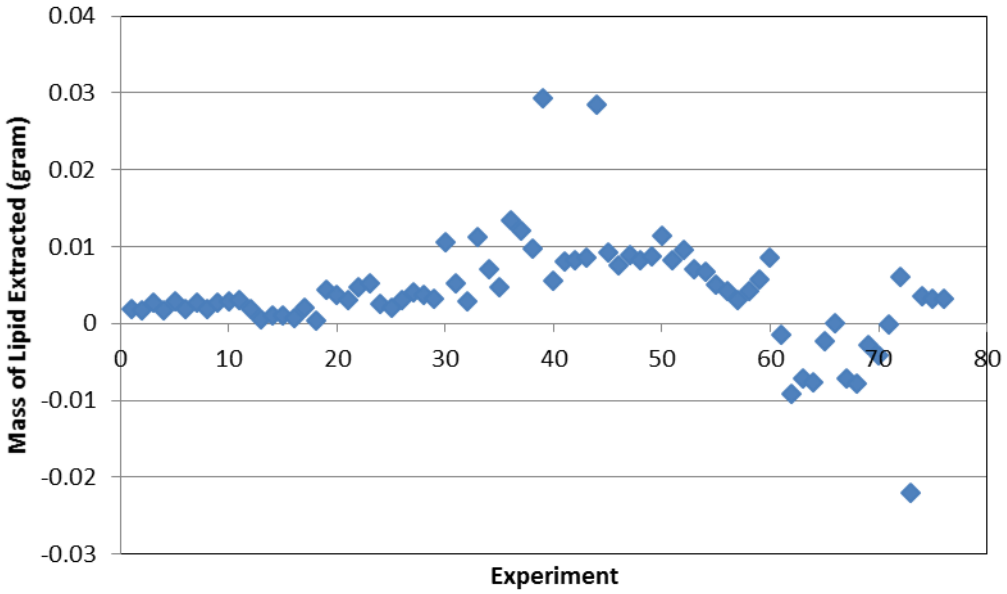

Figure 5.1 Lipid extraction data collected during *R. opacus* Bligh and Dyer

Figure 5.1 displays all data collected while cultivating *R. opacus*. The media utilized during this experiment was *R. opacus* with a maximum lipid yield of 30 mg and a minimum lipid yield of -22 mg. The maximum lipid mass of 0.03 g corresponds to 22% lipid mass/CDM, which is much lower than the expected 78% achieved by Alvarez. Three problems are illustrated in Figure 5.1: 1) the lipid mass is too variant (between 30mg and -22mg); 2) the lipid yield does not provide enough significant digits when measured gravimetrically since the precision of the balance used is accurate to 0.001 mg; and 3) the lipid percentage of several samples is below zero due to inefficiencies in the chemical extraction and low lipid percentages. The results from experimentation with *R. opacus* were replicated and closely monitored to ensure that there were not any inconsistencies between the literature methods and laboratory methods. The resulting

low lipid percentages, which could not be explained by the MSU Microbiology Laboratory, required the experiments to focus on alternative medias and microorganisms.

Once these inconsistencies were identified, the project was reassessed. A new experimental procedure was developed to increase the precision of the data collected. The new experimental procedure used a more effective growth media and yeast which was readily available in the MSU Microbiology Laboratory. The method used for the following experiments was discussed in the "Materials and Methods" chapter of this report.

5.2 Soybeans

Soybeans are a proven source of oil. However, existing processes for extracting the oil are labor-intensive and costly (Farsaie, et al., 1985). The current method for extracting lipids from soybeans involves machining the soybeans into thin flakes, using a solvent to extract the lipids from the soybean flakes, and refining the extracted lipids through solvent removal. Work by Dornbos et al. (1992) has shown that soybeans contain between 20 and 23% lipids. The lipid content of the seed varies with the conditions of the growth period from which the seed was harvested (Smith and Huyser 1987). Preliminary Bligh and Dyer extraction of soybeans acquired from Mississippi Soybean Promotion Board member, Jan Deregt, resulted in an initial lipid concentration in the range of 19-23%, which is consistent with the literature values reported (Dornbos, 1992). Achieving similar results as the literature states ensures that our laboratory had increased proficiency of the Bligh and Dyer extraction.

Othmer and Jaatinen (1959) used soybean flakes (i.e., processed soybeans with a thickness between 0.023 and 0.007 inches) to increase the efficiency of lipid extraction.

This was replicated in the lab by crushing the soybeans and sieving the crushed hulls. The portion of the hulls which passed through the #20 sieve and were retained on the #40 sieve were used for each experiment, to ensure uniformity between each sample. The soybeans were then tested using the modified Bligh and Dyer process discussed in the "Methods and Materials" chapter of this paper. Several Bligh and Dyer extractions were completed to accurately determine the initial lipid concentration of the machined soybeans. Once these initial extractions were complete, the machined soybeans were subjected to electroporation conditions to determine if electroporation had an effect on lipid concentration. The soybean experiments also utilized a negative control. A negative control (soybean placed in buffer solution in a cuvette with no voltage potential placed across the cell) was used to test and record the effect of the buffer solution on the milled, non-electroporated soybeans.

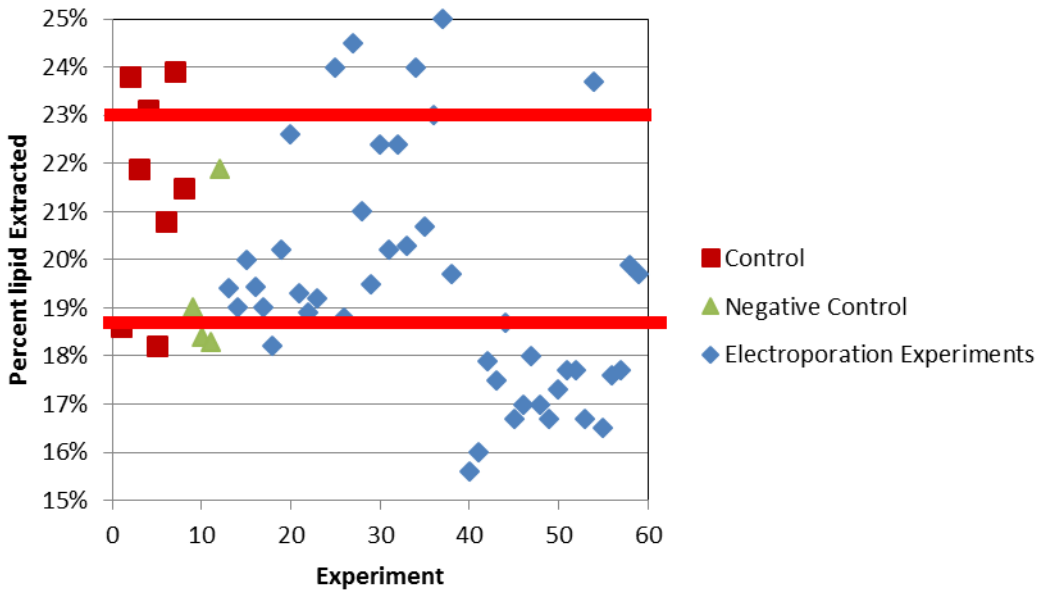

Figure 5.2 Graph of lipid percentage in crushed soybeans with boundaries (noted with bold lines) of literature-reported lipid percentages at 19 and 23%

Data collected during soybean investigation are displayed in Figure 5.2. The data were analyzed with SAS v9.2 software to accurately assess the output. The entire data set consists of 60 experimental observations, including 12 controls. The data collected were analyzed using a ridge regression model for the response surface to identify trends for future experiments. Table 5.1 shows the r-square for the regression model and has a fit of 0.2924, which is not significant, thus the model is a poor fit. The raw data collected with respect to the EP of soybeans can be seen in Appendix A.

Table 5.1 Output from regression model run on soybean electroporation data

Response Mean	0.197505
Root MSE	0.02405
R-Square	0.2924
Coefficient of Variation	12.177

Table 5.1 implies that there is too much variance associated with the data collected to accurately assess the effect of electroporation on soybean lipids. Figure 5.2 illustrates that a majority of the data collected fall between the lipid percentages for soybeans reported in the literature (Dornbos, 1992).

5.3 *Rhodotorula glutinis* (Yeast)

It was impossible to obtain high lipid contents using *R. opacus;* therefore, the focus of this project shifted to yeast. The Microbiology Laboratory in the Swalm School of Chemical Engineering at MSU had a proven method to efficiently produce high lipid contents while maintaining high cell mass values. Due to issues discussed in section 5.2 it was decided to focus on *R. glutinis*. Therefore, remainder of this chapter discusses the data collected from EP of *R. glutinis*.

Four Box-Behnken experimental matrices were performed using *R. glutinis,* with groups of experiments aimed at exploring the various adjustable parameters of the BTX 830 electroporator. Each matrix tested three independent variables and one dependent variable. The first two matrices discussed manipulated the following three parameters: voltage, pulse duration, and electrode spacing. The final two matrices manipulated the following three parameters: voltage, pulse duration, and multiple pulses. For every experiment conducted, the dependent variable was the amount of lipid extracted chemically after cell treatment, EP.

5.3.1 Matrix 1 – Low Voltage and Single Pulse

The first experimental matrix manipulated voltage, pulse duration, and electrode spacing to test the effect of these parameters on the amount of intracellular lipids extracted. The independent variables had the following settings:

Table 5.2 Matrix 1 parameters

Parameter	Minimum	Median	Maximum
Voltage (Volts)	10	250	490
Pulse Duration (microseconds)	10	500	990
Electrode Spacing (millimeter)	5	10	15

This matrix design utilized the low voltage settings of the BTX 830. Using the Box-Behnken experimental design, the data were analyzed using SAS v9.2. The RSREG Procedure was used to analyze the response surface to estimate the parameters of the model by least squares regression and to obtain information about the fit in the form of an analysis of variance. All of the raw data collected for Matrix 1 are displayed in Appendix A, Table A.2. Figure 5.3 is a graph of the raw data collected during these experiments.

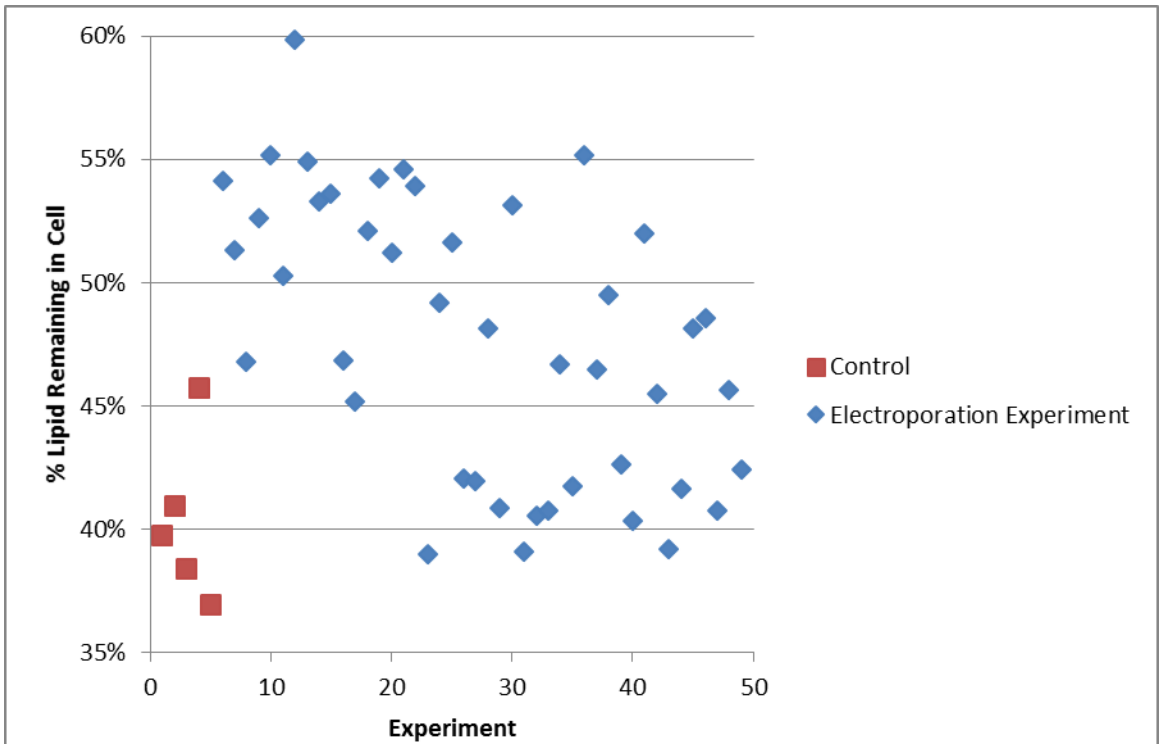

Figure 5.3 Graph of lipid percentage data collected during Matrix 1 tests with control experiments on left and EP experiments on right

Table 5.3 displays the results from the ridge analysis, which estimates that the cell will have 36% intracellular lipids following electroporation. This is equal to the lowest lipid percentage from the non-electroporated cells.

Table 5.3 Minimum ridge analysis of Matrix 1 Box-Behnken experimental design (from Appendix B.2, SAS Output)

Estimated Intracellular Lipids Remaining in Cell	PULSE DURATION (μs)	VOLTAGE (V)	ELECTRODE SPACING (mm)
43%	495	245	8
43%	487	244	7
42%	482	244	6
42%	479	244	5
41%	476	245	5
40%	475	245	4
40%	474	245	3
39%	473	246	2
38%	472	247	2
37%	472	247	1
36%	471	248	0.01

This regression model had an r-square value of 0.48, Table 5.4. The lack-of-fit test compares the variation around the model with pure variation within replicated observations. This measures the adequacy of the quadratic response surface model. The lack of fit for the model is not significant. The hypothesis tests can be used to gain an idea of the importance of the effects; here the cross-product terms are not significant. Parameter estimates and the factor ANOVA are shown in Appendix B.2. Looking at the parameter estimates, one can see that the cross-product terms are not significantly different from zero, as noted previously. The Estimate column contains estimates based on the raw data, and the Parameter Estimate from Coded Data column contains estimates based on the coded data. The factor ANOVA table displays tests for all four parameters corresponding to each factor—the parameters corresponding to the linear effect, the quadratic effect, and the effects of the cross-products with each of the other two factors.

The only factor with a significant overall effect is electrode spacing, indicating that the level of noise left unexplained by the model is still too high to estimate the effects of pulse duration and voltage accurately (see Appendix B.2).

Table 5.4 Output from regression model run on Matrix 1 electroporation data

Response Mean	**0.47**
Root MSE	**0.05**
R-Square	**0.48**
Coefficient of Variation	**10.04**

The results of the experimental design were also plotted using SAS v9.2. Figure 5.4 was created to visualize the effect of each independent variable on the dependent variables.

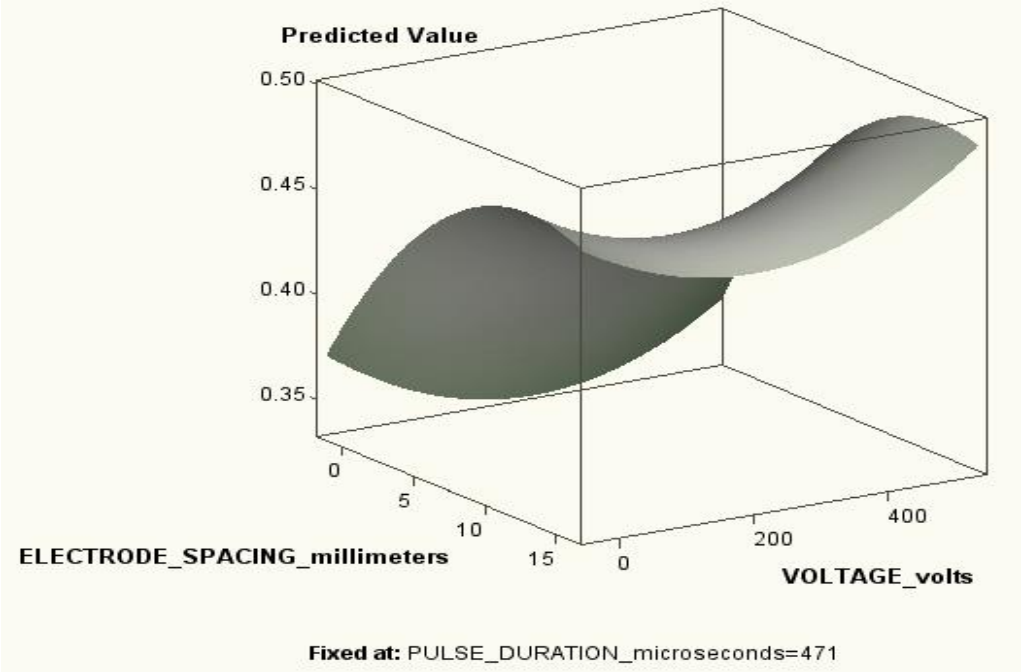

(A)

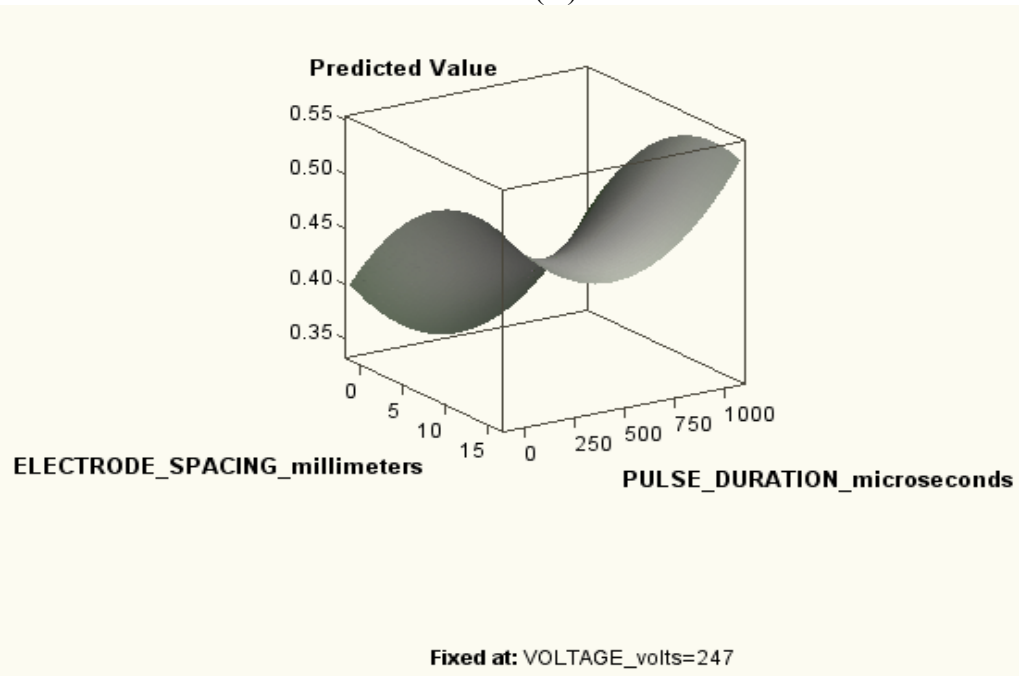

(B)

Figure 5.4 Model prediction for Matrix 1 variables (voltage, pulse duration, and electrode spacing): A) Surface graph comparing voltage and electrode spacing on lipid extraction, B) surface graph comparing pulse duration and electrode spacing on lipid extraction, and C) surface graph comparing voltage and pulse duration on lipid extraction. (see Appendix B.2: SAS Output)

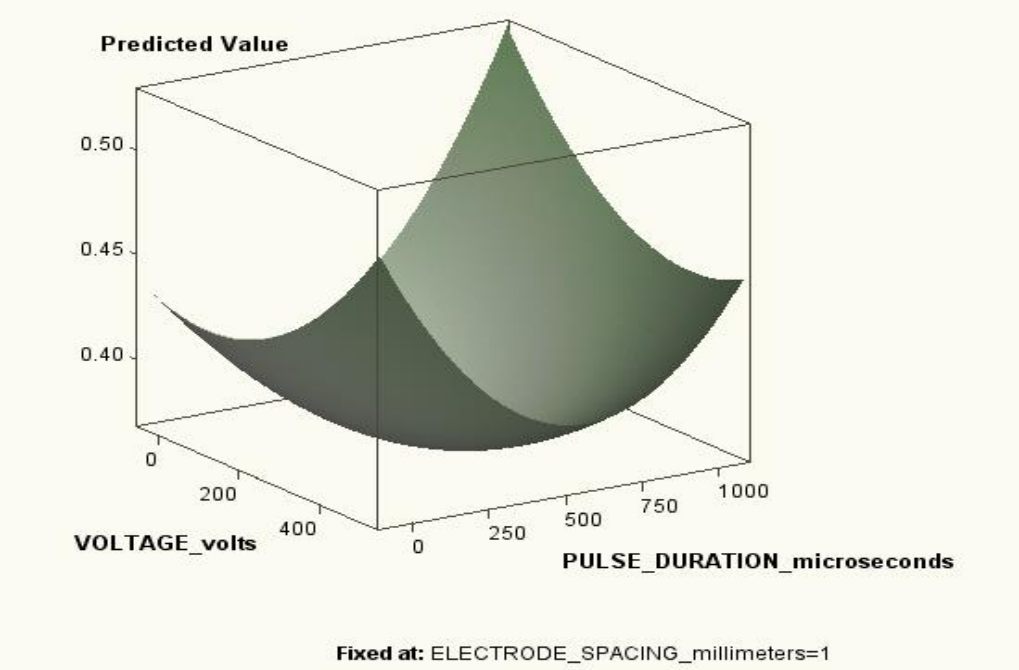

(C)

Figure 5.4 (Continued)

Figure 5.4 shows the graphical result of the response surface analysis with the predicted value being the model prediction of intracellular lipids extracted chemically. The units for all surface plots in Figure 5.4 are: VOLTAGE (volts); PULSE DURATION (microseconds); ELECTRODESPACING (millimeters); Predicted Value is the percentage of lipids remaining after EP. For each graph, one variable is held constant. This allows two independent variables to be graphed with the dependent variable on the z-axis. Figures 5.4A and 5.4B contain a saddle point, which means the parameters tested do not contain extremes. Figure 5.4C has a minimum, which means that under the parameters tested in Matrix 1, voltage and pulse duration have reached their minimum lipid extraction potential.

The canonical output in the Ridge Regression analysis completed in SAS produced eigenvalues and eigenvectors. These values can be helpful when trying to determine which variable or groups of variables have the most significant effect on the dependent variable. The output (from Appendix B.2) is displayed in Table 5.5. The canonical analysis (SAS Output: Appendix B.2) indicates that the predicted response surface is shaped like a saddle. Positive eigenvalues indicate directions of upward curvature, and negative eigenvalues indicate directions of downward curvature. The eigenvalue of 0.056 shows that the valley orientation of the saddle is slightly more curved than the hill orientation, with an eigenvalue of -0.0298. The larger the absolute value of an eigenvalue, the more pronounced is the curvature of the response surface in the associated direction. The coefficients of the associated eigenvectors show that the valley is more aligned with pulse duration and that the hill is more aligned with electrode spacing.

Table 5.5 Eigenvalues and eigenvectors from ridge analysis of Matrix 1

	Eigenvectors		
Eigenvalues	**PULSE DURATION (μs)**	**VOLTAGE (V)**	**ELECTRODE SPACING (mm)**
0.056	0.94	-0.33	-0.006
0.018	0.33	0.94	0.04
-0.029	-0.007	-0.04	0.99

The eigenvalues do not have the same sign; therefore, a saddle point is present. The estimated surface is typically curved: it contains a ***hill*** with the peak occurring at the unique estimated point of maximum response; a ***valley,*** or a ***saddle surface,*** with no unique minimum or maximum. The saddle point graph can be seen in Figures 5.4A and

5.4B, with a saddle point of 0.45. Since the focus of this study is to find the parameters that minimize the amount of lipids remaining in the cells after EP, the smallest eigenvalue is of the most interest. The smallest eigenvalue for Matrix 1 is -0.029 and the largest eigenvector associated with that eigenvalue is electrode spacing. Comparing the eigenvalues in Table 5.5 and the contour plots in Figure 5.4, one can infer that electrode spacing has the most significant effect on the amount of lipids extracted from the cell from EP. The Estimated Ridge of Minimum Response for Variable % Lipids Extracted indicates that minimum yields result from higher pulse duration (471 microseconds), lower voltage (248 volts), and lower electrode spacing (less than 1 mm) (see Appendix B.2).

5.3.2 Matrix 2- High Voltage and Single Pulse

The second experimental matrix manipulated higher voltage, pulse duration, and electrode spacing to test the effect that these parameters had on the amount of lipids extracted through Bligh and Dyer chemical extraction treatment. The independent variables voltage, pulse duration, and electrode spacing had the following settings:

Table 5.6 Matrix 2 parameters

Parameter	Minimum	Median	Maximum
Voltage (Volts)	1000	2000	3000
Pulse Duration (microseconds)	10	50	90
Electrode Spacing (millimeter)	10	15	20

This matrix design utilized the high voltage settings of the BTX 830. Using the Box-Behnken experimental design, the data were analyzed using SAS v9.2 with a canonical and ridge regression. All of the data collected for Matrix 2 are displayed in Table A.3. Figure 5.5 is a graph of the data collected during these experiments.

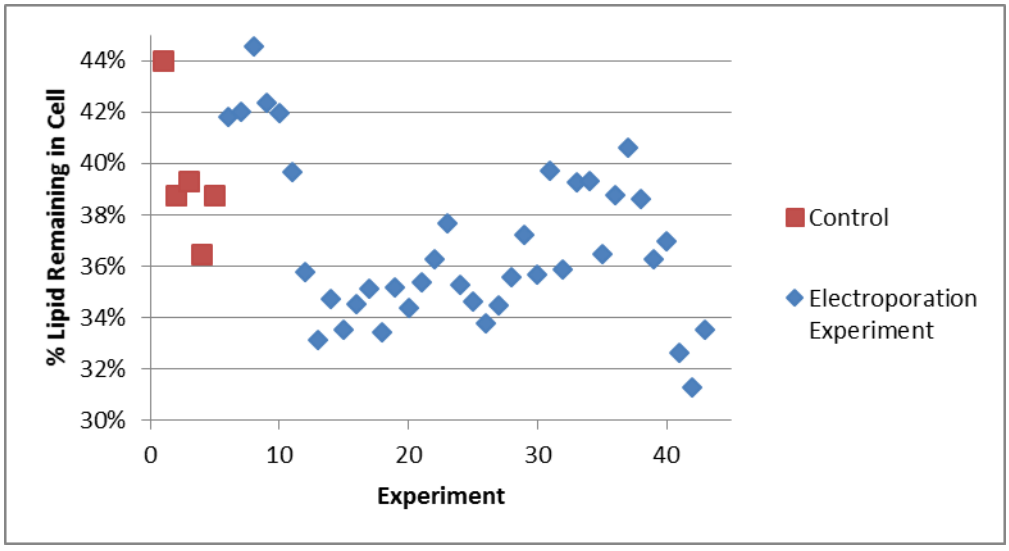

Figure 5.5 Data collected during Matrix 2 tests with control experiments on left and EP experiments on right

Table 5.7 displays the results from the ridge analysis, which estimates that the cell will have 32% intracellular lipids following electroporation. Comparing the output from the ridge analysis and the data collected, seen in Figure 5.5, the minimum amount of intracellular lipids remaining after EP is 32%. This is less than the control minimum of 36%. Comparing Table 5.7 to Figure 5.5, there would be 4% less lipids in the treated cells than in the untreated cells when using a 12-microsecond pulse, a voltage value of 1628 volts, and an electrode spacing of 3 mm.

Table 5.7 Minimum ridge analysis of Matrix 2 Box-Behnken experimental design

Estimated Intracellular Lipids Remaining in Cell	PULSE DURATION (μs)	VOLTAGE (V)	ELECTRODE SPACING (mm)
34%	45	1500	10
34%	42	1604	10
34%	38	1673	10
33%	34	1712	9
33%	29	1730	9
33%	25	1733	8
33%	22	1723	7
33%	19	1705	6
33%	16	1682	5
33%	14	1656	4
32%	12	1628	3

This regression model had an r-square value of 0.556, Table 5.8. The lack-of-fit test compares the variation around the model with ***pure*** variation within replicated observations. This measures the adequacy of the quadratic response surface model, which was highly significant. Yet, the lack of fit for the model is also significant; therefore, more complicated modeling or further experimentation with additional variables should be performed before firm conclusions are made concerning the underlying process. For

the hypothesis tests (e.g., Matrix 1), the cross-product terms are not significant. Parameter estimates and the factor ANOVA are shown in Appendix B.3. Looking at the parameter estimates, the cross-product terms are not significantly different from zero, as noted previously. The only factor with a significant overall effect is voltage, indicating that the level of noise left unexplained by the model is still too high to estimate the effects of pulse duration and electrode spacing accurately (see Appendix B.3).

Table 5.8 Minimum ridge analysis of Matrix 2 Box-Behnken experimental design

Response Mean	**0.371**
Root MSE	**0.024**
R-Square	**0.556**
Coefficient of Variation	**6.475**

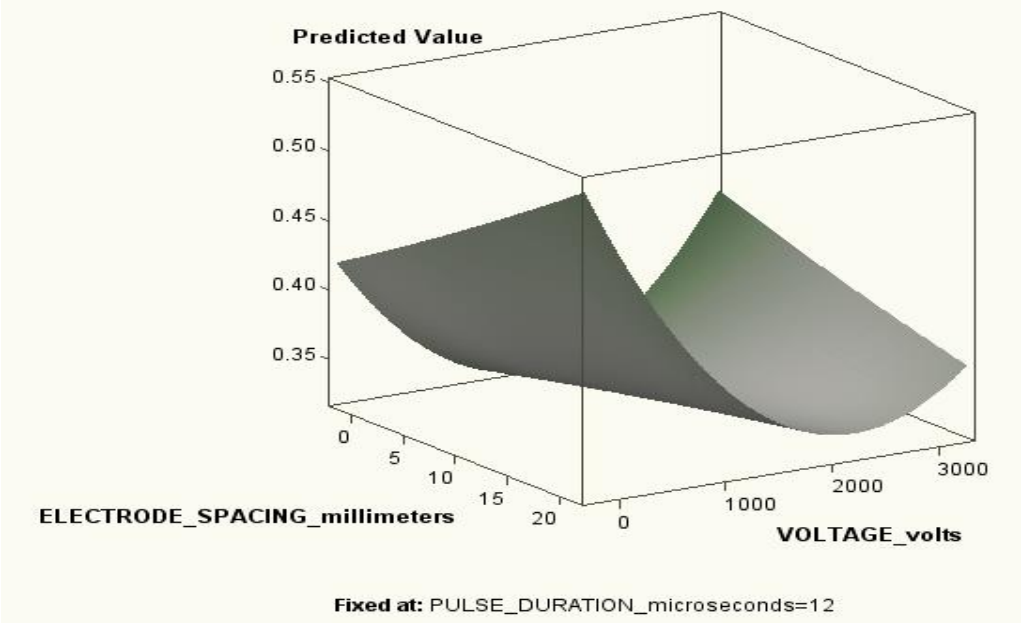

(A)

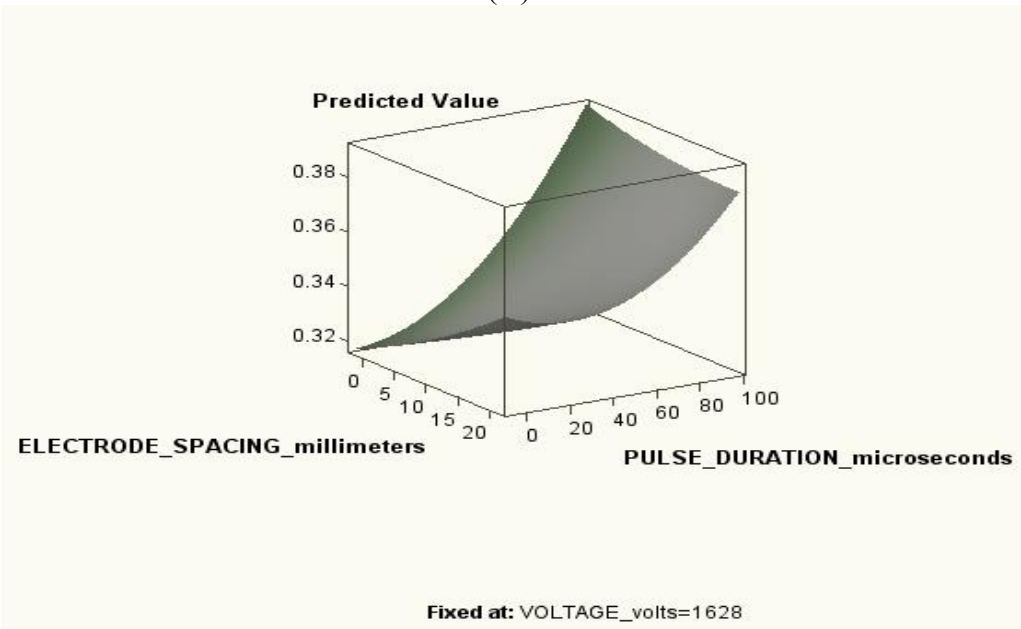

(B)

Figure 5.6 Model prediction for Matrix 2 variables (voltage, pulse duration, and electrode spacing): A) Surface graph comparing voltage and electrode spacing on lipid extraction, B) surface graph comparing pulse duration and electrode spacing on lipid extraction, and C) surface graph comparing voltage and pulse duration on lipid extraction

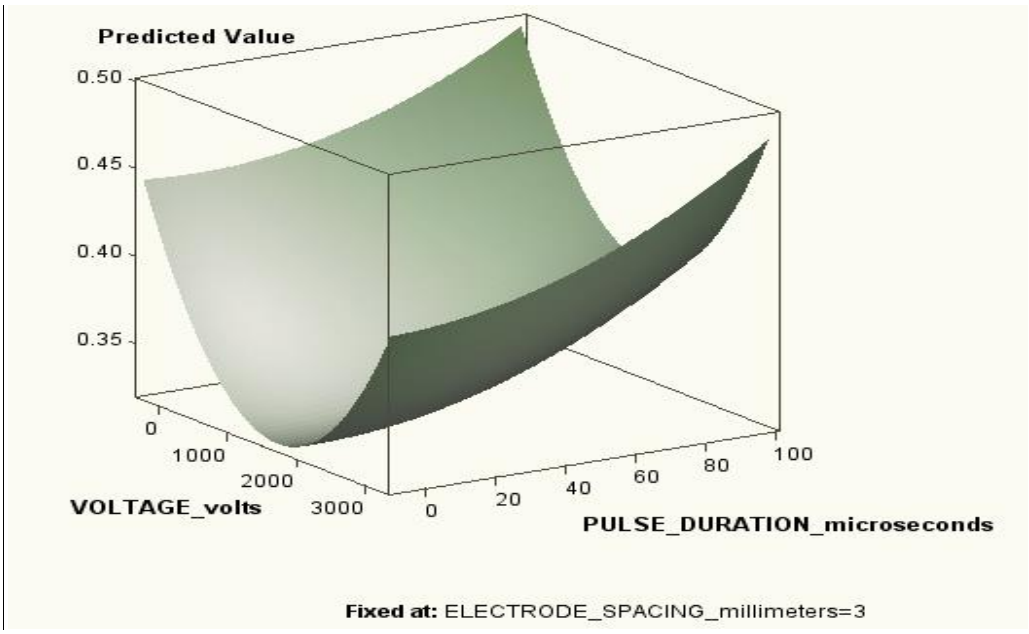

(C)

Figure 5.6 (Continued)

Figure 5.6 shows the graphical result of the response surface analysis. The units for all surface plots in Figure 5.6 are: voltage (volts); pulse duration (microseconds); and electrode spacing (millimeters); Predicted Value is the percentage of lipids remaining after EP. For each graph, one variable is held constant. This allows two independent variables to be graphed with the dependent variable on the z-axis. The contours displayed in Figure 5.6 do not have a minimum. The trends in the contour graphs are not clear; therefore, the eigenvalues and eigenvectors will be analyzed.

The ridge analysis completed in SAS produced eigenvalues and eigenvectors. These values can be helpful when trying to determine which variable or groups of variables have the most significant effect on the dependent variable. The output from this test is presented in Table 5.9. The canonical analysis (SAS Output: Appendix B.3) indicates that the predicted response surface is shaped like a saddle. The eigenvalue of

0.075 shows that the valley orientation of the saddle is slightly more curved than the hill orientation, with an eigenvalue of -0.0022. The coefficients of the associated eigenvectors show that the valley is more aligned with voltage and the hill is more aligned with electrode spacing. The Estimated Ridge of Minimum Response for Variable % Lipids Extracted indicates that minimum yields result from relatively higher pulse length, lower voltage, and higher electrode spacing (see Appendix B.3).

Table 5.9 Minimum ridge analysis of Matrix 2 Box-Behnken experimental design

	Eigenvectors		
Eigenvalues	**PULSE DURATION (μs)**	**VOLTAGE (V)**	**ELECTRODE SPACING (mm)**
0.075	0.047	0.977	-0.207
0.013	0.974	-0.090	-0.206
-0.0021	0.220	0.192	0.956

Comparing the eigenvalues in Table 5.9 and the contour plots in Figure 5.6, one can infer that pulse duration has the most significant effect on the amount of lipids remaining in the cell after EP. Figure 5.7 illustrates the effect of electrode spacing on intracellular lipid content. The first bar is the control from the experiment, zero value for electrode spacing since these cells were not subjected to electroporation. The values shown in Figure 5.7 are the average lipid contents for each group of electrode spacing experiments. An apparent trend is present in Figure 5.7 which affirms the statistical analysis stating that as electrode spacing is increased the amount of intracellular lipids decreases. Therefore, electrode spacing has the desired effect on cellular lipid content.

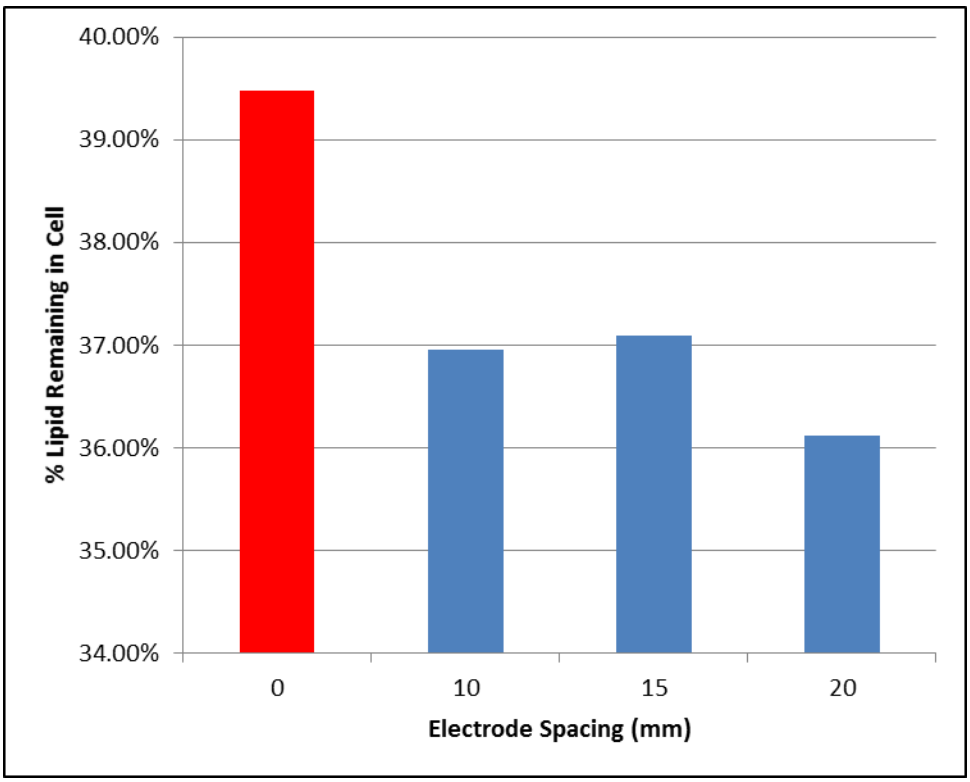

Figure 5.7 Data from Matrix 2 grouped by electrode spacing (control=0 and electroporated cells= 10, 15, and 20)

The estimated minimum response corresponds to reduction in the percentage of chemically extractable lipids after EP, which is positive, meaning that the high-voltage, single-pulse EP could theoretically extract lipids from *R. glutinis*. Table 5.7 shows that the minimum theoretical amount of lipid extracted from *R. glutinis* is 32%. This value can be obtained using the following parameters: 12 microseconds, 1628 volts, and 3 mm of electrode spacing. This percentage corresponds to a percent difference from the control. The control's average lipid percentage was 39% lipid/DCM and the cell mass was approximately 9 g/L. The theoretical optimal lipid extraction correlates to a mass extraction of 0.6 g/L extraction of lipids from *R. glutinis* utilizing EP.

5.3.3 Matrix 3- Low voltage, pulse duration, and number of pulses

The third experimental matrix manipulated voltage, pulse duration, and multiple pulses to test the effect these parameters had on the amount of lipids extracted through Bligh and Dyer chemical extraction treatment. The independent variables, voltage, pulse duration, and number of pulses, had the settings shown in Table 5.10.

Table 5.10 Matrix 3 parameters

Parameter	Minimum	Median	Maximum
Voltage (Volts)	10	260	500
Pulse Duration (microseconds)	10	505	1000
Number of Pulses	19	59	99

This matrix design utilized the low voltage and multiple voltage pulse settings of the BTX 830and the Teflon cuvette. When a sample is tested using multiple pulses, each individual pulse retains the identical settings. For example, if a sample was to be tested with parameters of 500 volts, 10 microseconds, and 50 pulses, each pulse would experience 500 volts and 10 microseconds. This experimental matrix was limited to 1000 microseconds because the technical support at BTX stated that after 1000 microseconds, cell viability would not be maintained. All raw data collected for Matrix 3 are presented in Appendix A, Table A-4. The data were analyzed using SAS v9.2 utilizing canonical

and ridge regression to produce a response surface for the parameters tested. The results from the model are shown in Table 5.11.

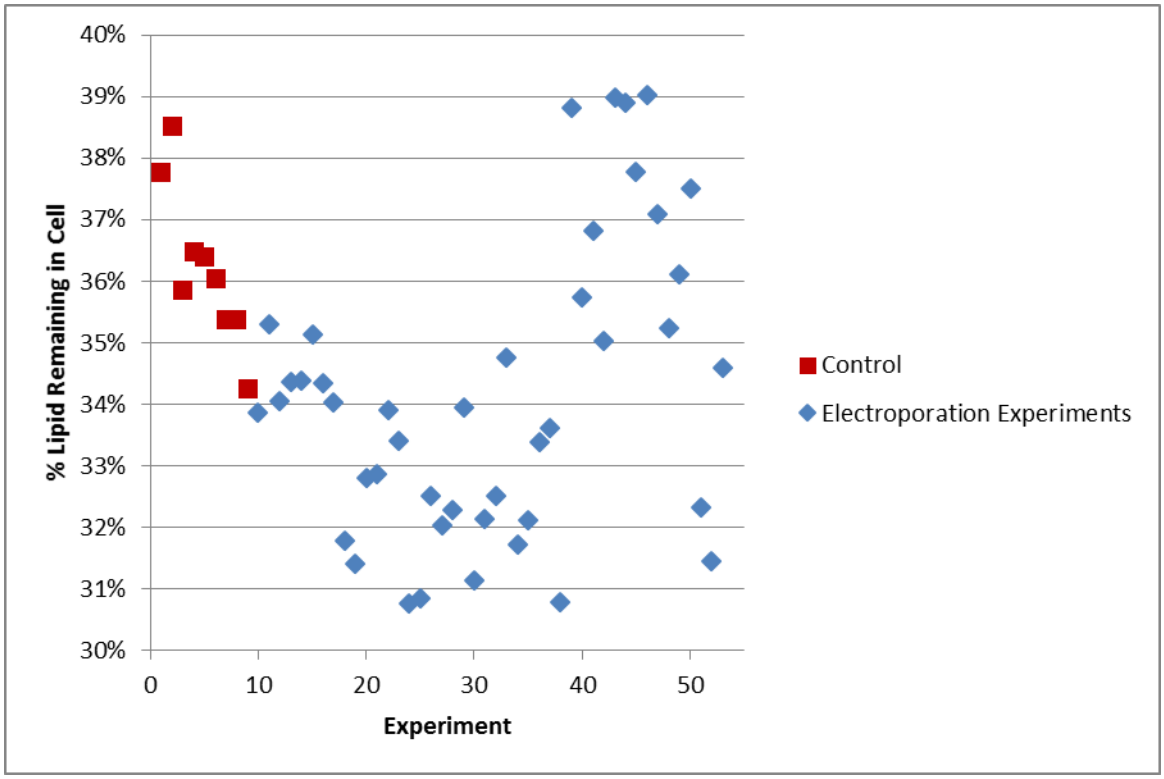

Figure 5.8 Graph of data collected during Matrix 3 tests with control experiments on left and EP experiments on right

Table 5.11 displays the results from the ridge analysis, which estimates that the cell will have 33% intracellular lipids following electroporation. Comparing the output from the ridge analysis and the data collected (seen in Figure 5.8), the minimum amount of intracellular lipids remaining after EP is 33%. This is less than the control minimum of 34%. Comparing Table 5.11 and Figure 5.8, there would be the possibility of 1% less lipids in the treated cells when using a 948-microsecond pulse, a voltage value of 325 volts, and an electrode spacing of 33 pulses.

Table 5.11 Minimum ridge analysis of Matrix 3 Box-Behnken experimental design

PERCENT INTRACELLULAR LIPIDS Remaining in Cell	PULSE DURATION (μs)	VOLTAGE (V)	NUMBER OF PULSES
35%	500	250	50
35%	496	275	49
35%	491	299	48
35%	548	316	44
35%	627	317	42
35%	687	319	40
34%	742	320	39
34%	795	321	37
34%	847	322	36
33%	898	323	35
33%	948	325	33

This regression model had an r-square value of 0.43 (Table 5.8). The lack-of-fit test compares the variation around the model with pure variation within replicated observations. This measures the adequacy of the quadratic response surface model, which was highly significant. Yet, the lack of fit for the model is not significant. In the hypothesis tests, unlike in Matrices 1 and 2, the cross-product terms are just significant. Parameter estimates and the factor ANOVA are shown in B.4. Looking at the parameter estimates, one can see that the only cross-product terms that are significantly different from zero are the number of pulses and the pulse duration. All of the factors indicate significant overall effect (see Appendix B.4).

Table 5.12 Output from regression model run on Matrix 3 electroporation data

Response Mean	**0.34**
Root MSE	**0.02**
R-Square	**0.43**
Coefficient of Variation	**5.69**

The results of the experimental design were also plotted using SAS v9.2. Figure 5.9 was created to visualize the effect of each independent variable on the dependent variable.

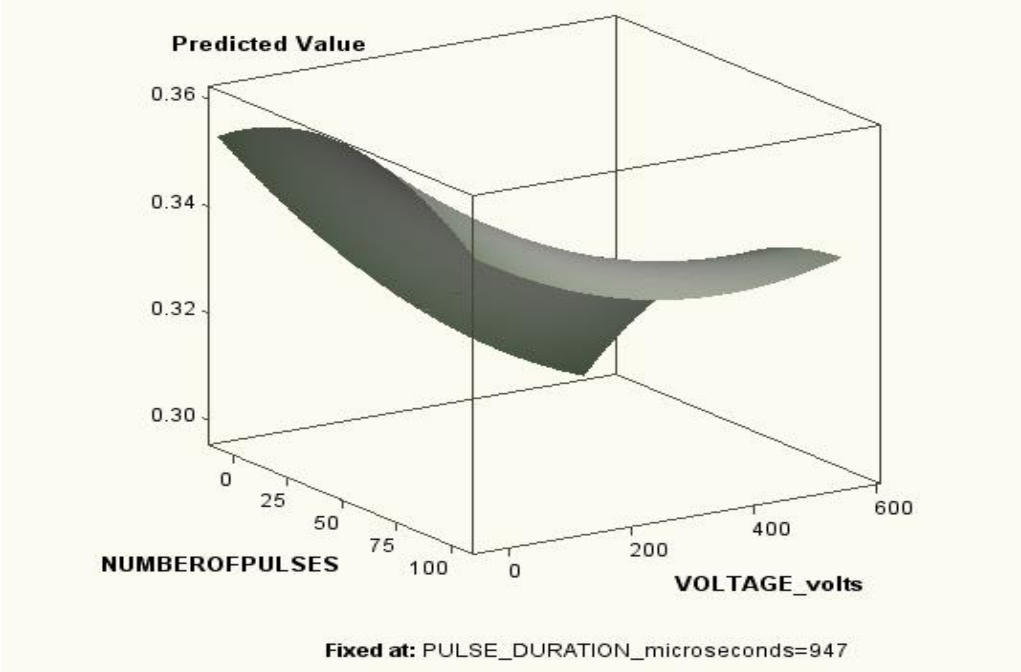

(A)

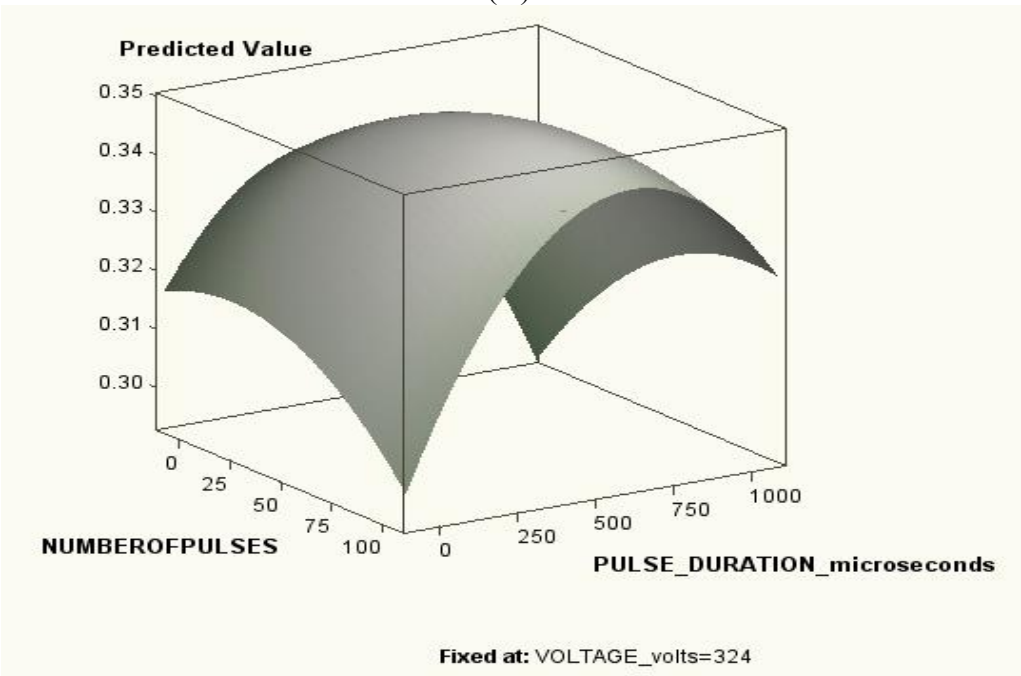

(B)

Figure 5.9 Model prediction for Matrix 3 variables (voltage, pulse duration, and number of pulses): A) Surface graph comparing voltage and number of pulses on lipid extraction, B) surface graph comparing pulse duration and number of pulses on lipid extraction, and C) surface graph comparing voltage and pulse duration on lipid extraction.

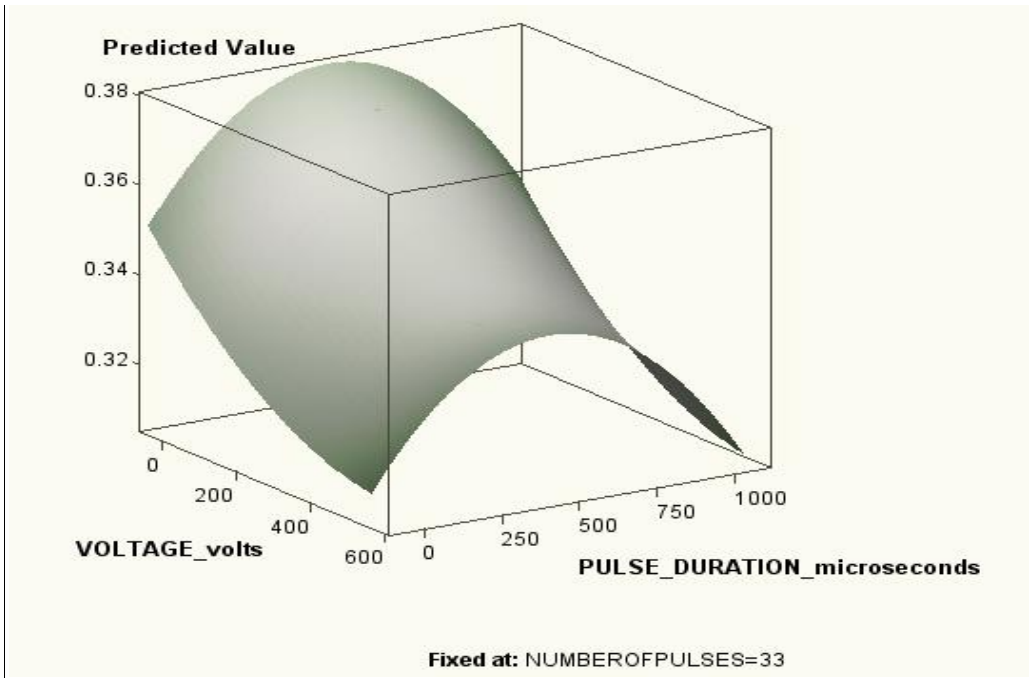

(C)

Figure 5.9 (Continued)

The ridge analysis completed in SAS produced eigenvalues and eigenvectors. These values can be helpful when trying to determine which variable or groups of variables have the most significant effect on the dependent variable. The output from this test is displayed in Table 5.13. The canonical analysis (SAS Output: Appendix B.4) indicates that the predicted response surface is shaped like a saddle. The eigenvalue of 0.007 shows that the valley orientation of the saddle is slightly more curved than the hill orientation, with an eigenvalue of -0.023. The coefficients of the associated eigenvectors show that the valley is more aligned with pulse duration and the hill is more aligned with the number of pulses. The Estimated Ridge of Minimum Response for Variable % Lipids Extracted indicates that minimum yields result from relatively higher pulse duration, higher voltage, and higher number of pulses (see Appendix B.4).

Table 5.13 Output from regression model run on Matrix 3 electroporation data

	Eigenvectors		
Eigenvalues	**PULSE DURATION (μs)**	**VOLTAGE (V)**	**NUMBER OF PULSES**
0.007	0.038	0.957	0.289
-0.007	0.268	-0.288	0.919
-0.023	0.963	0.043	-0.267

Comparing the eigenvalues in Table 5.13 with the contour plots in Figure 5.9, one can infer that pulse duration has the most significant effect on the amount of lipids remaining in the cell after EP. As pulse duration decreases the amount of lipids remaining in each cell after treatment decreases. Visual inspection of Figure 5.9C suggests that as voltage increase and pulse duration decreases the intracellular lipids available for chemical extraction will decrease. 5.10 illustrates the effect of pulse duration on intracellular lipid content. The first bar is the control from the experimental matrix, zero value for pulse duration since the cells were not subjected to electroporation. The values shown in Figure 5.10 are the average lipid contents for each group of pulse duration experiments. An apparent trend is present in Figure 5.10 which affirms the statistical analysis stating that as pulse duration is increased the amount of intracellular lipids decreases. Therefore, pulse duration has the desired effect on cellular lipid content.

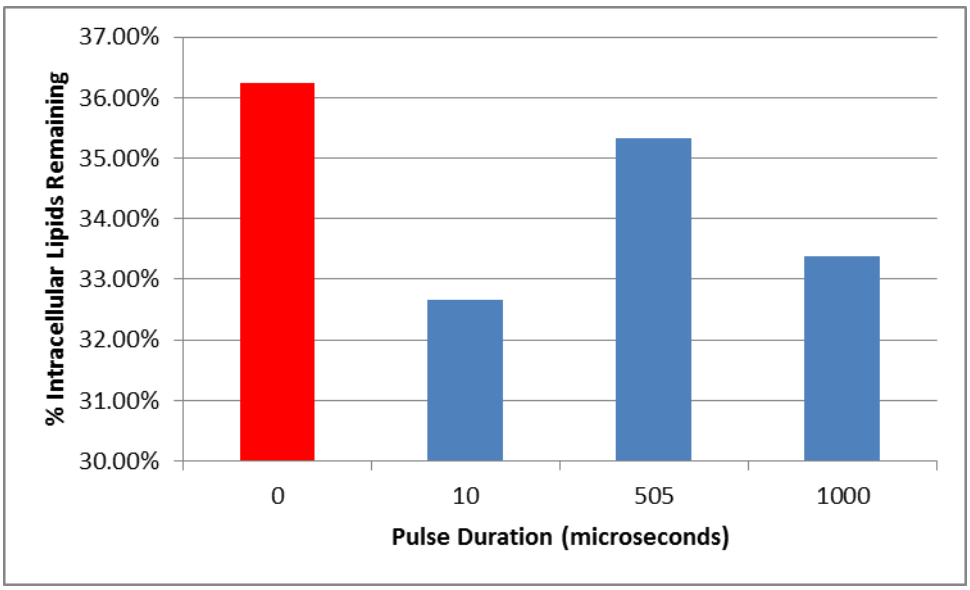

Figure 5.10 Data from Matrix 3 grouped by pulse duration (control=0 and electroporated cells= 10, 505, and 1000)

The estimated minimum response corresponds to a reduction in the percentage of chemically extractable lipids after EP, which is positive. This means that the high-voltage, single-pulse EP could theoretically extract lipids from *R. glutinis*. Table 5.11 shows that the minimum theoretical amount of lipid extracted from *R. glutinis* is 33%, which can be obtained using the following parameters: 948 microseconds, 325 volts, and 33 pulses. This percentage corresponds to a percent difference from the mean of the control. The control's average lipid percentage was 39% lipid/DCM and the cell mass was approximately 10 g/L. The theoretical optimal lipid extraction correlates to a mass extraction of lipids from *R. glutinis* of 0.6 g/L utilizing EP.

5.3.4 Matrix 4: High voltage, pulse duration, and number of pulses

The fourth experimental matrix manipulated high voltage, pulse duration, and multiple pulses to test the effect of these parameters on the amount of lipids remaining in

the cell after treatment. The independent variables voltage, pulse duration, and electrode spacing had the following settings:

Table 5.14 Matrix 4 parameters

	Minimum	Median	Maximum
Voltage (Volts)	690	1845	3000
Pulse Duration (microseconds)	20	60	100
Number of Pulses	19	59	99

This matrix design utilized the high voltage settings of the BTX 830. The Box-Behnken experimental matrix design was utilized for this experimental matrix. The raw data collected for Matrix 4 are displayed in Appendix A, Table A-5. The data were analyzed with SAS v9.2, utilizing canonical and ridge regression to produce a response surface for the parameters tested. The results from the model are displayed in Table 5.15.

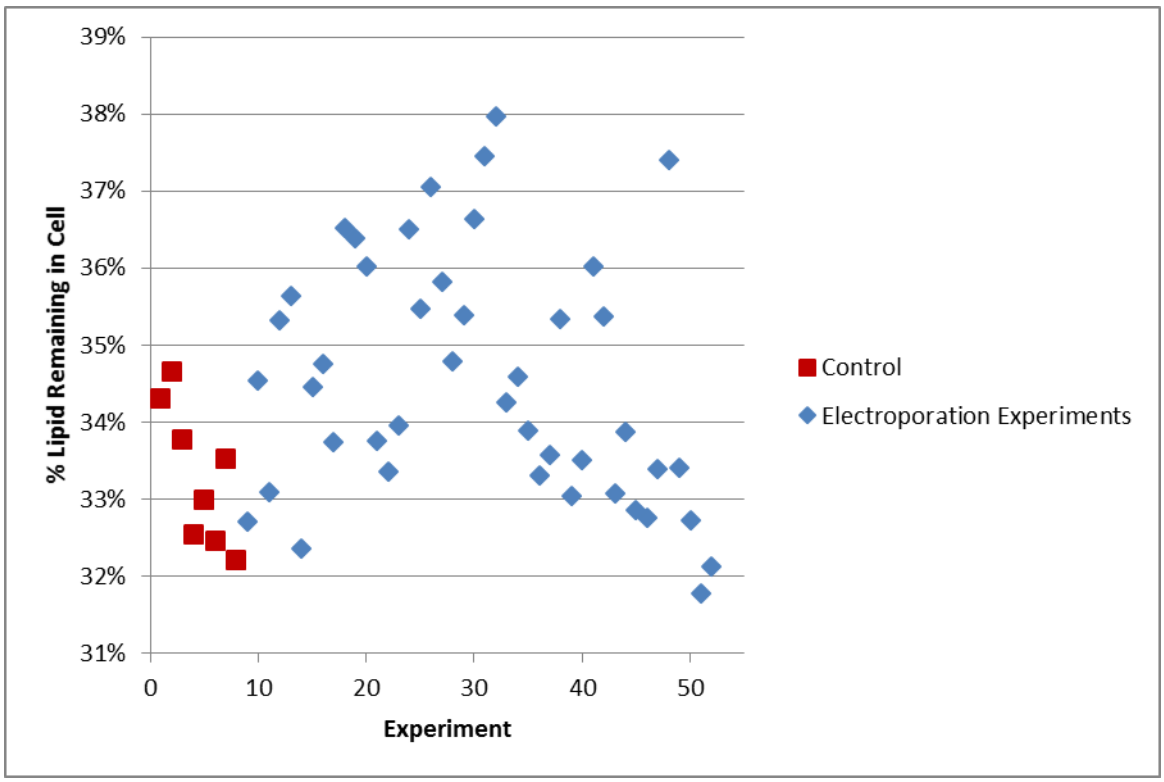

Figure 5.11 Graph of data collected during Matrix 4 tests (control experiments on left and EP experiments on right)

Table 5.15 displays the results from the ridge analysis, which estimates that the cell will have 32% intracellular lipids following electroporation. Comparing the output from the ridge analysis to the data collected (Figure 5.11), the minimum amount of intracellular lipids remaining after EP is 32%, which is equal to the control minimum of 32%.

Table 5.15 Minimum ridge analysis of Matrix 4 Box-Behnken experimental design

PERCENT INTRACELLULAR LIPIDS Remaining in Cell	PULSE DURATION (μs)	VOLTAGE (V)	NUMBER OF PULSES
0.33	500	1500	50
0.33	466	1391	49
0.33	444	1254	48
0.33	430	1104	48
0.33	422	949	48
0.33	417	793	48
0.33	414	638	49
0.32	413	483	49
0.32	412	329	49
0.32	412	176	49
0.32	413	23	50

This regression model had an r-square value of 0.570 (Table 5.16). The lack-of-fit test compares the variation around the model with pure variation within replicated observations. This measures the adequacy of the quadratic response surface model, which was highly significant. The lack of fit for the model is not significant. In the hypothesis tests, as in Matrices 1 and 2, the cross-product terms are not significant. Parameter estimates and the factor ANOVA are shown in Appendix B Table B.5. Looking at the parameter estimates, one can see that the cross-product terms are not significantly different from zero, as noted previously. The only factor which does not have a significant overall effect is voltage, indicating that the level of noise left unexplained by the model is still too high to estimate the cross effects accurately (see Appendix B.5).

Table 5.16 Output from regression model run on Matrix 4 electroporation data

Response Mean	0.344
Root MSE	0.011
R-Square	0.570
Coefficient of Variation	3.290

The results of the experimental design were then plotted using SAS v9.2 to get a visual interpretation of the data collected. Graphs were created to visualize the effect of each independent variable on the dependent variables. The graphs are displayed in Figure 5.12.

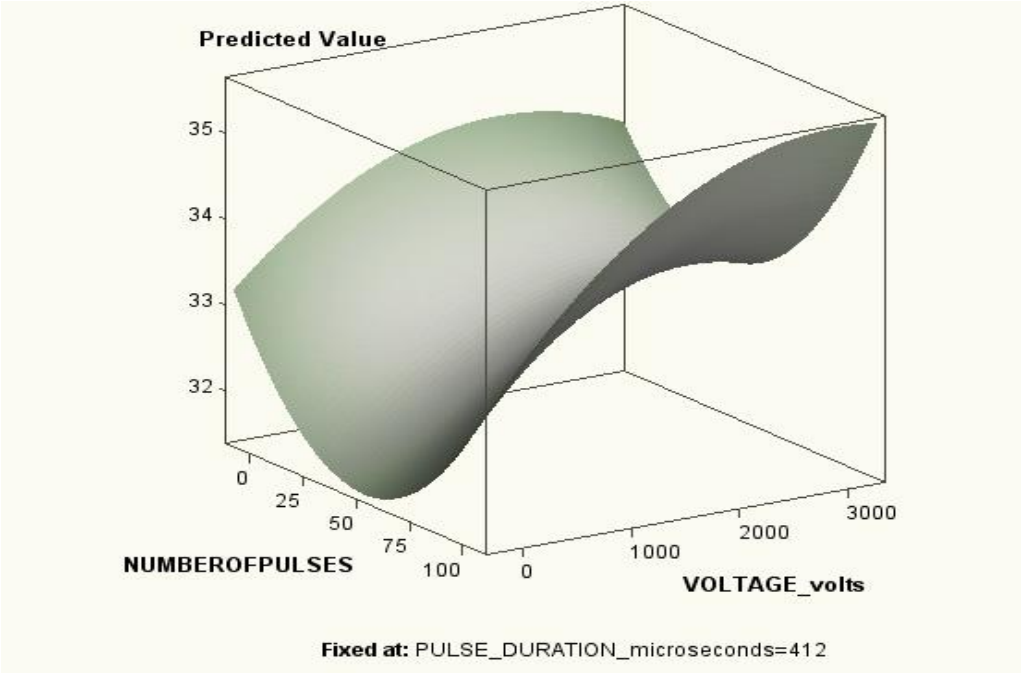

(A)

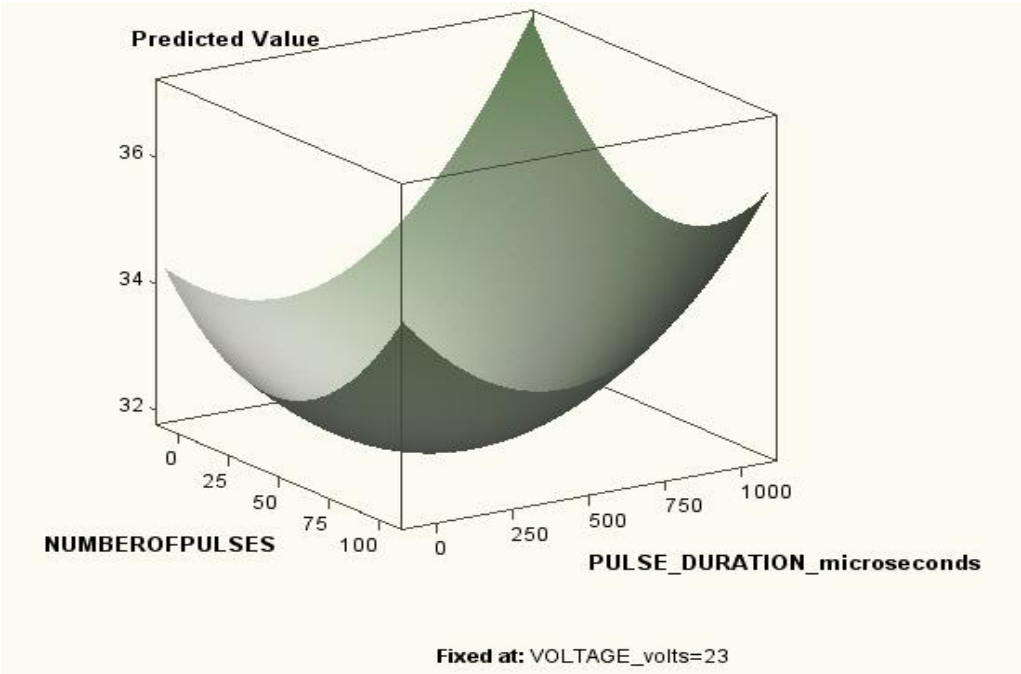

(B)

Figure 5.12 Model prediction for Matrix 4 variables (voltage, pulse duration, and number of pulses): A) Surface graph comparing voltage and number of pulses on lipid extraction, B) surface graph comparing pulse duration and number of pulses on lipid extraction, and C) surface graph comparing voltage and pulse duration on lipid extraction.

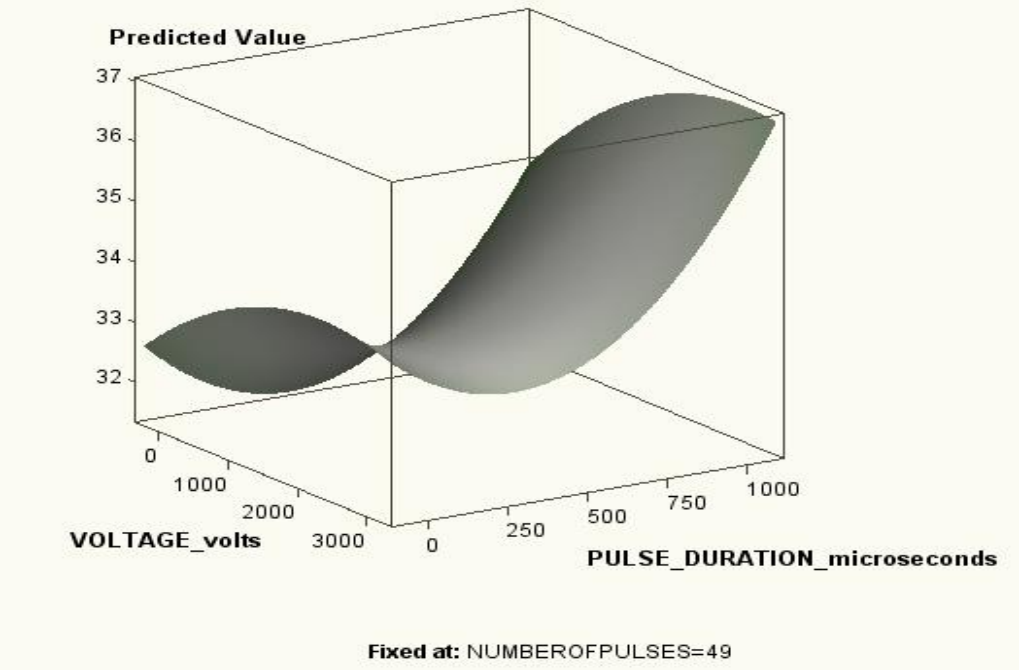

(C)

Figure 5.12 (Continued)

The ridge analysis completed in SAS produced eigenvalues and eigenvectors. These values can be helpful when trying to determine which variable or groups of variables have the most significant effect on the dependent variable. The output from this test is displayed in Table 5.17. The canonical analysis (SAS Output: Appendix B.5) indicates that the predicted response surface is shaped like a saddle. The eigenvalue of 0.0147 shows that the valley orientation of the saddle is slightly more curved than the hill orientation, with an eigenvalue of -0.00569. The coefficients of the associated eigenvectors show that the valley is more aligned with pulse duration, while the hill is more aligned with voltage. The Estimated Ridge of Minimum Response for Variable %

Lipids Extracted indicates that minimum yields result from relatively higher pulse duration, lower voltage, and lower number of pulses (see Appendix B.5).

Table 5.17 Output from regression model run on Matrix 3 electroporation data

	Eigenvectors		
Eigenvalues	PULSE DURATION (μs)	VOLTAGE (V)	NUMBER OF PULSES
0.015	0.897	0.013	-0.443
0.011	0.440	0.091	0.893
-0.006	-0.052	0.996	-0.076

Comparing the eigenvalues in Table 5.17 to the contour plots in Figure 5.12, one can infer that voltage has the most significant effect on the amount of lipids remaining in the cell after EP.

5.4 Scanning Electron Microscopy

Scanning electron microscopy (SEM) images were produced by Dr. Jaclyn Hall in the SEM Laboratory at MSU. These images allowed a visualization of the effect of EP on *R. glutinis*.

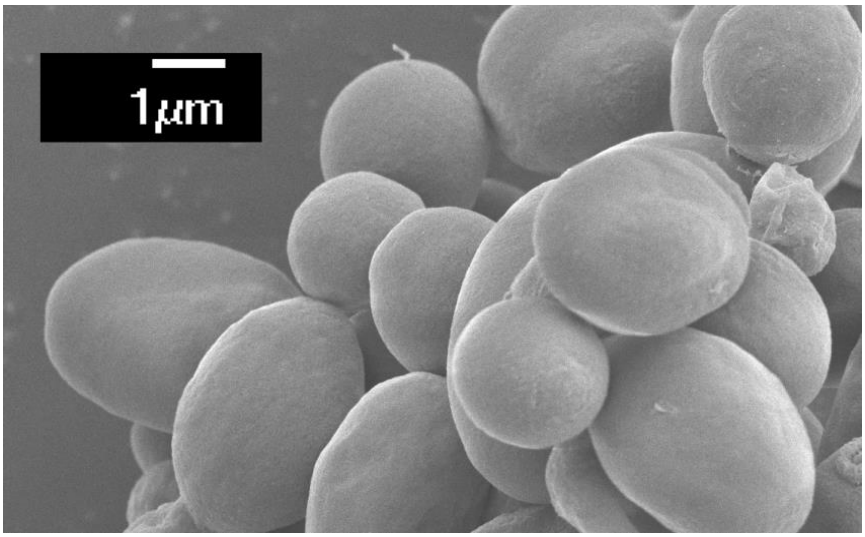

Figure 5.13 SEM photo of *Rhodotorula glutinis*, not subjected to EP

Figure 5.13 displays non-EP-treated *R. glutinis*. All samples photographed were cultivated using the procedure described in the "Materials and Methods" chapter. Neumann et al. (1989) discussed the visual effect of EP on microorganisms, and state that when cells are treated with EP, indentations form and bowl-shaped or volcano-shaped deformations can be seen when using a microscope. Microphotographs were taken of electroporated *R. glutinis* to visually inspect for differences between electroporated cells and non-electroporated cells. Figure 5.14 is an image of electroporated cells. The image shows indentations approximately 1 micrometer in width.

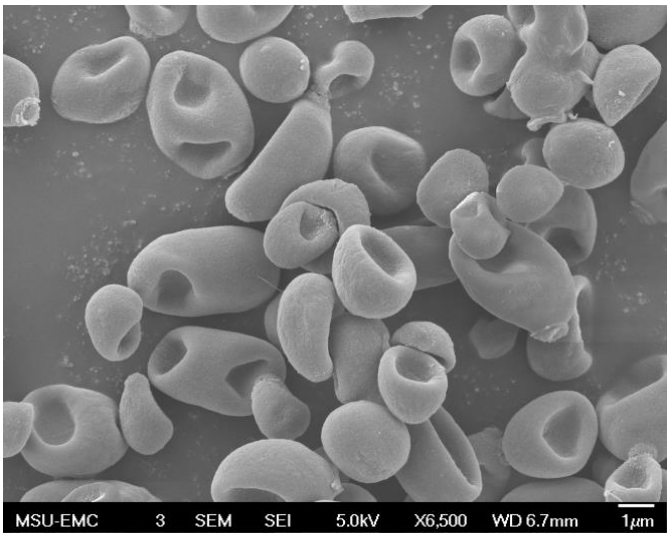

Figure 5.14 SEM microphotographs of *R. glutinis* after EP treatment (3000 volts, 100 microseconds, and 59 pulses)

Figure 5.14 displays a reversible EP experiment with parameters of 1500 volts, 100 microseconds, 59 pulses, and an electrode spacing of 4 mm. Weaver et al. (1996) noticed indentions in the cell membrane when a reversible EP experiment was conducted. Figure 5.14 illustrates indentions in electroporated cells, which suggests that EP has occurred and the cell walls have formed pores caused by the induced electric field. The indentions in Figure 5.14 are not present in non-electroporated cells, Figure 5.13.

EP parameters which should result in irreversible cell breakdown experiments were also completed (490 volts, 10,000,000 microseconds, and three pulses). Figures 5.15 and 5.16 display the SEM microphotographs captured after the irreversible EP experiments were concluded.

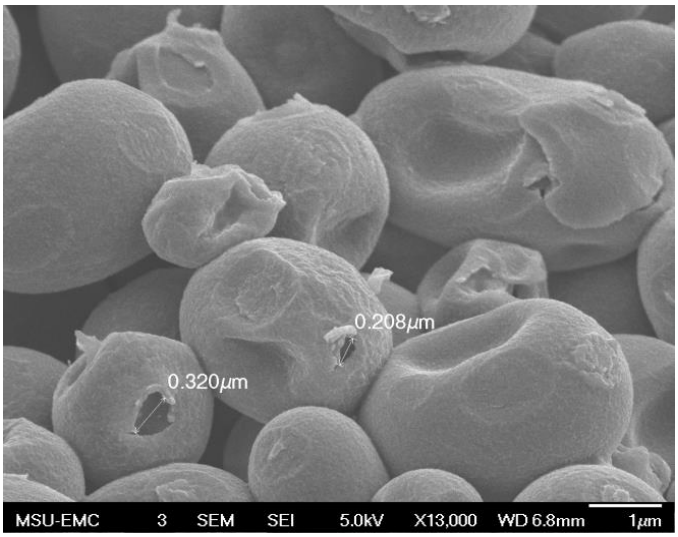

Figure 5.15 SEM of irreversible EP experiments illustrating cell membrane failure (490 volts, 10 seconds, and 3 pulses)

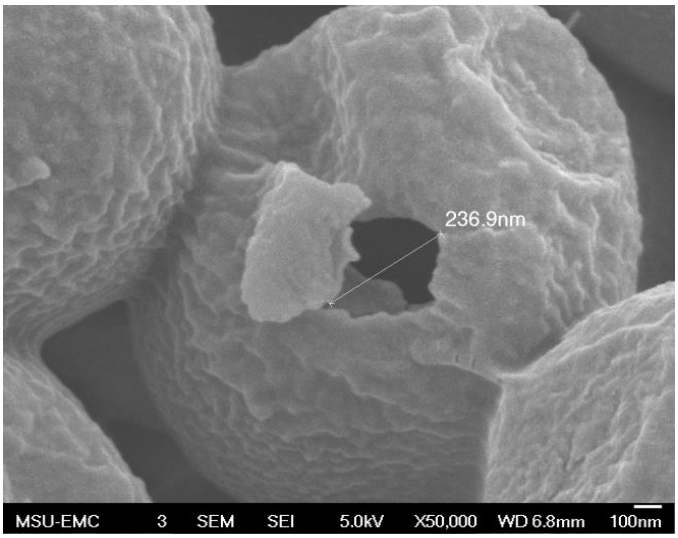

Figure 5.16 Enhanced SEM of irreversible EP experiments with cell membrane failure (490 volts, 10 seconds, and 3 pulses)

Figure 5.15 shows multiple cells with apparent cell membrane breakdowns. The right side of the image shows that a large section of the cell membrane, approximately 1 micrometer in width, has been dislocated. Figure 5.16 displays an enlarged

microphotograph of a cell membrane failure, which occurred during an EP experiment with a magnitude of 490 volts, a pulse duration of 10,000,000 microseconds (10 seconds), ten EP pulses, and an electrode spacing of 4 mm. The pulse duration tested in this particular experiment exceeds the pulse duration limit suggested by Freeman et al. (1994) of limiting pulse lengths to 1000 microseconds.

5.4.2 Irreversible Electroporation Experiments

As stated in the previous section, experiments were conducted to rupture the cell membrane. The purpose of these experiments was to test the amount of lipids expelled from *R. glutinis* during irreversible electroporation. Figure 5.16 is proof that cell walls ruptured under large pulse durations (1 second) and low voltages (500 volts). Three experiments were conducted utilizing parameters that should rupture the cell membrane. The parameters tested were 490 volts, 10,000,000 microseconds (10 seconds), and three pulses. The data collected during these tests are displayed in Table 5.18. Tests 4, 5, and 6 yielded approximately half of the lipids present in the controls and in tests 1, 2, 3, 7, 8, and 9. The experiments listed below are the only experiments completed under irreversible parameters, since the focus of this study was to remove microbial lipids while maintaining cell viability.

Table 5.18 Data collected during irreversible EP experiments

Test Number	Electroporation Parameters			% Lipid Extracted
	Voltage (V)	Pulse Duration (ms)	Number of Pulses	
1	3000	100	59	48.9%
2	3000	100	59	45.3%
3	3000	100	59	44.2%
4	490	10,000,000	3	23.9%
5	490	10,000,000	3	24.5%
6	490	10,000,000	3	20.3%
7	10	1000	59	47.0%
8	10	1000	59	47.3%
9	10	1000	59	46.9%
C1	0	0	0	41.3%
C2	0	0	0	44.2%
C3	0	0	0	43.0%

Figure 5.17 illustrates the data from Table 5.18 averaged for each experiment with C1-C3 being the controls for these experiments. The irreversible EP experiment, the second bar, is approximately half the value of the control. When a reversible EP experiment was completed on this batch of *R. glutinis,* the average intracellular lipids value measured was close to the amount of intracellular lipids present in the control. Therefore, when this batch of *R. glutinis* was subjected to 490 volts, 10,000,000 microseconds, and three pulses, 46.5% of the intracellular lipids were not available for chemical extraction. This suggests that EP successfully removed intracellular lipids.

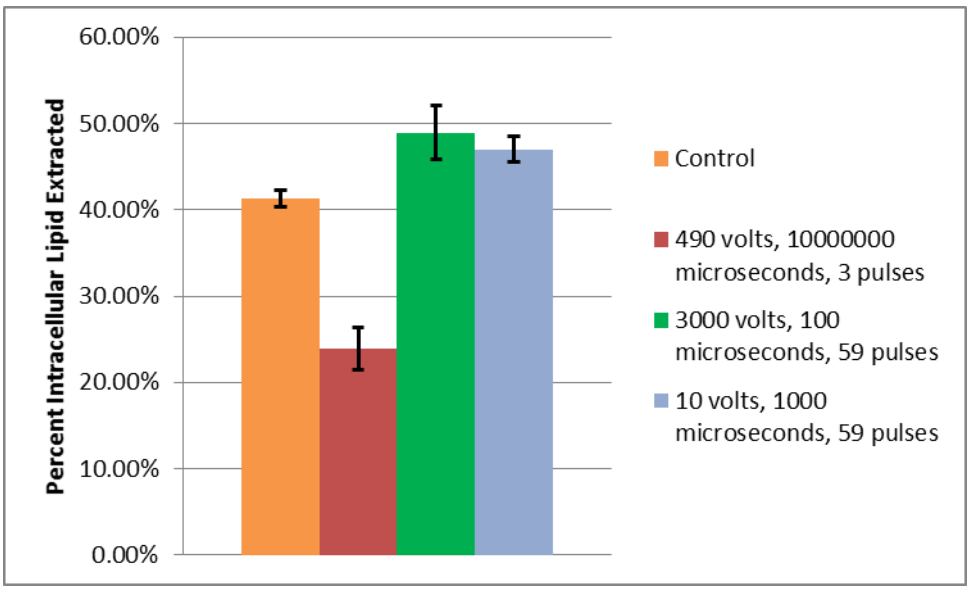

Figure 5.17 Average percent intracellular lipid extracted during the irreversible electroporation experiments

CHAPTER VI

CONCLUSIONS AND RECOMMENDATIONS

6.1 Conclusion

The overall goal of this study was to determine if EP can be an effective method for removing lipids from specific oleaginous microorganisms and soybeans. Based on the results of this study, it appears EP was ineffective for removing lipids from soybeans and EP has a limited effect for lipid extraction from oleaginous yeast organisms. Additional conclusions and observations are provided as follows.

- The Bligh and Dyer method of extraction is an effective lipid removal procedure when 10 grams/liter dry cell mass and 40% or higher lipid content is present. However, separate methods should be used if the lipid mass is below 30 mg because the Bligh and Dyer method is dependent on gravimetric analysis.
- The Bligh and Dyer method was very good for soybean lipid extraction, but EP did not significantly impact the soybean lipid extraction.
- The oleaginous yeast used in this study was able to produce lipid concentrations as high as 50% of the DCM as measured by the Bligh and Dyer extraction method.
- EP was successful in removing lipids from the oleaginous yeast used in this study. However, under the EP conditions investigated, the maximum lipid yield was 0.7 g/L of the 3.9 g/L available lipids (17.9% lipid extraction). This result was achieved in Matrix 2, which utilized high voltage and low pulse durations. Therefore, at these low extraction levels and under the parameters tested, reversible EP is not a viable extraction method.
- Initial tests show that irreversible EP removed 46.5% (Table 5.18) of microbial lipids. However, few experiments have been completed under these parameters.

6.2 Recommendations

Based on this study, the following recommendations are provided:

- Further research needs to focus on electrode spacing when using single-pulse EP.
  - Tables 5.5 and 5.9 illustrate that electrode spacing has the most significant effect on intracellular lipid extraction. Electrode spacing results in the largest eigenvector for the minimum eigenvalue.
- Future research should focus on pulse duration when using low voltage and multiple EP pulses.
  - Table 5.13 illustrates that pulse duration has the most significant effect on intracellular lipid extraction. Pulse duration results in the largest eigenvector for the minimum eigenvalue.
- Further investigation is needed regarding voltage effects when using high voltages and multiple pulses.
  - Table 5.17 illustrates that voltage has the most significant effect on intracellular lipid extraction. Voltage results in the largest eigenvector for the minimum eigenvalue.
- More experiments should be conducted using irreversible EP parameters and cell viability should be tested to determine if enough organisms survive EP to maintain a healthy community.
  - Experiments should focus on the number of individual cells that remain viable after a colony of cells is subjected to irreversible EP parameters. If a portion of cells remain viable, then a colony could be produced from the cells that survived irreversible EP.

REFERENCE

"International Petroleum (Oil) Consumption", U.S. Energy Information Administration, accessed February 19, 2012, http://www.eia.gov/emeu/international/oilconsumption.html

Abidor, I.G., Arakelyan, V.B., Chernomordik, L.V., Chizmadzhev, Yu. A., Pastushenko, V.F., and Tarasevich, M.R. (1979) Electric Breakdown of Bilayer Lipid Membranes: I. The main experimental facts and their qualitative discussion. *Bioelectrochem. Bioenerg*. 6 37-52

Abidor, I.G., Chemomordik, L.V., Sukharev S.I., and Chizmadzhev, Yu.A. (1982) The reversible electrical breakdown of bilayer lipid membranes modified by uranyl ions. *Bioelectrochem. Bioenerg*. 9 141-148.

Alvarez H.M., Kalscheuer R., and Steinbüchel A. (1997a) Accumulation of storage lipids in species of *Rhodococcus* and *Nocardia* and effect of inhibitors and polyethylene glycol. Fett/Lipid 99:239– 246

Alvarez HM, Luftmann H, Silva RA, Cesari AC, Viale A, Waterman M, and Steinbüchel A (2002) Identification of phenyldecanoic acid as a constituent of triacylglycerols and wax esters produced by Rhodococcus opacus PD630. Microbiology 148:1407–1412

Alvarez HM, Pucci OH, and Steinbüchel A (1997b) Lipid storage compounds in marine bacteria. Appl Microbiol Biotechnol 47:132–139

Alvarez, H., Mayer, F., Fabritius, D., and Steinbüchel, A. (1996) Formation of intracytoplasmic lipid inclusions by *Rhodococcus opacus* strain PD630, *Arch Microbiol* 165: 377–386

Arakelyan, V.B. (1979) 250 - Electric breakdown of bilayer lipid membranes V. Consideration of the kinetic stage in the case of the membrane containing an arbitrary number of defects. *Bioelectrochemistry and Bioenergetics 6.1*: 81-87.

Asgharian, N. and Schelly, Z.A. (1999) Electric field-induced transient birefringence and light scattering of synthetic liposomes. *Biochim. Biophys*. Acta 1418 295– 306.

Bargale, PC, Ford, R.J., Sosulski, F.W., Wulfsohn, D, and Irudayaraj, J. (1999) Mechanical oil expression from extruded soybean samples. *Journal of the American Oil Chemists Society*. 76:223-229.

Barnett, A. and Weaver, J.C. (1991) Electroporation: A unified, quantitative theory for reversible electrical breakdown and rupture. *Bioelectrochem. Bioenerg*. 25 163-182.

Bartoletti, D.C., Harrison, G.I. and Weaver, J.C. (1989) The number of molecules taken up by electroporated cells: quantitative determination. *FEBS Lett*. 256 4-10.

Beebe, S.J., Fox, P.M., Rec, L.J., Willis, E.L., and Schoenbach, K.H. (2003) Nanosecond, high-intensity pulsed electric fields induce apoptosis in human cells. *FASEB J*. 7 3 –5.

Benz, R. and Conti, F. (1981) Reversible electrical breakdown of squid giant axon membrane. *Biochim. Biophys. Acta*. 645 115-123.

Benz, R. and Zimmermann, U. (1980a) Pulse-length dependence of the electrical breakdown in lipid bilayer membranes. *Biochim. Biophys. Acta*. 597 637-642. 1980a

Benz, R. and Zimmermann, U. (1980b) Relaxation studies on cell membranes and lipid bilayers in the high electric field range. *Bioelectrochem. Bioenerg*. 7 723-739. 1980b

Benz, R. and Zimmermann, U. (1981) The resealing process of lipid bilayers after reversible electrical breakdown. *Biochim. Biophys. Acta*. 640 169-178.

Benz, R., Beckers, F., and Zimmermann, U. (1979) Reversible electrical breakdown of lipid bilayer membranes: A charge pulse relaxation study. *Journal of Membrane Biology*. 181-204.

Bligh, E.G. and Dyer, W.J. (1959) A rapid method for total lipid extraction and purification. *Can. J. Biochem. Physiol.* 37:911-917.

Box G.E. and Behnken D. (1960) Some new three level designs for the study of quantitative variables. *Technometrics*; 2(4):455-475.

Canakci, M. and Sanli, H., (2008) Biodiesel production from various feedstocks and their effects on the fuel properties. J. Ind. Microbiol. Biotechnol. 35, 431-441.

Chakrabarti, R., Wylie, D.E., and Schusster, S.M. (1989) Transfer of monoclonal antibodies into mammalian cells by electroporation. *J. Biol. Chem*. 264 15494-15500.

Chang, D and Reese, T. (1990) Changes in membrane structure induced by electroporation as revealed by rapid-freezing electron microscopy. *Biophysical Journal*. Volume 58, issue, pp 1-12.

Chang, D.C., Chassy, B.M., Saunders, J.A., and Sowers, A.E. (1992) "Guide to Electroporation and Electrofusion," Academic Press.

Chernomordik, L.V., Sukharev, S.I., Abidor, I.G., and Chizmadzhev, Yu. A. (1982) The study of the BLM reversible electrical breakdown in the presence of UO_2^{2+}. *Bioelectrochem. Bioenerg*. 9 149-155.

Chizmadzhev, Yu.A. (1979) 248 - Electric breakdown of bilayer lipid membranes III. Analysis of possible mechanisms of defect origination. *Bioelectrochemistry and Bioenergetics 6.1*: 63-70.

Crowley, J.M. (1973) Electrical breakdown of bimolecular lipid membranes as an electromechanical instability. *Biophys J.*; 13(7):711–724.

Dai C, Tao J, Xie F, Dai Y, and Zhao M. (2007) Biodiesel generation from oleaginous yeast *Rhodotorula glutinis* with xylose assimilating capacity. *African Journal of Biotechnology*; 6(18).2130-4.

Daniel H.J., Otto R.T., Binder M., Reuss M., and Syldatk C. (1999) Production of sophorolipids from whey: development of a two-stage process with *Cryptococcus curvatus* ATCC 20509 and *Candida bombicola* ATCC 22214 using deproteinized whey concentrates as substrates. Applied Microbiology and Biotechnology 51:40-45.

D'Annibale A., Sermanni G.G., Federici F., and Petruccioli M. (2005) Olive-mill wastewaters: a promising substrate for microbial lipase production. Bioresource Technology 97. DOI: 10.1016/j.biortech.2005.09.001.

Davis J.B. (1964) Cellular Lipids of a *Nocardia* Grown on Propane and n-Butane. Applied Microbiology 12:301-304.

De Andrus C, Espuny MJ, Robert M, Mercade ME, Manresa A, and Guinea J (1991) Cellular lipid accumulation by *Pseudomonas aeruginosa* 44T1. Appl Microbiol Biotechnol 35:813–816

Dimitrotrov, D.S. (1984) Electric breakdown of lipid bilayers and cell membranes: a thin visco elastic film model. *J. Membrane Biol.* 78, 53-60

Dornbos, D.L., Jr., and Mullen, R.E. (1992) Soybean Seed Protein and Oil Contents and Fatty Acid Composition Adjustments by Drought and Temperature. *JAOCS* vol. 69, no. 3 pp 228-231.

Farsaie, A., DeBarthe, J.V., Kenworthy, W.J., Lessley, B.V., and Wiebold, W.J. (1985) Analysis of Producing Vegetable Oil as an Alternative Fuel. *Energy in Agriculture*. 4 189-205.

Freeman SA, Wang MA, and Weaver JC. (1994) Theory of electroporation of planar bilayer membranes: Predictions of the aqueous area, change in capacitance, and pore-pore separation. *Biophys J*.;67(1):42-56.

Frierich, J., and List, G. (1981) Characterization of soybean oil extracted by supercritical carbon dioxide and hexane. USDA pp. 192-193.

Gabriel, B., and Teissie, J. (1994) Generation of reactive-oxygen species induced by electropermeabilization of Chinese hamster ovary cells and their consequence on cell viability. *Eur. J. Biochem*. 223 25–33.

Gabriel, B., and Teissie, J. (1995) Control by electrical parameters of short and long-term cell death associated to Chinese hamster ovary cell electropermeabilization. *Biochim. Biophys. Acta* 1266 171– 178.

Gabriel, B., and Teissie, J. (1995) Spatial compartmentation and time resolution of photooxidation of a cell membrane probe in electropermeabilized Chinese hamster ovary cells. *Eur. J. Biochem*. 228 710–718.

Gabriel, B., and Teissie, J. (1999) Time courses of mammalian cell electropermeabilization observed by millisecond imaging of membrane property changes during the pulse. *Biophys. J*. 76 2158– 2165.

Gao, D., Zeng, J., Zheng, Y., Yu, X., and Chen, S., (2013) Microbial lipid production from xylose by *Mortierella isabellina*. Bioresource. Technol. 133, 315-321.

Gift, E.A., and Weaver, J.C. (1995) Observation of Extremely Heterogeneous Electroporative uptake which changes with electric field pulse amplitude. *Biochem. Biophys. Acta*. 1234 52-62.

Golzio, M., Mora, M.P., Raynaud, C., Delteil, C., Teissie, J., and Rols, M.P. (1998) Control by osmotic pressure of voltage-induced permeabilization and gene transfer in mammalian cells. *Biophys. J*. 74 3015–3022.

Gross, D., Loew, L.M., and Webb, W.W. (1986) Optical imaging of cell membrane potential changes induced by applied electric fields. *Biophys. J*. 51 339– 348.

Haberl, S., Miklavčič, D., Sersa, G., Frey, W., and Rubinsky, B. (2013) Cell Membrane Electroporation—Part 2: The Applications, *IEEE Dielectrics and Electrical Insulation Society.* Vol. 29, no. 1, pp.29-37,.

Hall, J. (2012) Cultivation of Oleaginous Microorganism Consortium on Municipal Wastewater for the Production of Lipids. Dissertation. Mississippi State University

Harbich, W. and Helfrich, W. (1979) Alignment and opening of giant lecithin vesicles by electric fields. *Z. Naturforsch*. 34a 1063–1065.

Helfrich, W. (1974) Deformation of lipid bilayer spheres by electric fields. *Z. Naturforsch*. 29c 182–183.

Hetzler, S., Bröker, D., and Steinbüchel, A. (2013) Saccharification of Cellulose by Recombinant *Rhodococcus opacus* PD630 Strains. Appl. Environ. Microbiol. vol. 79 no. 17 5159-5166

Hibino, M., Itoh, H., and Kinosita, K., Jr. (1993) Time courses of cell electroporation as revealed by submicrosecond imaging of transmembrane potential. *Biophys. J*. 64 1789–1800

Hibino, M., Shigemori, M., Itoh, H., Nagayama, K., and Kinosita, K., Jr. (1991) Membrane conductance of an electroporated cell analyzed by submicrosecond imaging of transmembrane potential. *Biophys. J*. 59 209– 220.

Holdsworth JE, Ratledge C (1988) Lipid turnover in oleaginous yeasts. J Gen Microbiol 134:339–346

Hu, Q., Joshi, R.P., and Schoenbach, K.H. (2005) Simulations of nanopore formation and phosphatidylserine externalization in lipid membranes subjected to high-intensity, ultrashort electric pulses. *Phys. Rev. E.,* 72 031902-1–031902-10.

Hyuga, H., Kinosita, K., and Wakabayashi, N. (1991) Deformation of vesicles under the influence of strong electric fields. *Jpn. J. Appl. Phys.* 30 1141–1148

Jarm, T., Cemazar, M., Miklavcic, D., and Sersa, G. , (2010) Antivascular effects of electrochemotherapy: Implications in treatment of bleeding metastases, Expert Rev. Anticancer Ther. , vol. 10, no. 5, pp. 729–746.

Kakorin, S. and Neumann, E. (1998) Kinetics of the electroporative deformation of lipid vesicles and biological cells in an electric field. *Ber. Bunsenges. Phys. Chem*. 102 670– 675.

Kaneko H, Hosohara M, Tanaka M, and Itoh T. (1976) Lipid composition of 30 species of yeast. *Lipids*.;11(12):837-844.

Kavadia A, Komaitis M, Chevalot I, Blanchard F, Marc I, and Aggelis G (2001) Lipid and gamma-linolenic acid accumulation in strains of *Zygomycetes* growing on glucose. J Am Oil Chem Soc 78:341–346

Kinosita, K., Jr. and Tsong, T.Y. (1977) Hemolysis of human erythrocytes by transient electric field. *Proc. Natl. Acad. Sci*. U. S. A. 74 1923–1927.

Kinosita, K., Jr. and Tsong, T.Y. (1979) Voltage induced conductance in human erythrocyte membranes. *Biochim. Biophys. Acta*. 554 479-497.

Knowles JR (1980) Enzyme-catalyzed phosphoryl transfer reactions. Annu. Rev. Biochem. 49: 877–919.

Koronkiewicz, S., Kalinowski, S., and Bryl, K. (2002) Programmable chronopotentiometry as a tool for the study of electroporation and resealing of pores in bilayer lipid membranes. *Biochim. Biophys. Acta* 1561 222–229.

Kotnik, T., Bobanovic, F., and Miklavcic, D. (1997) Sensitivity of transmembrane voltage induced by applied electric fields—A theoretical analysis, *Bioelectrochem. Bioenerg*. 43 285–291.

Kotnik, T., Kramar, P., Pucihar, G., Miklavčič, D., and Tarek, M. (2013) Cell Membrane Electroporation—Part 1: The Phenomenon, *IEEE Dielectrics and Electrical Insulation Society.* Vol. 29, no. 1, pp.14-23,

Koutb, M. and Morsy, F. M., (2011) A potent lipid producing isolate of *Epicoccum purpurascens* AUMC5615 and its promising use for biodiesel production. Biomass Bioenergy 35, 3182-3187.

Lambert, H., Pankov, R., Gauthier, J., and Hancock, R. (1990) Electroporation-mediated uptake of proteins into mammalian cells. *Biochem. Cell. Biol*. 68 729-734.

Li Q, Du W, and Liu D. (2008) Perspectives of microbial oils for biodiesel production. *Appl Microbiol Biotechnol*.;80(5):749-756.

Lister, J.D. (1974) Stability of lipid bilayers and red blood cell membranes. *Phys Lett.* 53A 193-194.

Loginova, K. V., Vorobiev, E., Bals, O., and Lebovka, N. I. (2011) Pilot study of countercurrent cold and mild heat extraction of sugar from sugar beets, assisted by pulsed electric fields, *J. Food Eng.* , vol. 102, no. 4, pp. 340–347.

Lojewska, Z., Farkas, D., Ehrenberg, B., and Loew, L.M. (1989) Analysis of the effect and membrane conductance on the amplitude and kinetics of membrane potentials induced by externally applied electric fields. *Biophys. J*. 56 121– 128.

Lopez, A., Rols, M.P., and Teissie, J. (1988) 31P NMR analysis of membrane phospholipid organization in viable, reversibly electropermeabilized Chinese hamster ovary cells. *Biochemistry* 27 1222–1228.

Makula R.A., Lockwood P.J., and Finnerty W.R. (1975) Comparative Analysis of the Lipids of *Acinetobacter* Species Grown on Hexadecane. Journal of Bacteriology 121:250-258.

Mir, L.M., Banoun, H., and Paoletti, C. (1988) Introduction of definite amounts of nonpermenant molecules into living cells after electropermeabilization: Direct access to cytosol. *Exp. Cell. Res*. 175 15-25.

Muller, K.J., Sukhorukov, V.L., and Zimmermann, U. (2001) Reversible electropermeabilization of mammalian cells by high-intensity, ultra-short pulses of submicrosecond duration. *J. Membr. Biol*. 184 161–170

Neumann, E. and Kakorin, S. (1996) Electroptics of membrane electroporation and vesicle shape deformation. Curr. Opin. *Colloid Interface* 1 790–799.

Neumann, E. and Kakorin, S. (1998) Digression on membrane electroporation and electroporative delivery of drugs and genes. *Radiol. Oncol*. 32 7–17.

Neumann, E., Kakorin, S., and Toensing, K. (1999) Fundamentals of Electroporative delivery of drugs and genes. *Bioelectrochem. Bioenerg*. 48 3–16.

Neumann, E., Sowers A., and Jordan, C. (1989) "Electroporation and Electrofusion in Cell Biology." Plenum, New York.

Neumann, E., Toensing, K., Kakorin, S., Budde, P., and Frey, J. (1998) Mechanism of electroporative dye uptake by mouse B cells. *Biophys. J*. 74 98– 108.

Noguchi, H. (2008) Membrane simulation models from nm to μm scale, *J. Phys. Soc. Jpn.* 78, 041007.

Ohshima, T., Hama, Y. and Sato, M. (2000) "Releasing profiles of gene products from recombinant *Escherichia coli* in a high-voltage pulsed electric field," *Biochem. Eng. J.*, vol. 5, no. 2, pp. 149–155

Othmer, D., and Jaatinen, W. (1959) Extraction of Soybeans Mechanism with Various Solvents. *Industrial and Engineering Chemistry* vol. 51, no. 4 pp 543-546.

Pastushenko, V.F. (1979a) 247 - Electric breakdown of bilayer lipid membranes II. Calculation of the membrane lifetime in the steady-state diffusion approximation. *Bioelectrochemistry and Bioenergetics 6.1* Mar 1979: 53-62,.

Pastushenko, V.F. (1979b) 251 - Electric breakdown of bilayer lipid membranes VI. A stochastic theory taking into account the processes of defect formation and death: Membrane lifetime distribution function. *Bioelectrochemistry and Bioenergetics 6.1* Mar 1979: 89-95

Pastushenko, V.F. (1979c) 251 bis - Electric breakdown of bilayer lipid membranes VII. A stochastic theory taking into account the processes of defect formation and death: Statistical properties. *Bioelectrochemistry and Bioenergetics 6.1* Mar 1979: 97-104.

Pastushenko, V.F., Chizmadzhev, Yu.A., and Arakelyan, V.B. (1979d) Electric breakdown of bilayer lipid membranes: IV. Consideration of the kinetic stage in the case of the single-defectmembrane, *Journal of Electroanalytical Chemistry and Interfacial Electrochemistry*, Volume 104, , Pages 71-79, ISSN 0022-0728, http://dx.doi.org/10.1016/S0022-0728(1979)81009-8

Popov, S.V., Svitkina, T.M., Margolis, L.B., and Tsong, T.Y. (1991) Mechanism of cell protrusion formation in electrical field: the role of actin. *Biochim. Biophys. Acta* 1066 151–158.

Prausnitz, M.R., Lau, B.S., Milano, C.D., Conner, S., Langer, R., and Weaver, J.C. (1993) A quantitative study of electroporation showing a patuea in net molecular transport. *Biophys. J.* 65 414-422.

Prausnitz, M.R., Milano, C.D., Grimm, J.A., Langer, R., and Weaver, J.C. (1994) Quantitative study of molecular transport due to electroporation: Uptake of bovine serum albumin by human red blood cell ghosts. *Biophys. J*. 66 1522-1530.

Puc, M., Corovic, S., Flisar, K., Petkovsek, M., Nastran, J., and Miklavcic, D. (2004) Techniques of signal generation required for electropermeabilization. Survey of electropermeabilization devices. *Bioelectrochemistry* 64 113– 124.

Puc, M., Kotnik, T., Mir, L.M., and Miklavcic, D. (2003) Quantitative model of small molecules uptake after in vitro cell electropermeabilization. *Bioelectrochemistry* 60 1– 10.

Qiang, L., Du, W., and Liu, D. (2008) Perspectives of microbial oils for biodiesel production. *Applied Microbial Biotechnol*. 80:749-756.

Ramsey, R.W., and Harris, F.D. (1982) On-farm soybean oil expression. Plant and Vegetable Oils as Fuels, 2-4. American Society of Agricultural Engineers. pp 252-255.

Ratledge C. (1994) Microbial conversions of agro-waste materials to high-valued oils and fats. ICHEME Symposium series 137:25-33.

Ratledge C. (2002) Regulation of lipid accumulation in oleaginous micro-organisms. Biochemical Society Transactions 30:1047-1050.

Raza Z.A., Rehman A., Khan M.S., and Khalid Z.M. (2007) Improved production of biosurfactant by a *Pseudomonas aeruginosa* mutant using vegetable oil refinery wastes. Biodegradation 18:115-121.

Riske, K.A., and Dimova, R. (2005) Electro-deformation and poration of giant vesicles viewed with high temporal resolution. *Biophys. J*. 88 1143– 1155.

Rols, M.P. and Teissie, J. "Electropermeabilization of mammalian cells. Quantitative analysis of the phenomenon." *Biophys. J.* 58 (1990) 1089– 1098.

Rols, M.P. and Teissie, J. "Experimental evidence for the involvement of the cytoskeleton in mammalian cell electropermeabilization." *Biochim. Biophys. Acta* 1111 (1992) 45– 50.

Rosenthal, A., Pyle, D.L., and Niranjan, K. (1996) Aqueous and enzymatic processes for edible oil extraction. *Enzyme and Microbial Technology* 19 402-420

Sack, M., Sigler, J., Frenzel, S., Eing, C., Arnold, J., Michelberger, T., Frey, W., Attmann, F., Stukenbrock, L., and Muller, G. (2010) Research on industrialscale electroporation devices fostering the extraction of substances from biological tissue, *Food Eng. Rev.*, vol. 2, no. 2, pp. 147–156,.

Sale, A.J. H., and Hamilton, W.A. (1967a) Effects of high electric fields on microorganisms: II. Killing of bacteria and yeasts. *Biochim. Biophys. Acta*. 148 789-800. 1967a

Sale, A.J. H., and Hamilton, W.A. (1967b) Effects of high electric fields on microorganisms: I. Killing of bacteria and yeasts. *Biochim. Biophys. Acta*. 148: 781-788. 1967b

SAS Institute Inc. 2011. SAS/STAT® 9.3 User's Guide. Cary, NC: SAS Institute Inc.

Sersa, G., Cufer, T., Paulin, S. M., Cemazar, M., and Snoj, M. (2012) Electrochemotherapy of chest wall breast cancer recurrence, *Cancer Treat. Rev.*, vol. 38, no. 5, pp. 379–386

Sharma, A., Khare, S.K., and Gupta, M. (2002) Three phase partitioning for extraction of oil from soybean. *Bioresource Technology* 85:327-329.

Smith, K., and Weaver, J. (2008) Active Mechanisms Are Needed to Describe Cell Responses to Submicrosecond, Megavolt-per-Meter Pulses: Cell Models for Ultrashort Pulses. *Biophysical Journal* 95: 1547-1563

Smith, K.J., and Huyser, W. (1987) World distribution and significance of soybean, In: Wilcox JR (ed) Soybeans: improvement, production, and uses. 2nd ed. *Agronomy* 16:23-48.

Suga, M., and Hatakeyama, T. (2009) Gene transfer and protein release of fission yeast by application of a high voltage electric pulse, *Anal. Bioanal. Chem.*, vol. 394, no. 1, pp. 13–16,

Sukharev, S.1., Chemomordik, L.V,Abidor, I.G., and Chizmadzhev, Yu.A. "Effects of UO_2^{+2} ions on the properties of bilayer membranes. *Bioelectrochem. Bioenerg.*", 9 (1982) I33- 140.

Sukhorukov, V.L., Mussauer, H., and Zimmermann, U. (1998) The effect of electrical deformation forces on the electropermeabilization of erythrocyte membranes in low- and high-conductivity media. *J. Membr. Biol*. 163 235– 245.

Teissie, J. and Tsong, T.Y. "Electric field induced transient pores in phospholipid bilayer vesicles. *Biochemistry* 20 1548–1554.

Teissie, J., and Rols, M.P. (1993) An experimental evaluation of the critical potential difference inducing cell membrane electropermeabilization. *Biophys. J*. 65 409–413.

Teissie, J., Golzio, M., and Rols, M.P. (2005) Mechanisms of Cell Membrane electropermeabilization: A mini review of our present (lack of?) knowledge. *Biochimica et Biophysica Acta*. 1724 270-280.

Tekle, E., Astumian, R.D., Friauf, W.A., and Chock, P.B. (2001) Asymmetric pore distribution and loss of membrane lipid in electroporated DOPC vesicles. *Biophys. J*. 81 960–968.

Tieleman, D.P., Leontiadou, H., Mark, A.E. and Marrink, S.J.. (2003) Simulation of pore formation in lipid bilayers by mechanical stress and electric fields. *J. Am. Chem. Soc.* 125, 6382-6383.

Tonsing, K., Kakorin, S., and Neumann, E. (1997) Annexin V and vesicle membrane electroporation. Eur. *Biophys. J.* 26 307– 318.

Vasilkoski, Z., Esser, A.T., Gowrishanker, T.R., Stewart, D.A., and Weaver, J.C. (2006) Membrane Electroporation: The Absolute rate equation and nanosecond timescale pore creation. *Phys. Rev*, E 74, 021904-1–021904–12

Wang, H. (2007) Microfluidic Electroporation and Cell Arrays. Ph.D. dissertation, Purdue University.

Weaver, J., and Chizmadzhev, Y. (1996) "Theory of Electroporation: A Review." *Bioelectrochem. Bioenerg*. 41 135-160

Weaver, J., and Chizmadzhev, Y. (2006) Electroporation. In F**.** S. Barnes, and B. Greenebaum. *Biological and Medical Aspects of Electromagnetic Fields*. CRC Press. 293-332.

Winterhalter, M., and Helfrich, W. (1988) Deformation of spherical vesicles by electric fields. *J. Colloid Interface Sci*. 122 583–586.

Wynn J.P., and Ratledge C. (2006) Microbial production of oils and fats. Food science and technology 148:443-472.

Wynn, J., and Ratledge, C. “Oils from Microorganisms. Bailey’s Industrial Oil and Fat Products.” 2005

Yoon, S.H., and Rhee, J.S. (1983) “Lipid from Yeast Fermentation: Effects of Cultural Conditions on Lipid Production and its Characteristics of *Rhodotorula glutinis*.” *Journal of American Oil Chemists’ Society.* Vol.60, no. 7 pp 1281-1286.

Zhan, Y., Martin, V. A., Geahlen, R. L., and Lu, C. (2010) One-step extraction of subcellular proteins from eukaryotic cells, *Lab Chip*, vol. 10, no. 16, pp. 2046–2048,.

Zhang, X., Yan, S., Tyagi, R.D., Drogui, P., and Surampalli, R.Y. (2014), Ultrasonication assisted lipid extraction from oleaginous microorganisms, Bioresource Technology, doi: http://dx.doi.org/10.1016/j.biortech.2014.01.132

APPENDIX A

DATA WITH PARAMETERS

A.1 Soybean Data

Table A.1 Soybean data with experimental parameters

PULSE DURATION(s)	VOLTAGE (V)	ELECTRODE SPACING (mm)	PERCENT LIPID EXTRACTED
0	0	0	19%
0	0	0	24%
0	0	0	22%
0	0	0	23%
0	0	0	18%
0	0	0	21%
0	0	0	24%
0	0	0	22%
0	0	0	19%
0	0	0	18%
0	0	0	18%
0	0	0	22%
9	490	15	19%
9	490	15	19%
9	490	15	20%
9	10	15	19%
9	10	15	19%
1	490	15	18%
1	490	15	20%
1	490	15	23%
1	10	15	19%
1	10	15	19%
9	250	20	19%
9	250	20	26%
9	250	20	24%
9	250	10	19%
9	250	10	25%
9	250	10	21%
1	250	20	20%
1	250	20	22%
1	250	20	20%
0.01	2000	20	22%
0.01	2000	20	20%
0.01	2000	20	24%

Table A.1 (Continued)

0.01	1500	20	21%
0.01	1500	20	23%
0.1	200	20	25%
0.1	200	20	20%
0.1	200	20	13%
0.5	200	20	16%
0.5	200	20	16%
0.5	200	20	18%
1	200	20	18%
1	200	20	19%
1	200	20	17%
3	200	20	17%
3	200	20	18%
3	200	20	17%
5	200	20	17%
5	200	20	17%
5	200	20	18%
1	500	20	18%
1	500	20	17%
1	500	20	24%
3	500	20	17%
3	500	20	18%
3	500	20	18%
5	500	20	20%
5	500	20	20%
5	500	20	21%

A.2 Data Collected for *R. glutinis*

Table A.2 Matrix 1 data with experimental parameters

PULSE DURATION (μs)	VOLTAGE (V)	ELECTRODE SPACING (mm)	PERCENT INTRACELLULAR LIPIDS Remaining in Cell
0	0	0	39.78%
0	0	0	40.99%
0	0	0	38.42%
0	0	0	45.75%
0	0	0	36.96%
990	490	10	54.10%
990	490	10	51.31%
990	490	10	46.79%
990	10	10	52.63%
990	10	10	55.16%
990	10	10	50.26%
10	490	10	59.85%
10	490	10	54.92%
10	490	10	53.27%
10	10	10	53.63%
10	10	10	46.84%
10	10	10	45.20%
990	250	15	52.08%
990	250	15	54.22%
990	250	15	51.24%
990	250	5	54.58%
990	250	5	53.93%
990	250	5	38.97%
10	250	15	49.18%
10	250	15	51.61%
10	250	15	42.05%
10	250	5	41.95%
10	250	5	48.14%
10	250	5	40.88%
500	490	15	53.15%
500	490	15	39.08%
500	490	5	40.56%
500	490	5	40.77%
500	490	5	46.68%
500	10	15	41.77%

Table A.2 (Continued)

500	10	15	55.18%
500	10	15	46.48%
500	10	5	49.51%
500	10	5	42.62%
500	10	5	40.34%
500	250	10	51.98%
500	250	10	45.50%
500	250	10	39.18%
500	250	10	41.64%
500	250	10	48.12%
500	250	10	48.54%
500	250	10	40.75%
500	250	10	45.66%
500	250	10	42.44%

Table A.3 Matrix 2 data with experimental parameters

PULSE DURATION (μs)	VOLTAGE (V)	ELECTRODE SPACING (mm)	PERCENT INTRACELLULAR LIPIDS Remaining in Cell
0	0	0	44%
0	0	0	39%
0	0	0	39%
0	0	0	36%
0	0	0	39%
90	3000	15	42%
90	3000	15	42%
90	3000	15	45%
90	1000	15	42%
90	1000	15	42%
90	1000	15	40%
10	3000	15	36%
10	3000	15	33%
10	3000	15	35%
10	1000	15	34%
10	1000	15	35%
10	1000	15	35%
90	2000	20	33%

Table A.3 (Continued)

90	2000	20	35%
90	2000	20	34%
90	2000	10	35%
90	2000	10	36%
90	2000	10	38%
10	2000	20	35%
10	2000	20	35%
10	2000	20	34%
10	2000	10	34%
10	2000	10	36%
10	2000	10	37%
50	3000	20	36%
50	3000	20	40%
50	3000	20	36%
50	3000	10	39%
50	3000	10	39%
50	3000	10	36%
50	1000	20	39%
50	1000	20	41%
50	3000	10	39%
50	3000	10	36%
50	2000	15	37%
50	2000	15	33%
50	2000	15	31%
50	2000	15	34%

Table A.4 Matrix 3 data with experimental parameters

PULSE DURATION (μs)	VOLTAGE (V)	NUMBER OF PULSES	PERCENT INTRACELLULAR LIPIDS Remaining in Cell
0	0	0	37.78%
0	0	0	38.53%
0	0	0	35.86%
0	0	0	36.48%
0	0	0	36.41%

Table A.4 (Continued)

0	0	0	36.05%
0	0	0	35.39%
0	0	0	35.39%
0	0	0	34.26%
1000	500	59	33.86%
1000	500	59	35.29%
1000	500	59	34.06%
1000	10	59	34.35%
1000	10	59	34.38%
1000	10	59	35.13%
10	500	59	34.35%
10	500	59	34.02%
10	500	59	31.79%
10	10	59	31.40%
10	10	59	32.81%
10	10	59	32.87%
1000	260	99	33.90%
1000	260	99	33.40%
1000	260	99	30.76%
1000	260	19	30.85%
1000	260	19	32.51%
1000	260	19	32.03%
10	260	99	32.28%
10	260	99	33.96%
10	260	99	31.14%
10	260	19	32.13%
10	260	19	32.52%
505	500	99	34.77%
505	500	99	31.71%
505	500	99	32.12%
505	500	19	33.38%
505	500	19	33.61%
505	500	19	30.78%
505	10	99	38.82%
505	10	99	35.73%
505	10	99	36.83%
505	10	19	35.03%
505	10	19	38.99%
505	10	19	38.90%

Table A.4 (Continued)

505	260	59	37.78%
505	260	59	39.03%
505	260	59	37.10%
505	260	59	35.23%
505	260	59	36.11%
505	260	59	37.51%
505	260	59	32.32%
505	260	59	31.45%
505	260	59	34.59%

Table A.5 Matrix 4 data with experimental parameters

PULSE DURATION (μs)	VOLTAGE (V)	NUMBER OF PULSES	PERCENT INTRACELLULAR LIPIDS Remaining in Cell
0	0	0	34.31%
0	0	0	34.66%
0	0	0	33.78%
0	0	0	32.54%
0	0	0	32.98%
0	0	0	32.47%
0	0	0	33.52%
0	0	0	32.20%
10	690	59	32.70%
10	690	59	34.54%
10	690	59	33.10%
1000	690	59	35.32%
1000	690	59	35.63%
1000	690	59	32.36%
10	3000	59	34.46%
10	3000	59	34.75%
10	3000	59	33.75%
1000	3000	59	36.53%
1000	3000	59	36.39%
1000	3000	59	36.03%
10	1845	19	33.76%
10	1845	19	33.36%
10	1845	19	33.96%

Table A.5 (Continued)

1000	1845	19	36.50%
1000	1845	19	35.47%
1000	1845	19	37.06%
10	1845	99	35.83%
10	1845	99	34.79%
10	1845	99	35.40%
1000	1845	99	36.64%
1000	1845	99	37.45%
1000	1845	99	37.97%
505	690	19	34.26%
505	690	19	34.59%
505	3000	19	33.89%
505	3000	19	33.31%
505	3000	19	33.57%
505	690	99	35.34%
505	690	99	33.04%
505	690	99	33.51%
505	3000	99	36.02%
505	3000	99	35.38%
505	3000	99	33.08%
505	1845	59	33.87%
505	1845	59	32.86%
505	1845	59	32.76%
505	1845	59	33.40%
505	1845	59	37.41%
505	1845	59	33.41%
505	1845	59	32.73%
505	1845	59	31.78%
505	1845	59	32.13%

APPENDIX B

SAS OUTPUT

B.1 Soybean SAS Output

Coding Coefficients for the Independent Variables		
Factor	**Subtracted off**	**Divided by**
PULSE DURATION	4.500000	4.500000
VOLTAGE	1000.000000	1000.000000
ELECTRODESPACING	10.000000	10.000000

Response Surface for Variable PERCENT_LIPID_EXTRACTED: PERCENT LIPID EXTRACTED	
Response Mean	0.197505
Root MSE	0.024050
R-Square	0.2924
Coefficient of Variation	12.1770

Regression	DF	Type I Sum of Squares	R-Square	F Value	Pr > F
Linear	3	0.008668	0.2121	5.00	0.0042
Quadratic	3	0.002265	0.0554	1.31	0.2831
Crossproduct	3	0.001018	0.0249	0.59	0.6264
Total Model	9	0.011950	0.2924	2.30	0.0303

Residual	DF	Sum of Squares	Mean Square	F Value	Pr > F
Lack of Fit	8	0.006636	0.000829	1.56	0.1652
Pure Error	42	0.022285	0.000531		
Total Error	50	0.028921	0.000578		

Parameter	DF	Estimate	Standard Error	t Value	Pr > |t|	Parameter Estimate from Coded Data
Intercept	1	0.208353	0.006938	30.03	<.0001	0.187763
PULSE DURATION	1	-0.014022	0.008324	-1.68	0.0983	-0.018333
VOLTAGE	1	0.000046656	0.000181	0.26	0.7974	-0.003348
ELECTRODESPACING	1	-0.000844	0.004622	-0.18	0.8559	0.005381
PULSE DURATION*PULSE DURATION	1	0.001207	0.000581	2.08	0.0428	0.024451
VOLTAGE*PULSE DURATION	1	-0.000004480	0.000006832	-0.66	0.5149	-0.020162
VOLTAGE*VOLTAGE	1	-1.717143E-8	2.1449087E-8	-0.80	0.4272	-0.017171
ELECTRODESPACING*PULSE DURATION	1	0.000356	0.000311	1.15	0.2576	0.016025
ELECTRODESPACING*VOLTAGE	1	0.000000450	0.000009776	0.05	0.9635	0.004501
ELECTRODESPACING*ELECTRODESPACING	1	-0.000033536	0.000235	-0.14	0.8873	-0.003354

Factor	DF	Sum of Squares	Mean Square	F Value	Pr > F	Label
PULSE DURATION	4	0.004540	0.001135	1.96	0.1147	PULSE DURATION (s)
VOLTAGE	4	0.003972	0.000993	1.72	0.1610	VOLTAGE (V)
ELECTRODESPACING	4	0.002932	0.000733	1.27	0.2952	ELECTRODE SPACING (mm

Canonical Correlation	Adjusted Canonical Correlation	Approximate Standard Error	Squared Canonical Correlation	Eigenvalues of Inv(E)*H = CanRsq/(1-CanRsq)			Test of H0: The canonical correlations in the current row and all that follow are zero				
				Eigenvalue	Proportion	Cumulative	Likelihood Ratio	Approximate F Value	Num DF	Den DF	Pr > F
0.460511	0.434586	0.102580	0.212070	0.2691	1.0000	1.0000	0.78792961	5.02	3	56	0.0037

Note: The F statistic is exact.

Canonical Analysis of Response Surface Based on Coded Data

Factor	Critical Value		Label
	Coded	Uncoded	
PULSE DURATION	0.061726	4.777768	PULSE DURATION (s)
VOLTAGE	-0.010146	989.854221	VOLTAGE (V)
ELECTRODESPACING	0.942940	19.429397	ELECTRODE SPACING (mm)
Predicted value at stationary point: 0.189752			

Eigenvalues	Eigenvectors		
	PULSE DURATION	VOLTAGE	ELECTRODESPACING
0.028460	0.953474	-0.199499	0.226024
-0.004056	-0.163522	0.287621	0.943681
-0.020478	0.253273	0.936736	-0.241617
Stationary point is a saddle point.			

Estimated Ridge of Minimum Response for Variable PERCENT_LIPID_EXTRACTED: PERCENT LIPID EXTRACTED					
			Uncoded Factor Values		
Coded Radius	Estimated Response	Standard Error	PULSE DURATION	VOLTAGE	ELECTRODESPACING
0.0	0.187763	0.066274	4.500000	1000.000000	10.000000
0.1	0.185907	0.072363	4.882261	1035.302896	9.607861
0.2	0.184015	0.083016	5.161532	1102.898507	9.116780
0.3	0.181880	0.095810	5.370057	1186.435707	8.663623
0.4	0.179411	0.109623	5.542737	1275.965175	8.263644
0.5	0.176573	0.124150	5.696502	1367.870703	7.903002
0.6	0.173349	0.139316	5.839268	1460.818368	7.569534
0.7	0.169731	0.155109	5.975091	1554.260098	7.255111
0.8	0.165713	0.171531	6.106244	1647.947626	6.954423
0.9	0.161293	0.188591	6.234100	1741.759670	6.663930
1.0	0.156468	0.206297	6.359537	1835.633612	6.381201

Estimated Ridge of Maximum Response for Variable PERCENT_LIPID_EXTRACTED: PERCENT LIPID EXTRACTED					
Coded Radius	Estimated Response	Standard Error	Uncoded Factor Values		
			PULSE DURATION	VOLTAGE	ELECTRODESPACING
0.0	0.187763	0.066274	4.500000	1000.000000	10.000000
0.1	0.189874	0.065153	4.056248	995.148923	10.158815
0.2	0.192426	0.066751	3.602745	1004.240825	10.150227
0.3	0.195491	0.069638	3.152854	1018.655865	10.056689
0.4	0.199097	0.073247	2.707423	1035.368763	9.918732
0.5	0.203257	0.077344	2.265498	1053.229109	9.755295
0.6	0.207976	0.081823	1.826163	1071.731431	9.576008
0.7	0.213258	0.086630	1.388746	1090.624843	9.386215
0.8	0.219104	0.091734	0.952771	1109.772440	9.189104
0.9	0.225517	0.097120	0.517902	1129.093792	8.986694
1.0	0.232496	0.102780	0.083897	1148.538793	8.780322

Multivariate Statistics and Exact F Statistics					
S=1 M=0.5 N=27					
Statistic	Value	F Value	Num DF	Den DF	Pr > F
Wilks' Lambda	0.78792961	5.02	3	56	0.0037
Pillai's Trace	0.21207039	5.02	3	56	0.0037
Hotelling-Lawley Trace	0.26914890	5.02	3	56	0.0037
Roy's Greatest Root	0.26914890	5.02	3	56	0.0037

Raw Canonical Coefficients for the VAR Variables		
		V1
VOLTAGE	VOLTAGE (V)	0.0019506114
PULSE DURATION	PULSE DURATION (s)	0.1314773102
ELECTRODESPACING	ELECTRODE SPACING (mm)	-0.12852891

Raw Canonical Coefficients for the WITH Variables	
	W1
PERCENT_LIPID_EXTRACTED	37.9

Standardized Canonical Coefficients for the VAR Variables		
		V1
VOLTAGE	VOLTAGE (V)	0.9325
PULSE DURATION	PULSE DURATION (s)	0.4423
ELECTRODESPACING		-1.0100

Standardized Canonical Coefficients for the WITH Variables	
	W1
PERCENT_LIPID_EXTRACTED	1.0000

Correlations Between the VAR Variables and Their Canonical Variables		
		V1
VOLTAGE	VOLTAGE (V)	0.4576
PULSE DURATION	PULSE DURATION (s)	0.1137
ELECTRODESPACING	ELECTRODE SPACING (mm)	-0.5178

Correlations Between the WITH Variables and Their Canonical Variables		
		W1
PERCENT_LIPID_EXTRACTED	PERCENT LIPID EXTRACTED	1.0000

Correlations Between the VAR Variables and the Canonical Variables of the WITH Variables

		W1
VOLTAGE	VOLTAGE (V)	0.2107
PULSE DURATION	PULSE DURATION (s)	0.0523
ELECTRODESPACING	ELECTRODE SPACING (mm)	-0.2385

Correlations Between the WITH Variables and the Canonical Variables of the VAR Variables		
		V1
PERCENT_LIPID_EXTRACTED	PERCENT LIPID EXTRACTED	0.4605

B.2 Matrix 1 SAS output

The RSREG Procedure

Coding Coefficients for the Independent Variables		
Factor	**Subtracted off**	**Divided by**
TIME	495.000000	495.000000
VOLTAGE	245.000000	245.000000
ELECTRODESPACING	7.500000	7.500000

Response Surface for Variable PERCENT_LIPIDS_EXTRACTED	
Response Mean	0.470327
Root MSE	0.047241
R-Square	0.4770
Coefficient of Variation	10.0444

Regression	DF	Type I Sum of Squares	R-Square	F Value	Pr > F
Linear	3	0.036417	0.2188	5.44	0.0032
Quadratic	3	0.036574	0.2197	5.46	0.0031
Crossproduct	3	0.006407	0.0385	0.96	0.4227
Total Model	9	0.079399	0.4770	3.95	0.0012

Residual	DF	Sum of Squares	Mean Square	F Value	Pr > F
Lack of Fit	4	0.007935	0.001984	0.88	0.4872
Pure Error	35	0.079103	0.002260		
Total Error	39	0.087038	0.002232		

Parameter	DF	Estimate	Standard Error	t Value	Pr > |t|	Parameter Estimate from Coded Data
Intercept	1	0.401783	0.020276	19.82	<.0001	0.433946
TIME	1	-0.000142	0.000081148	-1.75	0.0880	0.010573
VOLTAGE	1	-0.000103	0.000167	-0.62	0.5393	0.001209
ELECTRODESPACING	1	0.013542	0.006494	2.09	0.0436	0.046574
TIME*TIME	1	0.000000212	5.9381831E-8	3.57	0.0010	0.051930
VOLTAGE*TIME	1	-0.000000192	0.000000114	-1.69	0.0990	-0.023322
VOLTAGE*VOLTAGE	1	0.000000381	0.000000245	1.55	0.1286	0.022859
ELECTRODESPACING*TIME	1	8.5995877E-8	0.000005171	0.02	0.9868	0.000319
ELECTRODESPACING*VOLTAGE	1	0.000002245	0.000010937	0.21	0.8384	0.004125
ELECTRODESPACING*ELECTRODESPACING	1	-0.000528	0.000418	-1.26	0.2141	-0.029717

Factor	DF	Sum of Squares	Mean Square	F Value	Pr > F
TIME	4	0.037082	0.009270	4.15	0.0067
VOLTAGE	4	0.011517	0.002879	1.29	0.2906
ELECTRODESPACING	4	0.022372	0.005593	2.51	0.0576

Canonical Analysis of Response Surface Based on Coded Data

Factor	Critical Value	
	Coded	Uncoded
TIME	-0.142008	424.706204
VOLTAGE	-0.168473	203.724021
ELECTRODESPACING	0.771172	13.283790
Predicted value at stationary point: 0.451051		

Eigenvalues	Eigenvectors		
	TIME	VOLTAGE	ELECTRODESPACING
0.056032	0.943271	-0.331965	-0.006229
0.018842	0.331933	0.942406	0.041120
-0.029803	-0.007780	-0.040855	0.999135
Stationary point is a saddle point.			

The RSREG Procedure

Estimated Ridge of Minimum Response for Variable PERCENT_LIPIDS_EXTRACTED					
			Uncoded Factor Values		
Coded Radius	Estimated Response	Standard Error	TIME	VOLTAGE	ELECTRODESPACING
0.0	0.433946	0.014564	495.000000	245.000000	7.500000
0.1	0.428902	0.014747	486.752557	244.494614	6.760645
0.2	0.423301	0.015124	481.847631	244.271317	6.013464
0.3	0.417126	0.015849	478.658472	244.297456	5.263768
0.4	0.410366	0.017072	476.463573	244.514724	4.513212
0.5	0.403018	0.018910	474.896604	244.875775	3.762393
0.6	0.395079	0.021423	473.751963	245.345965	3.011543
0.7	0.386548	0.024622	472.905258	245.900315	2.260757
0.8	0.377424	0.028489	472.276747	246.520659	1.510067
0.9	0.367706	0.032992	471.812909	247.193584	0.759483
1.0	0.357393	0.038101	471.476463	247.909017	0.009003

Estimated Ridge of Maximum Response for Variable PERCENT_LIPIDS_EXTRACTED						
				Uncoded Factor Values		
Coded Radius	Estimated Response	Standard Error	TIME	VOLTAGE	ELECTRODESPACING	
0.0	0.433946	0.014564	495.000000	245.000000		7.500000
0.1	0.438485	0.014444	510.886305	245.539063		8.210134
0.2	0.442704	0.014283	544.784475	244.369248		8.796396
0.3	0.447120	0.014022	598.172878	238.944116		9.107625
0.4	0.452290	0.013692	654.025413	231.309350		9.237464
0.5	0.458443	0.013368	707.547210	223.190240		9.301581
0.6	0.465653	0.013134	759.200078	214.974919		9.338730
0.7	0.473949	0.013098	809.611401	206.746677		9.362379
0.8	0.483345	0.013376	859.186230	198.525091		9.378268
0.9	0.493848	0.014078	908.176417	190.314084		9.389263
1.0	0.505461	0.015275	956.743250	182.113401		9.396955

B.3 Matrix 2 SAS output

The RSREG Procedure

Coding Coefficients for the Independent Variables		
Factor	**Subtracted off**	**Divided by**
TIME	45.000000	45.000000
VOLTAGE	1500.000000	1500.000000
ELECTRODESPACING	10.000000	10.000000

Response Surface for Variable PERCENT_LIPIDS_EXTRACTED	
Response Mean	0.370863
Root MSE	0.024014
R-Square	0.5562
Coefficient of Variation	6.4751

Regression	DF	Type I Sum of Squares	R-Square	F Value	Pr > F
Linear	3	0.011006	0.2567	6.36	0.0016
Quadratic	3	0.011250	0.2624	6.50	0.0014
Crossproduct	3	0.001594	0.0372	0.92	0.4413
Total Model	9	0.023850	0.5562	4.60	0.0006

Residual	DF	Sum of Squares	Mean Square	F Value	Pr > F
Lack of Fit	3	0.009842	0.003281	10.71	<.0001
Pure Error	30	0.009187	0.000306		
Total Error	33	0.019030	0.000577		

Parameter	DF	Estimate	Standard Error	t Value	Pr > |t|	Parameter Estimate from Coded Data
Intercept	1	0.395428	0.010709	36.92	<.0001	0.342090
TIME	1	-8.140881E-8	0.000843	-0.00	0.9999	0.021804
VOLTAGE	1	-0.000098779	0.000031096	-3.18	0.0032	-0.030975
ELECTRODESPACING	1	0.004272	0.004604	0.93	0.3602	0.007947
TIME*TIME	1	0.000006189	0.000005721	1.08	0.2872	0.012533
VOLTAGE*TIME	1	6.5193982E-8	0.000000172	0.38	0.7072	0.004401
VOLTAGE*VOLTAGE	1	3.1899112E-8	7.2342429E-9	4.41	0.0001	0.071773
ELECTRODESPACING*TIME	1	-0.000017021	0.000034093	-0.50	0.6209	-0.007660
ELECTRODESPACING*VOLTAGE	1	-0.000002050	0.000001402	-1.46	0.1530	-0.030753
ELECTRODESPACING*ELECTRODESPACING	1	0.000018186	0.000222	0.08	0.9353	0.001819

Factor	DF	Sum of Squares	Mean Square	F Value	Pr > F
TIME	4	0.010288	0.002572	4.46	0.0054
VOLTAGE	4	0.011612	0.002903	5.03	0.0028
ELECTRODESPACING	4	0.003116	0.000779	1.35	0.2720

The RSREG Procedure

Canonical Analysis of Response Surface Based on Coded Data

Factor	Critical Value	
	Coded	Uncoded
TIME	-0.491575	22.879135
VOLTAGE	0.565681	2348.520879
ELECTRODESPACING	1.562876	25.628757
Predicted value at stationary point: 0.334180		

Eigenvalues	Eigenvectors		
	TIME	VOLTAGE	ELECTRODESPACING
0.075142	0.047024	0.977132	-0.207369
0.013140	0.974255	-0.090689	-0.206404
-0.002157	0.220490	0.192324	0.956240
Stationary point is a saddle point.			

Estimated Ridge of Minimum Response for Variable PERCENT_LIPIDS_EXTRACTED					
			Uncoded Factor Values		
Coded Radius	Estimated Response	Standard Error	TIME	VOLTAGE	ELECTRODESPACING
0.0	0.342090	0.012515	45.000000	1500.000000	10.000000
0.1	0.338691	0.012095	41.899179	1604.032866	9.789844
0.2	0.336029	0.011696	37.934006	1672.736676	9.543629
0.3	0.333856	0.011371	33.639671	1712.060654	9.207437
0.4	0.332020	0.011230	29.396980	1730.401258	8.727897
0.5	0.330422	0.011459	25.449339	1732.903999	8.072912
0.6	0.328988	0.012262	21.952691	1723.294560	7.251738
0.7	0.327657	0.013767	18.947679	1705.264350	6.310800
0.8	0.326384	0.015985	16.375560	1682.053003	5.302680
0.9	0.325136	0.018854	14.141774	1655.901745	4.264492
1.0	0.323894	0.022295	12.160057	1628.137366	3.216720

Estimated Ridge of Maximum Response for Variable PERCENT_LIPIDS_EXTRACTED					
			Uncoded Factor Values		
Coded Radius	Estimated Response	Standard Error	TIME	VOLTAGE	ELECTRODESPACING
0.0	0.342090	0.012515	45.000000	1500.000000	10.000000
0.1	0.346526	0.012950	46.998730	1369.198286	10.205708
0.2	0.352220	0.013440	48.171950	1226.187685	10.413529
0.3	0.359292	0.014058	48.858505	1079.003710	10.622534
0.4	0.367796	0.014891	49.264652	930.593942	10.831830
0.5	0.377761	0.016021	49.500984	781.943978	11.041062
0.6	0.389202	0.017517	49.628245	633.376448	11.250118
0.7	0.402127	0.019427	49.681717	484.986700	11.458982
0.8	0.416541	0.021776	49.683075	336.790208	11.667666
0.9	0.432449	0.024570	49.646302	188.775015	11.876192
1.0	0.449853	0.027806	49.580803	40.921090	12.084583

Canonical Correlation Analysis

Canonical Correlation	Adjusted Canonical Correlation	Approx. Standard Error	Squared Canonical Correlation	Eigenvalues of Inv(E)*H = CanRsq/(1-CanRsq)				Test of H0: The canonical correlations in the current row and all that follow are zero			
				Eigenvalue	Proportion	Cumulative	Likelihood Ratio	Approx. F Value	Num DF	Den DF	Pr > F
0.506630	0.476180	0.114698	0.256674	0.3453	1.0000	1.0000	0.7433256	4.49	3	39	0.0084

Note: The F statistic is exact.

Multivariate Statistics and Exact F Statistics					
S=1 M=0.5 N=18.5					
Statistic	**Value**	**F Value**	**Num DF**	**Den DF**	**Pr > F**
Wilks' Lambda	0.74332569	4.49	3	39	0.0084
Pillai's Trace	0.25667431	4.49	3	39	0.0084
Hotelling-Lawley Trace	0.34530531	4.49	3	39	0.0084
Roy's Greatest Root	0.34530531	4.49	3	39	0.0084

Canonical Correlation Analysis

Raw Canonical Coefficients for the VAR Variables	
	V1
VOLTAGE	-0.000213314
TIME	0.0268314194
ELECTRODESPACING	-0.130592724

Raw Canonical Coefficients for the WITH Variables	W1
PERCENT_LIPIDS_EXTRACTED	31.296717793

Canonical Correlation Analysis

Standardized Canonical Coefficients for the VAR Variables	V1
VOLTAGE	-0.2124
TIME	0.9206
ELECTRODESPACING	-0.7919

Standardized Canonical Coefficients for the WITH Variables	W1
PERCENT_LIPIDS_EXTRACTED	1.0000

Correlations Between the VAR Variables and Their Canonical Variables	
	V1
VOLTAGE	-0.2907
TIME	0.5498
ELECTRODESPACING	-0.5457

Correlations Between the WITH Variables and Their Canonical Variables	W1
PERCENT_LIPIDS_EXTRACTED	1.0000

Correlations Between the VAR Variables and the Canonical Variables of the WITH Variables	
	W1
VOLTAGE	-0.1473
TIME	0.2785
ELECTRODESPACING	-0.2765

Correlations Between the WITH Variables and the Canonical Variables of the VAR Variables	
	V1
PERCENT_LIPIDS_EXTRACTED	0.5066

B.4 Matrix 3 SAS output

The RSREG Procedure

Coding Coefficients for the Independent Variables

Factor	Subtracted off	Divided by
TIME	500.000000	500.000000
VOLTAGE	250.000000	250.000000
NUMBEROFPULSES	49.500000	49.500000

Response Surface for Variable PERCENT_LIPIDS_EXTRACTED	
Response Mean	0.278898
Root MSE	0.038098
R-Square	0.6490
Coefficient of Variation	13.6602

Regression	DF	Type I Sum of Squares	R-Square	F Value	Pr > F
Linear	3	0.017381	0.0977	3.99	0.0136
Quadratic	3	0.085384	0.4802	19.61	<.0001
Crossproduct	3	0.012650	0.0711	2.91	0.0455
Total Model	9	0.115416	0.6490	8.84	<.0001

Residual	DF	Sum of Squares	Mean Square	F Value	Pr > F
Lack of Fit	4	0.013157	0.003289	2.60	0.0505
Pure Error	39	0.049256	0.001263		
Total Error	43	0.062413	0.001451		

Parameter	DF	Estimate	Standard Error	t Value	Pr > |t|	Parameter Estimate from Coded Data
Intercept	1	0.317213	0.012123	26.17	<.0001	0.229062
TIME	1	-0.000315	0.000056093	-5.62	<.0001	0.013316
VOLTAGE	1	-0.000426	0.000117	-3.63	0.0007	-0.013099
NUMBEROFPULSES	1	0.001401	0.000644	2.18	0.0351	0.018169
TIME*TIME	1	0.000000276	4.6035543E-8	5.99	<.0001	0.068883
VOLTAGE*TIME	1	1.8191328E-8	8.7169145E-8	0.21	0.8357	0.002274
VOLTAGE*VOLTAGE	1	0.000000641	0.000000191	3.35	0.0017	0.040046
NUMBEROFPULSES*TIME	1	0.000001249	0.000000516	2.42	0.0199	0.030903
NUMBEROFPULSES*VOLTAGE	1	0.000000886	0.000001029	0.86	0.3939	0.010966
NUMBEROFPULSES*NUMBEROFPULSES	1	-0.000018992	0.000006239	-3.04	0.0040	-0.046535

Factor	DF	Sum of Squares	Mean Square	F Value	Pr > F
TIME	4	0.072783	0.018196	12.54	<.0001
VOLTAGE	4	0.021365	0.005341	3.68	0.0116
NUMBEROFPULSES	4	0.018386	0.004597	3.17	0.0229

Canonical Analysis of Response Surface Based on Coded Data

Factor	Critical Value	
	Coded	Uncoded
TIME	-0.136489	431.755328
VOLTAGE	0.144573	286.143313
NUMBEROFPULSES	0.166929	57.763009
Predicted value at stationary point: 0.228723		

Eigenvalues	Eigenvectors		
	TIME	VOLTAGE	NUMBEROFPULSES
0.071026	0.989333	0.059815	0.132822
0.040250	-0.067093	0.996442	0.051010
-0.048883	-0.129298	-0.059377	0.989826

Stationary point is a saddle point.

Estimated Ridge of Minimum Response for Variable PERCENT_LIPIDS_EXTRACTED

Coded Radius	Estimated Response	Standard Error	Uncoded Factor Values		
			TIME	VOLTAGE	NUMBEROFPULSES
0.0	0.229062	0.012077	500.000000	250.000000	49.500000
0.1	0.226374	0.012052	487.639465	259.473149	45.085605
0.2	0.223045	0.012009	488.392669	264.209486	40.078012
0.3	0.218823	0.012032	492.412810	267.265391	35.068374
0.4	0.213654	0.012221	497.533481	269.668602	30.088299
0.5	0.207523	0.012683	503.148143	271.756094	25.129751
0.6	0.200422	0.013522	509.026362	273.667109	20.185634
0.7	0.192349	0.014812	515.061799	275.469423	15.251383
0.8	0.183301	0.016590	521.198598	277.199995	10.324103
0.9	0.173278	0.018858	527.404594	278.880705	5.401905
1.0	0.162279	0.021598	533.659945	280.525343	0.483519

Estimated Ridge of Maximum Response for Variable PERCENT_LIPIDS_EXTRACTED

Coded Radius	Estimated Response	Standard Error	Uncoded Factor Values		
			TIME	VOLTAGE	NUMBEROFPULSES
0.0	0.229062	0.012077	500.000000	250.000000	49.500000
0.1	0.231973	0.012005	537.003382	237.846996	51.800483
0.2	0.235917	0.011837	584.542264	229.840342	52.967768
0.3	0.241141	0.011606	634.622536	225.240189	53.843133
0.4	0.247719	0.011352	685.275018	222.623096	54.620500
0.5	0.255680	0.011124	735.968740	221.183115	55.354493
0.6	0.265039	0.010990	786.560944	220.484069	56.065472
0.7	0.275804	0.011032	837.023248	220.278087	56.762688
0.8	0.287979	0.011337	887.361549	220.415859	57.450965
0.9	0.301567	0.011983	937.590807	220.802599	58.133079
1.0	0.316570	0.013019	987.726877	221.375387	58.810748

Canonical Correlation Analysis

Canonical Correlation	Adjusted Canonical Correlation	Approximate Standard Error	Squared Canonical Correlation	Eigenvalues of Inv(E)*H = CanRsq/(1-CanRsq)			Test of H0: The canonical correlations in the current row and all that follow are zero				
				Eigenvalue	Proportion	Cumulative	Likelihood Ratio	Approximate F Value	Num DF	Den DF	Pr > F
0.312633	0.259845	0.125121	0.097740	0.1083	1.0000	1.0000	0.90226047	1.77	3	49	0.1653

Note: The F statistic is exact.

Multivariate Statistics and Exact F Statistics					
S=1 M=0.5 N=23.5					
Statistic	Value	F Value	Num DF	Den DF	Pr > F

Wilks' Lambda	0.90226047	1.77	3	49	0.1653
Pillai's Trace	0.09773953	1.77	3	49	0.1653
Hotelling-Lawley Trace	0.10832740	1.77	3	49	0.1653
Roy's Greatest Root	0.10832740	1.77	3	49	0.1653

Canonical Correlation Analysis

Raw Canonical Coefficients for the VAR Variables	
	V1
VOLTAGE	-0.003931831
TIME	0.0013860796
NUMBEROFPULSES	-0.014606949

Raw Canonical Coefficients for the WITH Variables	
	W1
PERCENT_LIPIDS_EXTRACTED	17.100181965

Canonical Correlation Analysis

Standardized Canonical Coefficients for the VAR Variables

	V1
VOLTAGE	-0.7585
TIME	0.5306
NUMBEROFPULSES	-0.5108

Standardized Canonical Coefficients for the WITH Variables

	W1
PERCENT_LIPIDS_EXTRACTED	1.0000

Correlations Between the VAR Variables and Their Canonical Variables

	V1
VOLTAGE	-0.7891
TIME	0.1797
NUMBEROFPULSES	-0.5993

Correlations Between the WITH Variables and Their Canonical Variables

	W1
PERCENT_LIPIDS_EXTRACTED	1.0000

Correlations Between the VAR Variables and the Canonical Variables of the WITH Variables

	W1
VOLTAGE	-0.2467
TIME	0.0562
NUMBEROFPULSES	-0.1874

Correlations Between the WITH Variables and the Canonical Variables of the VAR Variables	
	V1
PERCENT_LIPIDS_EXTRACTED	0.3126

B.5 Matrix 4 SAS output

Coding Coefficients for the Independent Variables		
Factor	**Subtracted off**	**Divided by**
TIME	500.000000	500.000000
VOLTAGE	1500.000000	1500.000000
NUMBEROFPULSES	49.500000	49.500000

Response Surface for Variable PERCENT_LIPIDS_EXTRACTED	
Response Mean	0.343566
Root MSE	0.011302
R-Square	0.5700
Coefficient of Variation	3.2897

Regression	DF	Type I Sum of Squares	R-Square	F Value	Pr > F
Linear	3	0.003750	0.3005	9.78	<.0001
Quadratic	3	0.003227	0.2586	8.42	0.0002
Crossproduct	3	0.000135	0.0108	0.35	0.7876
Total Model	9	0.007111	0.5700	6.19	<.0001

Residual	DF	Sum of Squares	Mean Square	F Value	Pr > F
Lack of Fit	4	0.000629	0.000157	1.26	0.3023
Pure Error	38	0.004736	0.000125		
Total Error	42	0.005365	0.000128		

Parameter	DF	Estimate	Standard Error	t Value	Pr > |t|	Parameter Estimate from Coded Data
Intercept	1	0.334129	0.003884	86.02	<.0001	0.332955
TIME	1	-0.000032817	0.000019032	-1.72	0.0920	0.009955
VOLTAGE	1	0.000009893	0.000007509	1.32	0.1948	0.007993
NUMBEROFPULSES	1	-0.000412	0.000224	-1.84	0.0730	0.001684
TIME*TIME	1	5.5702239E-8	1.3969082E-8	3.99	0.0003	0.013926
VOLTAGE*TIME	1	2.391207E-9	5.4215056E-9	0.44	0.6614	0.001793
VOLTAGE*VOLTAGE	1	-2.464922E-9	2.2504871E-9	-1.10	0.2796	-0.005546
NUMBEROFPULSES*TIME	1	-0.000000133	0.000000158	-0.84	0.4056	-0.003281
NUMBEROFPULSES*VOLTAGE	1	3.3021827E-8	6.246285E-8	0.53	0.5998	0.002452
NUMBEROFPULSES*NUMBEROFPULSES	1	0.000004678	0.000001951	2.40	0.0210	0.011462

Factor	DF	Sum of Squares	Mean Square	F Value	Pr > F
TIME	4	0.004492	0.001123	8.79	<.0001
VOLTAGE	4	0.000760	0.000190	1.49	0.2231
NUMBEROFPULSES	4	0.001448	0.000362	2.83	0.0362

Canonical Analysis of Response Surface Based on Coded Data

Factor	Critical Value	
	Coded	Uncoded
TIME	-0.420045	289.977370
VOLTAGE	0.608746	2413.119325
NUMBEROFPULSES	-0.198695	39.664591
Predicted value at stationary point: 0.333130		

Eigenvalues	Eigenvectors		
	TIME	VOLTAGE	NUMBEROFPULSES
0.014749	0.896566	0.012871	-0.442723
0.010779	0.439859	0.091250	0.893419
-0.005687	-0.051897	0.995745	-0.076150

Stationary point is a saddle point.

Estimated Ridge of Minimum Response for Variable PERCENT_LIPIDS_EXTRACTED					
			Uncoded Factor Values		
Coded Radius	Estimated Response	Standard Error	TIME	VOLTAGE	NUMBEROFPULSES
0.0	0.332955	0.003550	500.000000	1500.000000	49.500000
0.1	0.331725	0.003568	466.331340	1390.623448	48.896396
0.2	0.330555	0.003577	443.563685	1254.228288	48.493232
0.3	0.329372	0.003600	429.754831	1103.990430	48.325383
0.4	0.328133	0.003675	421.601171	949.161878	48.328631
0.5	0.326812	0.003842	416.793967	793.487280	48.440613
0.6	0.325398	0.004137	414.026388	638.159809	48.621727
0.7	0.323884	0.004587	412.568366	483.480642	48.848488
0.8	0.322264	0.005201	411.994486	329.464563	49.106695
0.9	0.320538	0.005978	412.043786	176.043168	49.387408
1.0	0.318703	0.006908	412.548334	23.132198	49.684763

Coded Radius	Estimated Response	Standard Error	Uncoded Factor Values		
			TIME	VOLTAGE	NUMBEROFPULSES
0.0	0.332955	0.003550	500.000000	1500.000000	49.500000
0.1	0.334326	0.003512	542.265313	1577.939461	50.115810
0.2	0.335895	0.003454	589.195982	1631.757182	50.562547
0.3	0.337700	0.003380	638.273529	1670.176849	50.762533
0.4	0.339757	0.003298	688.290056	1698.967967	50.705037
0.5	0.342079	0.003223	738.672545	1721.504840	50.406359
0.6	0.344672	0.003177	789.129920	1739.779583	49.891508
0.7	0.347542	0.003186	839.505282	1755.020426	49.186846
0.8	0.350692	0.003282	889.712119	1768.021306	48.317171
0.9	0.354125	0.003488	939.703928	1779.317932	47.304673
1.0	0.357842	0.003821	989.458131	1789.285343	46.168695

Canonical Correlation Analysis

Canonical Correlation	Adjusted Canonical Correlation	Approximate Standard Error	Squared Canonical Correlation	Eigenvalues of Inv(E)*H = CanRsq/(1-CanRsq)			Test of H0: The canonical correlations in the current row and all that follow are zero				
				Eigenvalue	Proportion	Cumulative	Likelihood Ratio	Approximate F Value	Num DF	Den DF	Pr > F
0.548202	0.526943	0.097946	0.300526	0.4296	1.0000	1.0000	0.69947413	6.87	3	48	0.0006

Note: The F statistic is exact.

Multivariate Statistics and Exact F Statistics

S=1 M=0.5 N=23					
Statistic	**Value**	**F Value**	**Num DF**	**Den DF**	**Pr > F**
Wilks' Lambda	0.69947413	6.87	3	48	0.0006
Pillai's Trace	0.30052587	6.87	3	48	0.0006
Hotelling-Lawley Trace	0.42964544	6.87	3	48	0.0006
Roy's Greatest Root	0.42964544	6.87	3	48	0.0006

Raw Canonical Coefficients for the VAR Variables	
	V1
VOLTAGE	0.0001946204
TIME	0.0020011337
NUMBEROFPULSES	0.0083888108

Raw Canonical Coefficients for the WITH Variables	
	W1
PERCENT_LIPIDS_EXTRACTED	63.935020007

Canonical Correlation Analysis

Standardized Canonical Coefficients for the VAR Variables	
	V1
VOLTAGE	0.2009
TIME	0.7729
NUMBEROFPULSES	0.2903

Standardized Canonical Coefficients for the WITH Variables	
	W1
PERCENT_LIPIDS_EXTRACTED	1.0000

Canonical Structure

Correlations Between the VAR Variables and Their Canonical Variables	
	V1
VOLTAGE	0.5574
TIME	0.9233
NUMBEROFPULSES	0.6010

Correlations Between the WITH Variables and Their Canonical Variables	
	W1
PERCENT_LIPIDS_EXTRACTED	1.0000

Correlations Between the VAR Variables and the Canonical Variables of the WITH Variables	
	W1
VOLTAGE	0.3056
TIME	0.5061
NUMBEROFPULSES	0.3295

Correlations Between the WITH Variables and the Canonical Variables of the VAR Variables	
	V1
PERCENT_LIPIDS_EXTRACTED	0.5482